The influence of vegetation on acoustic properties of soils

Measurements of acoustic impedances of outdoor surfaces with application to traffic noise

L. A. M. van der Heijden

The influence of vegetation on acoustic properties of soils

Measurements of acoustic impedances of outdoor surfaces with application to traffic noise reduction

Promotor : prof. dr. H. F. Linskens
Co-promotor : prof. dr. H. Myncke

The influence of vegetation on acoustic properties of soils

Measurements of acoustic impedances of outdoor surfaces with application to traffic noise reduction

PROEFSCHRIFT

ter verkrijging van de graad van
doctor in de Wiskunde en Natuurwetenschappen
aan de Katholieke Universiteit te Nijmegen
op gezag van de Rector Magnificus
Prof. Dr. J. H. G. I. Giesbers
volgens besluit van het College van Dekanen
in het openbaar te verdedigen
op vrijdag 27 januari 1984
des namiddags te 2.00 uur

door

LEONARDUS ANTONIUS MARIA VAN DER HEIJDEN

geboren te Vlijmen

1984

krips repro meppel

Aan mijn ouders

Aan Gaia

Dankwoord/Acknowledgments

Gaarne wil ik aan het begin van dit proefschrift een woord van dank richten aan allen die op enigerlei wijze aan het tot-stand-komen ervan hebben bijgedragen.
In de eerste plaats wil ik mijn ouders bedanken die, niet zonder enige moeite, mijn universitaire studie mogelijk hebben gemaakt.
Voor de faciliteiten en de personele hulp ben ik de directeur van de Faculteit der Wiskunde en Natuurwetenschappen, dr. C.J.M. Aarts, en de afdelingen Botanie, Mechanische Ontwerp en Elektronica Research zeer erkentelijk; met name ben ik dank verschuldigd aan de heer A.H. Glaap en zijn medewerkers in de Botanische Tuin voor het onderhouden van de akoestische proefveldjes, de heren T. Groenen en M. Kaptein voor hun waardevolle adviezen bij de constructie van de stromingsweerstandmeter en de heer J. van Huet voor het ontwerp van de Pulse Sound Processor en voor zijn bereidheid steeds in te springen bij elektronische problemen. Voor hun inzet tijdens hun doctoraalstage en de bijdrage aan de experimentele en theoretische resultaten dank ik Joseph de Bie, Vincent Claessen, Niek de Cock, Peter Gotwalt, Hans Groenewoud, Wilko van Rens, Rob van Son en Herman Walthaus.
I am also very much indebted to dr. K. Attenborough, senior lecturer in Engineering Mechanics at the Faculty of Technology, the Open University, England, for his vivid interest in my work and his stimulating influence on my line of thought and on the direction of this research.

Mijn vrouw Gaia en dochters Anke en Elise dank ik voor hun steun en geduld.

Table of contents

1. Introduction 9
1.1 Scope of the present investigation 9
1.1.1 Historical background 9
1.1.2 Acoustically relevant physical soil parameters 10
1.1.3 Vegetation and physical soil characteristics. 11
1.2 Models of outdoor sound propagation 14
1.2.1 Sound interference above soil 14
1.2.2 Some calculations of the image source strength 16
1.2.2.1 Plane wave reflection coefficient 16
1.2.2.2 The Ingard solution 16
1.2.2.3 The Brekhovskikh solution 17
1.2.2.4 The Chessel solution 17
1.2.3 More sophisticated models 18
1.3 Acoustic characterization of outdoor surfaces 19
1.3.1 Characteristic and specific impedance 19
1.3.2 Specific flow resistance 19

2. Measurements of acoustic impedances of soils 21
2.1 Outdoor measurements with the inclined track method 21
2.1.1 Introduction 21
2.1.2 Materials and methods 22
2.1.2.1 Acoustic measuring set-up and apparatus 22
2.1.2.2 Computer analysis of the acoustic data 25
2.1.2.3 Soil physical methods 31
2.1.3 Results of the measurements 31
2.1.3.1 Description of measuring sites 31
2.1.3.2 Soil-physical results 37
2.1.3.3 Acoustical results 38
2.1.4 Discussion 61
2.1.4.1 Performance of the optimization 61
2.1.4.2 General behaviour of acoustic soil parameters 62
2.1.4.3 Layered character of outdoor surfaces 63
2.1.4.4 Influence of angle of incidence 63
2.1.4.5 Influence of soil water content 64
2.1.4.6 Influence of organic layer 64
2.1.4.7 Comparison with values from the literature 66
2.2 Indoor measurements with a short sound pulse 69
2.2.1 Introduction 69
2.2.2 Apparatus and experimental set-up 69
2.2.3 Calculation of impedances 72
2.2.3.1 In the time domain 72

2.2.3.2 In the frequency domain 73
2.2.4 Impedances of sand, peat, grass-sod and oak leaf layers 73
2.2.5 Conclusion. 82

3. Measurements of specific flow resistances of soil samples 85
3.1 Introduction 85
3.2 Materials and methods 86
3.3 Results 90
3.3.1 Measured specific flow resistances 90
3.3.2 Comparison of measured and acoustically derived resistivities . 94

4. Relative contributions of ground and vegetation to sound propagation . 97
4.1 Introduction 97
4.2 The 1/3-octave model 98
4.3 Results and discussion 100
4.3.1 Variation of model parameters 101
4.3.2 Comparison with measurements 106
4.4 Conclusions 114

5. The influence of forest floors on traffic noise propagation 115
5.1 Introduction 115
5.2 Theory of diffraction at the road edge 116
5.3 Results and discussion 118

Summary 125

Samenvatting 126

References 127

Curriculum vitae 139

Chapter 1

Introduction

1.1 Scope of the present investigation

1.1.1 Historical background

Many investigators are working at the moment on the problem of outdoor sound propagation. One of the problems encountered is a good approximation of the acoustical properties of soil surfaces. These values have to be used in outdoor sound propagation models which, in turn, are of great importance for the prediction of traffic noise [5, 91], for the study of the concept of coevolution of acoustical animal communication [21] and for the acoustic climate of the environment [79]. It is only recently that researchers have come to realize the importance of sound reflections by natural soils in the communication of birds [64, 86, 103], insects [86, 135] and mammals [131]. The basis for this research was laid ten years ago by H.F. Linskens of the Department of Botany when he and Van Huet measured a sound-absorbing influence of a hedge on the immission sound pressure level of the former's car (unpublished results). This preliminary experiment was followed by a large number of outdoor sound propagation measurements in forests carried out by students. The results were compiled and published in 1976 [79]. After this publication, the research was taken up by M.J.M. Martens of the Department of Botany, who increased the number of outdoor measurements and extended the investigations to model experiments in an anechoic room [85]. It subsequently became evident that the influence of vegetation on sound could be subdivided into two components: the influence of living, aboveground plant parts such as trunks, branches, twigs, leaves and nee-

dles, and the influence of dead plant parts lying on the forest floor. This is caused by the fact that sound heard in a forest is the result of the interference of a direct travelling sound wave and a ground reflected sound wave. Due to this interference, sound can be attenuated (with a phase difference between $\pi/2$ and $3\pi/2$) or amplified (otherwise). This phase difference is very much influenced by the geometry of the sound source and receiver above the floor. This makes the sound field very unpredictable.
The first attempt in our laboratory to gauge this ground effect was published by Martens in 1977 [81]. Sound propagation measurements were undertaken over asphalt and the sound pressure level differences between a number of measuring microphones and a reference microphone were determined. A plane wave model was used to calculate these differences for different amplitudes and phases of the reflection coefficient. Although the model results quite closely resembled the measured results, the calculated values for the reflection coefficient did not resemble the model values because the same reflection coefficients were used both as input for the reference and the measuring microphone. It was not then known that this coefficient depends on the angle of sound incidence. These angles were different for the reference and the measuring microphone.
I started this research in 1979 and was assigned to measure ground effect on the propagation of sound through forests. More specifically, it was my task to separate the floor influence from the vegetation influence. This was indeed necessary because the interference character of sound fields in forests makes reliable predictions of sound attenuation impossible without knowledge of the mechanism of the floor influence. The aim of this research was to find a set-up to measure this influence and the parameters necessary to describe this influence for any sound source and receiver geometry.
Although this project was based on existing theoretical models and experimental methods, the combination of these in the forest situation has given new insights and numerical values as tools for further applied (traffic noise) and pure (animal communication) research.

1.1.2 Acoustically relevant physical soil parameters

In a review article Attenborough [6] summarizes existing theories on the acoustical properties of porous media. From this it is apparent that acoustically relevant soil parameters are: air porosity, flow resistivity. tortuosity and the dynamic shape factor and that soils can be modeled as porous media with a rigid frame.
In sands and compact subsoils the solid particles lie close together, resulting in a low porosity. In medium-textured soils high in organic matter, the pore space (i.e. the space filled with air and water) will be high [17]. Considerable difference in the total pore space of various

soils exists. Sandy surface soils give values between 35 to 50 %, medium- to fine-textured soils vary from 40 to 60 % or even more in cases of high organic matter and marked granulation. According to Berenyi [12] the pore volume of dried samples of different kinds of soils are as follows: 78 % for lowland peat-soil, 59 % for sandy-soil with much humus, 55 % for sandy-soil containing humus, 48 % for sandy-soil, 50 % for clayey sandy-soil, 56 % for sandy clay and 59 % for heavy clay. Pore space also varies with depth; some subsoils can drop to as low as 25 %, but this is of no interest to acoustical considerations because it has been shown that only the upper 9 cm of soil partake in sound absorption (see section 2.2). It is apparent that total pore space is not a good measure of the acoustical absorption by soils because pore size distribution will have even more influence on sound absorption than total pore space itself. Macropores will give a better gas exchange than micropores, which are also often completely filled with water. Another drawback of the total pore space is the fact that all air spaces are included in the measurement of porosity, whereas only air voids that are connected with the free air are of interest for acoustic properties. These considerations make flow resistivity an interesting parameter (see section 1.3).

1.1.3 Vegetation and physical soil characteristics.

Vegetation has a great effect on two important physical soil parameters, i.e. the soil porosity and water content. In fig. 1.1 a summary can be found of a number of lines of influence.

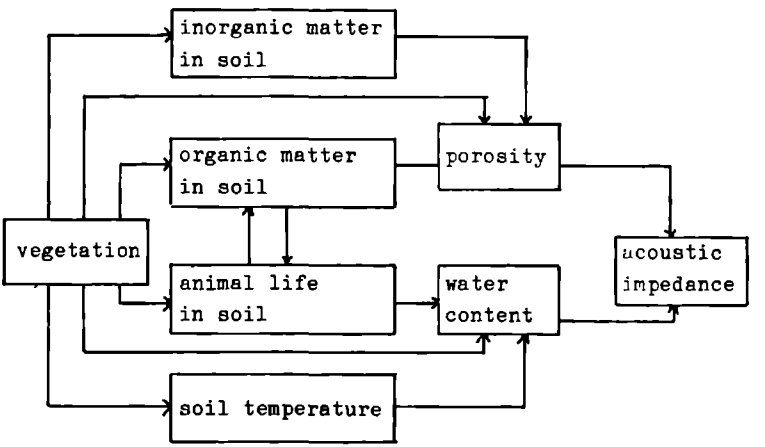

Fig. 1.1 Summary of the relations between biological and physical parameters affecting acoustic soil characteristics, here described by the acoustical impedance.

Vegetation has a direct influence on the porosity through the penetration of roots in the soil, the protection of soil crumbs from the destructive effect of rain drops and through the supply of decaying plant material [106]. After a test period of five years it was found that in a loamy soil the percentage of crumbs larger than 1 mm was 3 % in bare ground, 17 % in ground covered with straw and 34 % in grass-covered ground [106]. Not many acousticians will be aware of the fact that a healthy soil comprises millions of active little animals that continuously change the chemical and physical characteristics of the soil. Certain nematodes, centipedes,sowbugs, ants, fly and beetle larvae, termites (in the tropical regions), and especially earthworms and enchytraeid worms move gigantic masses of soil material, thereby increasing the soil porosity [106]. Earthworms, for example, can move up to 7.23 kg/m^2 per year in a meadow, leading to long pore channels in horizontal and vertical directions. These channels will affect the flow resistivity and the tortuosity. Each plant community clearly influences the kind and intensity of animal soil life. The activity of earthworms for example can vary from 0.98 kg/m^2 excretions per annum in garden soil , 3.44 kg/m^2 in a meadow, 1.71 kg/m^2 in a mixed forest and 1.99 kg/m^2 in a fir-wood [106]. Earthworms prefer a moist habitat that is reasonably well aerated. For this reason, they are found mostly in medium-textured upland soils where the moisture capacity is high, rather than in droughty sands or poorly drained lowlands. Another indication for the influence of vegetation on animal soil life is given by the total biomass in the soil. The total mass of all herbivores, large and small detritivores and predators can be 189.5 , 79.9 and 15.1 g/m^2 for a grassland meadow, an oak forest and a spruce forest respectively [106]. This shows that the metabolism is greatest under grasslands. The spruce with high pH leaves encourages acid conditions and slow organic breakdown. In addition to the activity of the macrofauna, the microfauna , consisting of microorganisms, has a stabilizing influence on the soil structure. Slime and other viscous microbial products probably encourage crumb development and exert a stabilizing influence [17].

Another important influence of vegetation on the composition of inorganic soil constituents influencing porosity is the acidification of the soils by the replacement of cations in the ground by protons [106]. As plants are highly selective in their ion uptake, it is evident that they can change the inorganic matter content drastically. And the type of absorbed cations definitely influences the formation of aggregates. It is known that sodium ions have a dispersive action on particles, while calcium ions encourage granulation by flocculation [17].

Vegetation will also greatly influence soil temperature [111] and ,indirectly, animal soil life and soil water content. The differences between soil surface temperatures and air temperatures can vary extremely for different vegetations. According to Stoutjesdijk [111] these differences under conditions of bright weather and a high sun can have the following

values: -10 °C for open shade, 1 °C for lush grassland, 6 °C under heather (Calluna), 12 °C under hair-grass (Deschampsia), 16 °C under crowberry (Empetrum nigrum L.) and even 35 °C on drymoss. Dense vegetation will promote a microclimate with few fluctuations in the soil temperature. As a result of the canopy temperatures on a plant-grown surface will not reach such extreme values as those found on an open plain [10]. Around noon of a summer day the soil temperature at a depth of 1 cm can rise up to 34 °C on a bare plain and only up to 27 °C on a sod-covered soil ([104]. This would cause the soil to remain wet and the air pores to remain filled with water, which would reduce the absorption of sound. It should be noted, however. that plants actively influence evapo-transpiration: the water flow from soil to plant and atmosphere is complicated by interactions between physical and plant-physiological processes. These are strongest at the interface between soil water and roots and phase change from liquid to vapor that occurs within leaves and which is greatly influenced by the stomatal movement [76].

Furthermore, the layer of decaying plant material constitutes a natural mulching material that forms a barrier to water evaporation [104]. The reduction of wind speed, common in closed vegetations, has the same effect [80] on evapo-transpiration in a plant canopy. Vegetations planted in rows however will promote the occurence of "tunnels" of fast moving air below the canopy [104], which will dry out the surface layer. All in all, however, a plant grown surface will lose more vapour to the air than bare ground. This is well illustrated by the measurements of Bartels and Friedrich as cited by Geiger [45]: the percentage of the total annual precipitation that evaporated again, was 26 or 51 % for a bare soil, 58 % for a surface covered with short grass, 78 % for a 3-8 year old pine tree stand and 85 % for a 4-8 year old oak tree stand. This increase in the loss of water is caused by the large total leaf area.

1.2.1 Sound interference above soil

Sound is the physical phenomenon of waves of alternating compressions and rarefactions of air. This can be completely described by either the pressure or the velocity wave equation. The pressure wave equation is written:

$$\frac{\delta^2 p}{\delta x^2} = \frac{1}{c^2}\frac{\delta^2 p}{\delta t^2} \tag{1.1}$$

where c is the speed of sound. For a point source in an infinite medium, the complex solution of this differential equation gives the pressure p_{ff} as a function of position and time:

$$p_{ff} = (A/kr_1)\, e^{i(kr_1-\omega t)} \tag{1.2}$$

where r_1 is the distance from the source, k is the wave number ($k=2\pi f/c$). ω is the angular frequency ($\omega = 2\pi f$). The factor A is an arbitrary constant. The real part of eq. 1.2 describes the measurable sound pressure.
The description of the sound field above a forest floor follows from fig. 1.1. The sound field is formed by the interference of sound coming directly from the source at point A and of the sound reflected by the ground surface. This reflected sound appears to be radiated by an "image source" situated in the ground at B. At the point of reflection the sound is somewhat absorbed and delayed: upon reflection sound loses energy and time. These two influences can be accounted for by the introduction of a complex relative image strength Q. The amplitude of Q describes the energy absorption; its phase, the time delay. With Q the sound interference above a ground surface can be modeled as:

$$p = (A/kr_1)\, e^{i(kr_1-\omega t)} + Q(A/kr_2)\, e^{i(kr_2-\omega t)} \tag{1.3}$$

A more convenient sound field description, independent of the source strength (i.e. of A), is the so-called sound pressure relative to the free field, p_{rff}:

$$p_{rff} = p/p_{ff} = 1 + Q(r_1/r_2)\, e^{ik(r_2-r_1)} \tag{1.4}$$

Finally, the measured sound pressure level relative to the free field is defined as:

$$L_{cr} = lg \{Re(p_{rff})\}^2 \qquad (1.5)$$

In the derivations of eqs 1.1-1.5 and of the following equations describing Q, certain assumptions have been made about the medium of sound propagation and about the reflecting surface. In all the models to be discussed in this thesis, the air is assumed to be without:

- vertical wind or temperature gradients
- turbulence
- atmospheric absorption
- diffracting elements
- scattering objects.

Furthermore, the reflecting surface is assumed to be completely smooth and homogeneous.

The small source-receiver distances and the low frequencies used in the models guaranteed that these conditions were met. Also, the point source directivity is assumed to be 1. but in section 2.1 , eqs 1.1-1.5 will be extended to the case of a non-uniform point source. There it will also be shown how sound absorption by air can be included in the calculations. In section 1.2.3 more sophisticated models will be given in which one or more of these limitations have been overcome.

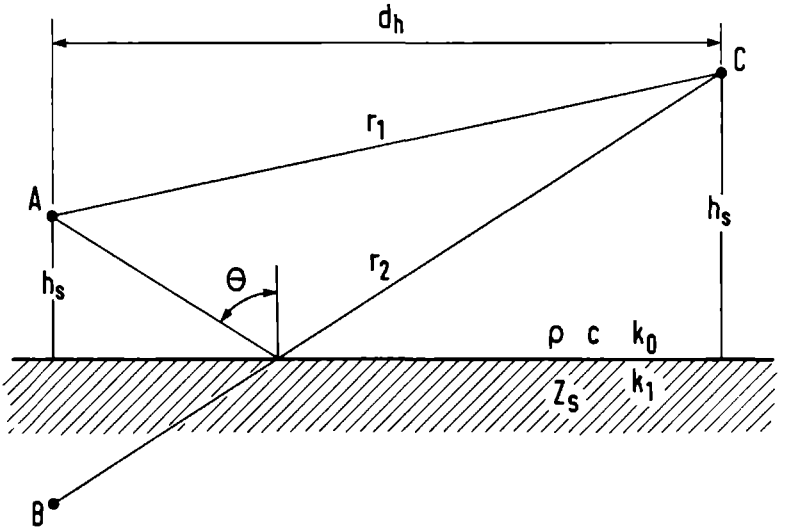

Figure 1.2. Geometrical conditions for the calculation of sound interference above soil. The sound source is located at A, the image source at B and the receiver at C.

1.2.2 Some calculations of the image source strength

The image source strength is a more or less complicated function of the source-receiver distance, the source height, the receiver height, the sound frequency and the specific acoustic impedance of the ground. Many ways exist to calculate Q. See [4, 99] for a review. Four of them will be described here. The purpose of this description is to give an as accurate account as possible of the calculation procedures followed and to show the assumptions and limitations inherent to the different calculations. For the derivations of the equations, the readers are referred to the literature.

1.2.2.1 Plane wave reflection coefficient

The most simple calculation of Q consists of assuming $Q=R_p$, where R_p is the plane wave reflection coefficient [92]:

$$R = \frac{\cos\theta - \rho c/Z_s}{\cos\theta + \rho c/Z_s} \tag{1.6}$$

In this equation the surface is assumed to be locally reacting, i.e. the incident sound has no horizontal components. This equation is only valid for $\theta \ll 90^o$ [99].

1.2.2.2 The Ingard solution

A solution in which the spherical character of the sound waves is taken into account was given by Ingard [58]. His solution also assumes local reaction. In this thesis the computer programme developed by Moerkerken [90] was used. In this approach Q is calculated as follows:

$$Q = 1 - 2r_2 k\beta \int_0^\infty \frac{\exp(-kr_2 t)}{DN}\, dt \qquad (\beta = Z_s/\rho c) \tag{1.7}$$

$$DN = \frac{\{\alpha_1 + \alpha_2 + i(\beta_1 + \beta_2)\}N}{\{(\alpha_1 + \alpha_2)^2 + (\beta_1 + \beta_2)^2\}^{1/2}} \tag{1.8}$$

$$N = \{\alpha_1^2 - \alpha_2^2 + \beta_1^2 - \beta_2^2 + 2i(\alpha_2\beta_1 - \alpha_1\beta_2)\}^{1/2} \tag{1.9}$$

$$\alpha_1 = Re\beta + \gamma_o \qquad ,\gamma_o = \cos\theta \tag{1.10a}$$

$$\beta_1 = Im\beta + \gamma_o t \tag{1.10b}$$

$$\alpha_2 = (1 - \gamma_o^2)^{1/2}\{t(t^2/4 + 1)^{1/2} + t^2/2\}^{1/2} \tag{1.11}$$

$$\beta_2 = -(1 - \gamma_o^2)^{1/2}\{t(t^2/4 + 1)^{1/2} - t^2/2\}^{1/2} \tag{1.12}$$

1.2.2.3 The Brekhovskikh solution

Brekhovskikh [18] used an algebraic approximation of the Ingard integral, resulting in the following Q:

$$Q = R_p + \frac{2i(Z/\rho c)(Z/\rho c + \cos\theta)}{kr_2(\cos\theta(Z/\rho c) + 1)^3} \tag{1.13}$$

R_p is calculated with eq. 1.6. Contrary to the solution of Ingard, this solution is also valid for non-locally reacting surfaces.

1.2.2.4 The Chessel solution

Chessel describes another approximation of the Ingard integral:

$$Q = R_p + F(w)(1 - R_p) \tag{1.14}$$

The factor F(w) can be calculated for small values of w ($|w| \leq 10$) with:

$$F(w) = 1 + i\sqrt{\pi w}\exp(-w) - 2w \times \exp(-w)\left[1 + \frac{w}{1!3} + \frac{w^2}{2!5} + \frac{w^3}{3!7}\ldots\right] \tag{1.15}$$

For $|w| > 10$ the following series is used:

$$F(w) = -\sum_{n=1}^{\infty} \frac{(2n)!}{2^n n!(2w)^n} = -\left[\frac{1}{2w} + \frac{1.3}{(2w)^2} + \frac{1.3.5}{(2w)^3} + \ldots\right] \tag{1.16}$$

The numerical distance w is given by:

$$w = \frac{\frac{1}{2}ik_1 r_2(\cos\theta + \rho c/Z_s)^2}{1 + \cos\theta(\rho c/Z_s)} \tag{1.17}$$

In 1980, a general solution of the sound reflection problem was given by Attenborough et al. [4]. They showed that most of the previously discussed approximations are special cases of their solution.

1.2.3 More sophisticated models

All the models so far discussed have limited value because of the assumptions made in section 1.2.1: no vertical wind or temperature gradients, no turbulence, no atmospheric absorption, no scattering by trees and the reflecting surface is completely smooth and homogeneous. In this section some references will be made to articles in which one or more of these assumptions are deemed unnecessary.

Models in which a vertically layered atmosphere with a vertical wind or temperature gradient is involved are those of de Jong [66, 67] and Tatarskij [117].

De Jong decomposes the incident sound field in its plane wave components with the aid of a discrete double spatial Fourier transform. He used a wave equation, modified to include the influence of any vertical temperature or wind gradient in a stratified medium, to find the derivatives of the sound pressure with respect to the horizontal distance. With the Taylor series he calculated the sound pressures in successive parallel planes. This method includes the effects of ground reflections, impedance discontinuities and screens.

Tatarskij [79] also presented a theory on sound propagation in a stratified atmosphere, but in the absence of a reflecting plane. He used a Fourier transform with respect to time and the horizontal coordinates to reduce his system of equations to two first-order equations for the vertical sound speed and pressure.

The influence of turbulence on the sound field above a forest floor consists of a reduction of the coherence of the direct and the ground reflected sound. Turbulence will therefore result in a flattened interference pattern [26]. Some models are able to include the influence of turbulence on the propagation of sound [22, 26, 27, 28, 116]. Vegetation will cause much turbulence in a stream of wind. Therefore, forests probably absorb less sound through turbulence than open plains do. More research is necessary in this direction.

The influence of sound diffraction by screens is dealt with by Isei et al. [59, 60] and De Jong [67]. The interaction between screen diffraction and ground reflection is sufficiently predictable with these theories. A number of theories also exist on the scattering of sound by trees or tree-like structures [16, 19, 41].

Obviously, forest floors are not smooth. They contain many irregularities in the form of living and dead plant material, holes, bumps and man-made channels. Models exist that take the inequality of the reflecting surface into account. They predict the existance of a surface wave with an amplitude that sometimes can even exceed the amplitude of direct sound [49, 123, 124, 127].

For a review of theories that deal with an inhomogeneous soil surface, i.e. with patches of different impedances, the reader is referred to 5.2.

1.3 Acoustic characterization of outdoor surfaces

As was seen in the previous section, the behaviour of sound above a forest floor is totally determined by only one acoustical parameter of the ground, the specific impedance. In this section those models will be described which can be used to calculate the specific impedance of soil on the basis of other properties of the soil. First, the influence of the layer structure of a soil on the relation between the specific and the characteristic impedance will be given. Then, a semi-empirical description of the characteristic impedance will be given. An excellent review of the acoustics of porous materials can be found elsewhere [6].

1.3.1 Characteristic and specific impedance

The specific or point impedance (Z_s) of a surface is defined as the ratio of speed of the air particles and air pressure just inside that surface. If the material of the reflecting surface is not infinitely thick, Z_s will be influenced by sound returning to the surface, and it will depend on the thickness of the material. For an infinitely extended medium, the ratio of particle speed and pressure is a material constant, the so-called characteristic or wave impedance (Z_c). In case of one layer backed by an infinitely hard background, the following equation applies [136]:

$$Z_s = Z_c \coth(kd) \tag{1.18}$$

with propagation constant k for the material of the layer. From this equation it can be seen that the acoustic description of a layered floor has three components: Z_c, k and d. It is also possible to extend this theory to a multi-layered floor [18].

1.3.2 Specific flow resistance

The most important parameter for the description of the acoustic properties of outdoor surfaces is the specific flow resistance or flow resistivity (R_s). The flow resistivity is defined as the ratio of pressure difference over a sample of unit thickness and the induced normal volume velocity of the gas at the surface of the material [14]. The characteristic acoustical impedance can be calculated from this flow resistivity with the empirical formulas of Delany and Bazley [31]:

$$Z_c/\rho c = 1+9.08(1000f/R_s)^{-0.75}+i11.9(1000f/R_s)^{-0.73} \tag{1.19}$$

$$k=(2\pi f/c)\{1+10.8(1000f/R_s)^{-0.70}+i10.3(1000f/R_s)^{-0.59}\} \tag{1.20}$$

These relationships assume a time dependence $\exp(-i\omega t)$ and use the convention that a positive imaginary part of the impedance means a stiffness-type reactance. Furthermore, the porosity is assumed to be 1.

Recently, a model was developed which not only includes the specific flow resistance in the calculation of Z_c, but also the porosity, the tortuosity and the shape factor [7]. This model appears to give predictions of Z_c superior to empirical formulae that use flow resistivity only. Unfortunately, we had no opportunity to test this model experimentally.

Chapter 2

Measurements of acoustic impedances of soils

2.1 Outdoor measurements with the inclined track method

2.1.1 Introduction

In 1969 Dickinson was the first investigator to measure the specific impedance of a natural ground surface [32]. A good description of the developments in this field of research is given in two review articles [6, 99]. Most impedance measurements have been performed on grass covered surfaces and until now only one investigator has specifically studied forest floors: Talaske from the Pennsylvania State University [115]. In this chapter I hope to present more acoustic data on forest floors, so badly needed, as was already stated in section 1.1.
The technique used by Talaske for measuring the specific acoustic impedances of forest floors was that of the impedance tube. This technique has two obvious disadvantages. Firstly, it is a destructive method: the penetration of the tube in the ground will disrupt the soil structure and therefore result in impedance artefacts. Secondly, forest floors are spatially very inhomogeneous, both in the horizontal and in the vertical plane. With the impedance tube, the impedance of only a very small ($100\ cm^2$) part of the forest floor is measured. To obtain a representative value for Z_s, investigators would need to do many experiments.
In this chapter a description will be given of the so-called inclined track method. It is a free field method, non-destructive and it takes into account a large area of reflection.

2.1.2.1 Acoustic measuring set-up and apparatus

Inclined track. A description of the geometry of the speaker and the microphone array can be found in fig. 2.1 and table 2.1. The distance between two adjacent microphones was chosen in such a way that the path length difference between the direct and the ground reflected wave increases 2 cm per position. This allows for an optimal spatial sampling of the interference pattern with 30 microphone positions. The essence of the inclined track method lies in the fact that the reflected sound reaches all microphones after the same angle of incidence on the floor. This is necessary because it has not yet been proven that the specific impedance is independent of the angle of incidence, i.e. that soils are locally reacting. If all distances could be measured with infinite accuracy, two microphones would suffice to determine the two parameters wanted (the real and imaginary parts of Z_s), but as with all impedance measurements, the accuracy in these distances is not so high. Therefore, a statistical approach is needed and the optimization of the difference between a model and measurements of the interference pattern is such an approach.

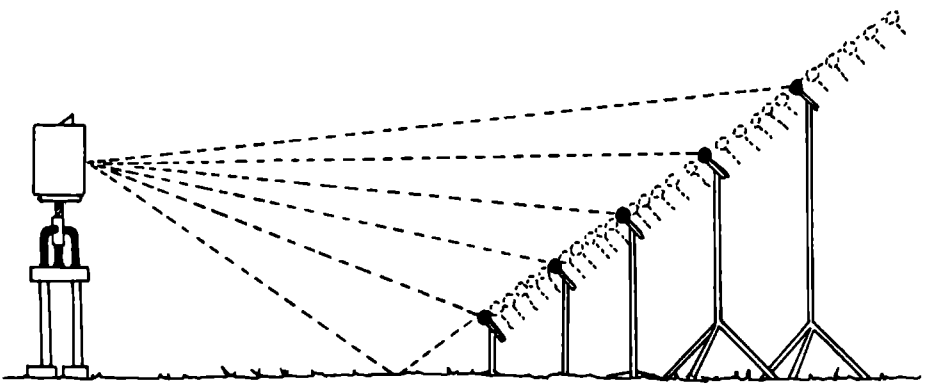

Figure 2.1. The geometry of the inclined track set-up.

Table 2.1 The positions of the microphones on the inclined track. Height of the sound source was 1.83 m.

microphone position	microphone number	horizontal distance	microphone height	$r_2 - r_1$
1	2	6.54	0.56	0.30
7	3	7.45	0.89	0.42
13	4	8.64	1.32	0.54
19	5	10.29	1.93	0.66
25	6	12.78	2.83	0.78
2	2	6.68	0.61	0.32
8	3	7.64	0.96	0.44
14	4	8.87	1.41	0.56
20	5	10.63	2.05	0.68
26	6	13.32	3.03	0.80
3	2	6.82	0.66	0.34
9	3	7.80	1.02	0.46
15	4	9.13	1.50	0.58
21	5	11.01	2.19	0.70
27	6	13.90	3.24	0.82
4	2	6.97	0.72	0.36
10	3	7.99	1.09	0.48
16	4	9.40	1.60	0.60
22	5	11.40	2.33	0.72
28	6	14.56	3.48	0.84
5	2	7.12	0.77	0.38
11	3	8.20	1.16	0.50
17	4	9.67	1.70	0.62
23	5	11.82	2.48	0.74
29	6	15.27	3.74	0.86
6	2	7.28	0.83	0.40
12	3	8.41	1.24	0.52
18	4	9.97	1.81	0.64
24	5	12.28	2.65	0.76
30	6	16.95	4.35	0.90

Description of apparatus The sound was transmitted by a Dynacord D 310 speakerbox with only the woofer switched on. The frequency characteristic of the speaker is shown in table 2.2. The 22 pure tones (200-1600 Hz, see table 2.2) were generated by a Brüel and Kjaer 1023 sine generator. The sound analyzing system comprised five General Radio 1962.9601 1/2-inch microphones with General Radio 1560-p42 preamplifiers. The sound levels were

registrated with a Brüel and Kjaer 2306 level recorder with an accuracy of 1 dB. The measuring system was calibrated before and after each measuring session with a General Radio 1562-A sound level calibrator. The current through the speaker box was monitored during the session to be able to calculate the free field sound pressure level from measurements in an anechoic room and above an asphalt surface. With a sound source on a hard surface, the measured sound field equals the free field plus 6.02 dB. The free field level, used in the computer programme (see table 2.2), was calculated by averaging these measurements according to:

$$L_3 = 20 \lg \{ (10^{L_1/20} + 10^{(L_2 - 6.02)/20})/2 \} \qquad (2.1)$$

with

L_1: the free field sound pressure level measured in the anechoic room;
L_2: the sound pressure level measured above the asphalt floor;
L_3: the free field sound pressure level used for the analysis.

The influence of background noise on the inclined track measurement was reduced by means of the application of a 1/3-octave filter. The influence of this filter on the non-center frequencies was corrected for.

Table 2.2. The free field sound pressure levels of the Dynacord D 310 speaker used in the computer programme.
Distance between speaker and microphone: 10.0 m; heights 1.0 m.

Freq. Hz	Volt. 10^{-4} V	SPL dB	Freq. Hz	Volt. 10^{-4} V	SPL dB
100	0.21	62.6	630	1.1	75.8
125	0.6	65.1	700	1.1	75.8
160	0.9	68.2	800	1.1	75.5
200	1.08	69.4	900	1.1	74.5
250	1.07	71.3	1000	1.0	74.0
300	1.1	72.7	1100	0.9	76.7
315	1.18	72.3	1200	1.07	75.6
350	1.21	72.2	1250	0.9	74.3
400	1.2	72.9	1300	0.9	73.5
450	1.3	74.2	1400	0.8	75.0
500	1.3	74.1	1500	0.9	77.1
550	1.2	74.5	1600	0.9	77.9
600	1.13	76.0			

Meteorological measurements. During the inclined track measurements the air temperature was measured with a mercury thermometer and the air humidity with a ventilated wet-dry bulb Assmann psychrometer. The measuring times were recorded to enable us to correct for changes in the meteorological situation during the acoustical measurement. The wind speed was measured at 1.5 m above the ground with a cup anemometer, its direction was roughly estimated and expressed in the form of the angle between the wind vector and the direction of the sound. In general, measurements were stopped with wind speeds exceeding 2 m/s.

2.1.2.2 Computer analysis of the acoustic data

General description of the programme.

A FORTRAN IV programme was written to analyse the measurements and to calculate the impedances of the measured floors. The programme was run under an MVS/TSO operating system on an IBM-compatible computer from the computer center of the Catholic University (URC).

A number of steps can be distinguished in the programme. See also figure 2.3.

1. All data are read.
   These include: the measured sound pressure levels and voltages over the source, the positions of the microphones and the speaker the frequencies used, the times of sound pressure level measurements, the air temperatures and humidities and the times at which these were measured.
2. The measured sound pressure levels relative to the free field are calculated from the measured sound pressure levels.
   This is done in two steps. First, the free field levels for all microphone positions and frequencies are calculated; secondly, the measured levels are corrected for departures of the voltages during the inclined track measurements from the voltages during the free field measure ments.
3. The model sound pressure levels relative to the free field are calculated for a certain starting value of the impedance.
   In this calculation, the air temperatures and humidities are used to calculate the sound speeds, wave numbers and attenuation constants for each measuring point. In the case of a measurement with 30 microphones and 22 frequencies this amounts to 660 values. These variables are then used as input for the chosen outdoor sound propagation model (see section 1.2). In this model a correction for the non-spherical character of the Dynacord speaker is applied.
4. The impedance is found.
   This is accomplished by an optimization routine that minimizes the sum of squares of the differences between measured and model sound pressure levels by iterative changes of the input impedance.

Figure 2.3 A schematical representation of the computer programme used to calculate the impedances from the inclined track measurements.

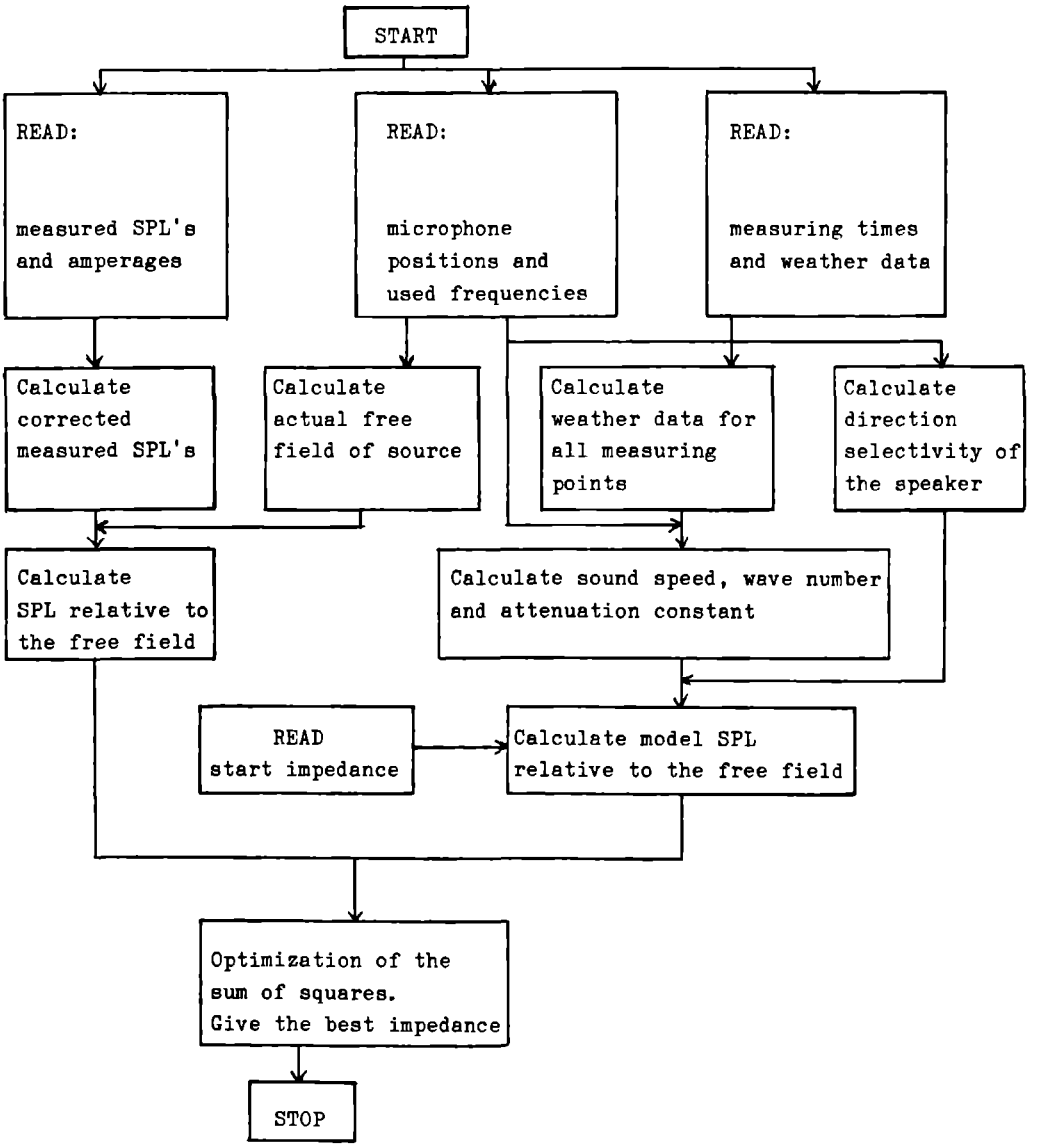

Calculation of the measured sound pressure levels relative to the free field First, the actual free field sound pressure levels during the inclined track measurement are calculated. The equation used was:

$$L_2 = L_1 - 20 \lg \{(r_1/10.0)\times(V_1/V_2)\} - 20 \lg D(\theta) \qquad (2.2)$$

with

L_1 : the free field sound pressure level during the free field measurement (see table 2.2);

L_2 : the actual free field sound pressure level during the inclined track measurement;

V_1 : the voltage across the speaker during the free field measurement;

V_2 : the voltage during the inclined track measurement;

r_1 : the linear distance between source and receiver;

$D(\theta)$: the directivity factor of the speaker;

θ : the angle between the emitted sound ray and the normal of the speaker.

The factor $r_1/10.0$ accounts for the change in sound pressure level caused by the change in distance between source and receiver. The factor V_1/V_2 deals with the fluctuations in source strength caused by drift in the electronic equipment. The factor $D(\theta)$ takes care of the non-spherical character of the speaker (see: calculation of the directivity factor of the Dynacord). Lastly, the measured sound pressure level relative to the free field, L_{mr}, is calculated with:

$$L_{mr} = L_m - L_2 - (r_1/100)a_{tot} \qquad (2.3)$$

with

L_m : the measured sound pressure levels on the inclined track;

a_{tot} : the absorption loss coefficient in dB/100 m.

From eqs. 2.2 and 2.3 it is clear that the measured sound pressure level relative to the free field is corrected for the 1/r-law, the frequency characteristic of the speaker and the absorption of sound by air.

Calculation of sound speed and wave number

The speed of sound in air depends on air humidity, temperature and atmospheric pressure. The speed in m/s of sound in dry air and in moist air was calculated according to Sutherland [113]:

$$c_{dry} = 331.6\times(1 + t/273.15)^{1/2} \qquad (2.4)$$

with t as the air temperature in ^{o}C. Sound speed c in moist air is:

$$c = \left[\frac{c_{dry}^2 \, (1 + 0.239019\ a)}{(1 + a/3) \times (1 - 0.376050\ a)} \right]^{1/2} \tag{2.5a}$$

$$a = \{ b \times RH \times 101.325 / (76 \times p_{amb}) \}^{1/2} \tag{2.5b}$$

$$b = 10^{\{20.5318 - 2939/(t + 273.15) - 4.922\ \lg(t + 273.15)\}} \tag{2.5c}$$

with RH as the relative humidity of the air and p_{amb} as the ambient atmospheric pressure in kPa. The wave number is calculated as $k=2\pi f/c$.

Calculation of the directivity factor of the Dynacord

The sound pressure emitted under an angle θ with the normal axis of the speaker differs considerably from the pressure in front of the speaker, especially for high frequencies. This directivity of the loudspeaker can be modelled as a vibrating membrane mounted on a baffle [98] and described as:

$$D(\theta) = p_\theta / p_0 \tag{2.6}$$

with

$D(\theta)$: the directivity factor;

p_θ : the sound pressure emitted under an angle θ with the normal of the membrane;

p_0 : the sound pressure emitted on the normal (θ=0).

$$D(\theta) = \frac{2J_1(kr_s \sin\theta)}{kr_s \sin\theta} \tag{2.7}$$

$$J_1(x) = \frac{1}{\pi} \int_0^{\pi} \cos(x\sin\theta - \theta)\ d\theta \tag{2.8}$$

with

$J_1(x)$: first order spherical Bessel function;

k : wave number;

r_s : radius of the vibrating membrane.

The sound emitted by the Dynacord speaker in an anechoic room was measured for pure tones between 125 and 2000 Hz for θ = 0, 5, 10, 15, 20, 25 and 30° and an estimation was made of the apparent r_s of the Dynacord by fitting eq. 2.7 to these measurements. With the result, r_s = 0.1334 m, the directivity factor was calculated for eq. 2.2.

Calculation of the absorption loss coefficient

Sound is absorbed in air by classical losses, molecular absorption losses for rotational relaxation of oxygen and nitrogen molecules, and molecular absorption losses for vibrational relaxation of oxygen and nitrogen molecules. We use the theory developed by Sutherland et al. [113], to calculate the absorption loss coefficient from the input parameters pure tone sound frequency, air temperature, humidity and atmospheric pressure. First, the classical plus rotational losses are calculated with:

$$a_{cl} + a_{rot} = 1.6 \times 10^{-8} (T/293.15)^{1/2} f^2 / (p_{amb}/101.325) \qquad (2.9)$$

$$T = t + 273.15$$

with t as the air temperature in ^{o}C, f the sound frequency in Hz, and p_{amb} the ambient atmospheric pressure in kPa. The molecular vibration losses are then calculated for oxygen and nitrogen:

$$a_{vib,o} = 868.6 \mu_{max,o} \frac{f_{m,o}}{c} \frac{(f/f_{m,o})^2}{1 + (f/f_{m,o})^2} \qquad (2.10a)$$

$$a_{vib,n} = 868.6 \mu_{max,n} \frac{f_{m,n}}{c} \frac{(f/f_{m,n})^2}{1 + (f/f_{m,n})^2} \qquad (2.10b)$$

$$c = 343.23 (T/293.15)^{1/2} \qquad (2.10c)$$

with

c : speed of sound;
$\mu_{max,o}$: maximum loss in intensity per wavelength for oxygen;
$\mu_{max,n}$: id. for nitrogen;
$f_{m,o}$: frequency of maximum loss per wavelength for oxygen;
$f_{m,n}$: id. for nitrogen.

These maximum losses are calculated as follows:

$$\mu_{max,o} = 0.20928 \, (4\pi)(C_{i,o}/R)/35 \qquad (2.11a)$$

$$\mu_{max,n} = 0.78084 \, (4\pi)(C_{i,n}/R)/35 \qquad (2.11b)$$

with

$$C_{i,o}/R = (2239.1/T)^{2} e^{-2239.1/T} (1 - e^{-2239.1/T})^{-2} \qquad (2.11c)$$

$$C_{i,n}/R = (3352.0/T)^{2} e^{-3352.0/T} (1 - e^{-3352.0/T})^{-2} \qquad (2.11d)$$

The frequencies at which the maximum losses occur depend on the relative humidity of the air, RH, and are calculated as follows:

$$f_{m,o} = (p_{amb}/101.325)\{ 24 + 44100 \times b \times RH \left[\frac{0.05 + b \times RH}{0.391 + b \times RH}\right] \} \qquad (2.12a)$$

$$f_{m,n} = \frac{p_{amb}/101.325}{(T/293)^{1/2}} \{9 + 350 \times b \times RH\, e^{-6.142[(293/T)^{1/3} - 1]}\} \qquad (2.12b)$$

The factor b is calculated with eq. 2.5c.
The total absorption loss coefficient in dB/100 m , a_{tot}, is finally calculated with:

$$a_{tot} = a_{cl} + a_{rot} + a_{vib,o} + a_{vib,n} \qquad (2.13)$$

The optimization routine

To find the impedance, we used optimization routine E04FCF from the NAG subroutine library [95]. This routine is meant to find an unconstrained minimum of a sum of squares of M nonlinear functions in N variables - in our case M=15 or 30 (the number of measuring points on the inclined track) and N=2 (the real and imaginary parts of the impedance). The routine tries to minimize the sum of squares of the differences between measured and calculated sound fields:

$$F = \sum_{i=1}^{M} [\, L_{mr,i} - L_{cr,i} \,]^2 \qquad (2.14)$$

with

$L_{mr,i}$: the measured sound pressure field relative to the free field;
$L_{cr,i}$: the calculated sound pressure level relative to the free field.

A more detailed description of this corrected Gauss-Newton method can be found elsewhere [46]. The method is designed to ensure that steady progress is made in the optimization, whatever the starting impedance, and to have the rapid ultimate convergence of the method of Newton.

2.1.2.3 Soil physical methods

From each measurement site five 70 cm^3 samples of the upper part of mineral soil just underneath the litter and humus layers were collected and the water, air and solid matter contents and the organic matter content subsequently determined. Furthermore, in some cases the thickness of the organic layer (litter plus humus) was measured as was the total area of the leaves on 1 m^2. The water content of the soil samples was measured by taking the difference in weight before and after drying. For measurements 4-11 the drying took place for 6 hours at 110 °C, for measurements 12-22 for 24 hours at 100 °C. The volume of the solid soil parts was determined by replacing the air in the dried samples by 96 % alcohol. The air content was found by subtracting the volumes of the solid and water from the total sample volume. The organic matter contents of sieved samples was determined with the loss-on-ignition method [129]. Samples of 5 grams were burned for 2.5 hours at a temperature of 550-580 °C. The samples were weighed before and after burning and the difference was equal to the weight of the organic matter. Care was taken that the temperature did not exceed 600 °C as this would cause the carbonate salts to dissociate. Sifting the soil samples (mesh-width 2 mm) before burning resulted in smaller standard errors in the measured organic matter contents.
To determine soil texture, we applied mechanical analysis of the soil samples. First, soil particles > 2 mm (gravel and stones) were removed from the sample by sifting (mesh-width 2 mm). Then, binding substances (humic material, hydroxides and carbonates) were removed by heating with hydrochloric acid and hydrogen peroxide. Particles with dimensions < 2 mm and > 50 µm (the sand fraction), were separated out with a sieve and weighed after drying. Smaller particles were analysed with the precipitation method [106]. The ratio of the different fractions of soil particles was used as the key in separating the soils into textural classes according to the classification of the US Department of Agriculture [17].

2.1.3 Results of the measurements

2.1.3.1 Description of measuring sites

In this section the 23 measuring sites are described. The descriptors used are: measuring date, vegetational type, description of the surface, and meteorological conditions. The measuring sites involve 4 pine-forests, 7 deciduous forests, 5 grass-covered surfaces and 7 barren sandy plains.

Measurement number: 1 Date: 1980-04-17
Location: Botanical Garden, Nijmegen
Vegetational type: Querco-Carpinetum. See also measurement 6.
Description of surface : covered with a 2.2 cm thick layer of leaves. The weight of these leaves was 674.4 g/m^2; the total area of leaves lying on 1 m^2 of forest floor was 10.6 m^2.
Air temperature: 13.6-19.8 °C ; R.H.: 72-34 %
Wind: 0-2 m/s, direction 0°

Measurement number: 2 Date: 1980-07-25
Location: Experimental Garden, Nijmegen
Vegetational type: lawn. Very dense, short grass.
Description of surface: the same soil as in measurements 3, 16 and 17. The grass was regularly mown.
Air temperature: 27.5°C ; R.H.: 45 %
Wind: 0-2 m/s, direction 160°

Measurement number: 3 Date: 1980-07-25
Location: Experimental Garden, Nijmegen
Vegetational type: barren sandy plain. No vegetation present (see also measurements 11,16 and 17).
Description of the surface: A dense, regularly compacted, sandy soil.
Air temperature: 24.0 °C ; R.H.: 60 %
Wind: 1-2 m/s, direction 160°

Measurement number: 4 Date: 1982-08-15
Location: Venray
Description of vegetation: mixed forest with firs (Pinus sylvestris L.), oaks (Quercus sp.) and birches (Betula sp.). The lower undergrowth consisted of about 50 % Calluna vulgaris (L) Hull., 30 % Sphagnum sp., 10 % Molinia caerulea (L) Moench. and 30 % Mnium hornum Hedw.
Description of surface: the organic layer varied between 1 cm of fir needles and 3 cm of oak and birch leaves. At the point where the sound was reflected the moss layer was approximately 8 cm thick.
Air temperature: 26.8°C ; R.H.: 51.2 %
Wind: 0-1 m/s, sky half covered with thin clouds

Measurement number: 5 Date: 1980-09-01
Location: gliding club airport, Malden
Description of vegetation: bare plain without trees or shrubs About 40 % of the overgrowth was Molinia caerula (L.) Moench. and 40 %

Calluna vulgaris (L.) Hull.
Description of surface: bare sandy soil, with some dry leaves of grass.
Air temperature: 18.6°C ; R.H.: 56.8 %
Wind: 0-3 m/s, sky sunny and clear

Measurement number: 6 Date: 1980-09-16
Location: Botanical Garden, Nijmegen
Description of vegetation: mixed forest with oak (Quercus sp.), hornbeam (Carpinus betulus L.) and some fir-trees (Pinus sylvestris L.). The herb layer contained only Glechoma hederacea L., which had a covering of about 30 %.
Description of surface: the thickness of the leaf layer on the ground was 1-3 cm. The weight of 1 m^2 of this layer was 3,388 kg., with a total effective area of 13.5 m^2.
Air temperature: 16.8°C ; R.H.: 82.3 %
Wind: no wind; cloudy sky

Measurement number: 7 Date: 1980-09-18
Location: Botanical Garden, Nijmegen
Description of vegetation: mixed forest with oak (Quercus sp.) and birch (Betula pendula Roth.). Lower trees were mountain-ash (Sorbus aucuparia), maple-tree (Acer pseudoplatanus L.), American bird-cherry (Prunus serotina Ehrh.), mountain elder (Sambucus racemosa L.) and sweet chestnut (Castanea sativa Mill.). There was very little undergrowth, sometimes Solanum dulcamara L. and some clumps of grass.
Description of surface: at the sound reflecting point there was only a 5 cm thick organic layer. This layer contained many beech leaves from the beeches along a nearby alley. 1 m^2 of this leaf layer weighed 6.800 kg and had a total area of 42.3 m^2.
Air temperature: 17.5°C ; R.H.: 69.8 %
Wind: no wind; cloudy sky

Measurement number: 8 Date: 1980-09-23
Location: Venray
Description of vegetation: shifting sand. This was a bare sandy plain with 5 % Festuca tenuifolia Sibth.
Description of surface: see above
Air temperature: 19.8°C ; R.H.: 80.0 %
Wind: 0-1 m/s; sky sunny following mist

Measurement number: 9 Date: 1980-09-25
Location: Graalburcht
Description of vegetation: meadow. There was low vegetation without trees or shrubs with the following plants: Holcus lanatus L., 75 %; Plantago lanceolata L., 10 %; Achillea millefolium L., < 5 %; Taraxacum officinale Dahlst., < 5 %; Lolium perenne L., < 5 % and some papilionaceous flowers , Medicago lupulina L., Vicia hirsuta (L.) S.F.Gray., Trifolium dubium Sibth., Trifolium arvense and Trifolium campestre Schreb., all < 5%.
Description of surface: see above
Air temperature: 16.1°C ; R.H.: 75.4 %
Wind: 0-1 m/s; overcast sky

Measurement number: 10 Date: 1980-10-02
Location: Westermeerwijk, Nijmegen
Description of vegetation: spruce-fir forest. This was a monoculture with only spruce-firs (Picea abies (L.) Karsten).
Description of surface: there was no undergrowth; the soil was covered with a carpet of fir needles and dead twigs. The thickness of the organic layer was about 3-5 cm.
Air temperature: 14.3°C ; R.H.: 67.5 %
Wind: 0-1 m/s; sky half covered with thin clouds

Measurement number: 11 Date: 1980-12-16
Location: Experimental Garden, Nijmegen
Description of vegetation: barren sandy plain without weeds
Description of surface: see above
Air temperature: 6.9°C ; R.H.: 73.0 %
Wind: 0-1 m/s; sky approximately 10 % covered with thin clouds

Measurement number: 12 Date: 1982-04-16
Location: Botanical Garden, Nijmegen
Vegetational type: mixed deciduous forest with oak (Quercus robur), birch (Betula pubescens) and beech (Fagus sylvatica).
Description of the surface: floor covered with a 3-4 cm thick layer of leaves.
Air temperature: 14.0-16.0°C ; R.H.: 38.0-46.0 %
Wind: 0-0.5 m/s, direction 90°; sky lightly overcast

Measurement number: 13 Date: 1982-05-14
Location:Flevo-polder
Vegetational type: Beech-forest. A young monoculture of beech trees, Fagus sylvatica. No undergrowth present.
Description of surface: soil covered with a 4-8 cm thick layer of leaves.
Air temperature: 16.5-20.0°C ; R.H.: 34.5-46.5 %
Wind: 0-2 m/s, direction 90°; slightly overcast

Measurement number: 14 Date: 1982-05-17
Location: Botanical Garden, Nijmegen
Vegetational type: mixed deciduous forest with oak (see also measurement 12).
Description of surface: 100% covered with ivy (Hedera helix). The height was 15-20 cm.
Air temperature: 23.0-24.0°C ; R.H.: 47.0-52.5 %
Wind: 0 m/s; no clouds

Measurement number: 15 Date: 1982-05-21
Location: Venray
Vegetational type: pine-forest with only Pinus sylvestris.
Description of surface: no undergrowth,soil covered with a 6-7 cm thick layer of needles.
Air temperature: 18.0°C ; R.H.: 63.5-72.5 %
Wind: no wind; heavily overcast sky

Measurement number: 16 Date: 1982-06-08
Location: Experimental Garden,Nijmegen
Description of vegetation: barren sandy plain. No vegetation present (see also measurements 3,11 and 17).
Air temperature: 22.0-25.0°C ; R.H.: 54.0-64.0 %
Wind: 1-3 m/s, direction 30°; no clouds

Measurement number: 17 Date: 1982-07-08
Location: Experimental Garden,Nijmegen
Description of vegetation: barren sandy plain. No vegetation present (see also measurements 3,11,16). Description of surface: a dense, regularly compacted sandy soil.
Air temperature: 25.5-26.0°C ; R.H.: 49.0-51.5 %

Measurement number: 18 Date: 1982-07-12
Location: Ooypolder
Description of vegetation: meadow. with Lolium perenne, Plantago lanceolata, Rumex acetosa and Trifolium repens. Grass height 8-10 cm.
Air temperature: 26.0-28.0°C ; R.H.: 52.0-62.0 %
Wind: 0-3 m/s, direction 10°; no clouds

Measurement number: 19 Date: 1982-07-15
Location: Venray
Description of vegetation: sand dunes , without vegetation
Air temperature: 24.0-28.5°C ; R.H.: 45.0-61.0 %
Wind: 0-3 m/s, direction 180°; a slightly overcast sky

Measurement number: 20 Date: 1982-07-21
Location: Venray
Description of vegetation: fir-wood with only Pseudotsuga menziesii
Description of surface: no undergrowth, a 1-2 cm thick layer of needles.
Air temperature 22.0-24.0°C ; R.H.: 60.0-68.0 %
Wind: no wind; sky half-clouded

Measurement number: 21 Date: 1982-07-22
Location: Venray
Description of vegetation: deciduous forest with only elm-trees Ulmus minor.
Description of surface: no undergrowth, a 12-15 cm thick layer of leaves.
Air temperature: 18.0-22.0°C ; R.H.: 57.0-60.0 %
Wind: 0-1 m/s, direction 120°; sky half-clouded

Measurement number: 22 Date: 1982-09-10
Location: Park in Botanical Garden, Nijmegen
Description of vegetation: lawn
Description of surface: only grass with a height of 2-3 cm.
Air temperature: 24.0-27.0°C ; R.H.: 50.0-57.5 %
Wind: 1 m/s, direction 40°; no clouds

Measurement number: 23 Date: 1983-02-03
Location: Wezep
Description of vegetation: barren sandy terrain. No vegetation present.
Description of surface: homogeneous barren sandy terrain.

Air temperature: 1.0-4.0°C ; R.H.: 75.0-89.0 %
Wind: 3-5 m/s, direction 90°; sky heavily clouded

2.1.3.2 Soil-physical results

The results from the soil-physical analysis of the soil samples are represented in table 2.4 (organic matter contents and volume percentages of air, water and solid matter) and table 2.3 (soil texture). The soils show such a large variation in solid matter contents, from 10 to 65 vol. %, that a similar large variation in acoustic floor properties is expected. A comparison of the organic matter contents and the solid matter contents shows absolutely no correlation (correlation coefficient of -0.09). Therefore, the expected relation between organic matter and soil porosity [106] could not be affirmed. Soil porosities can be derived from table 2.4; they equal 100 x (100 % - vol. % solid matter). This means that the porosities ranged from 0.35 to 0.9. The air contents of the soils during the acoustic measurements ranged from 7.3 (meadow, silty clay) to 49.3 vol. % (spruce-fir forest, sandy soil). The low air content of silty clay is caused by the many water-filled micropores, the high air content of sand by the air-filled macropores.

Table 2.3 The classification of soil textures determined by mechanical analysis.

measurement number	fraction 1 50 µm-2 mm (sand) %	fraction 2 2 µm-50 µm (silt) %	fraction 3 < 2 µm (clay) %	classification
12	78.8	14.5	6.9	loamy sand
13	89.4	8.5	2.1	sand
14	76.1	15.7	8.2	loamy sand
15	93.2	4.4	2.4	sand
16	76.6	22.1	1.3	loamy sand
17	76.6	22.1	1.3	loamy sand
18	5.4	54.7	39.9	silty clay
19	97.4	1.8	0.8	sand
20	87.5	12.1	0.4	sand
21	80.1	16.1	3.8	loamy sand
22	73.5	24.1	2.4	sandy loam

Table 2.4 Results of soil physical measurements of the soil samples taken from the 23 measuring sites.

measurement number	organic matter weight %	water content vol %	solid matter vol %	air content vol %
1	.	16.1±1.8	41.0±7.0	43.0±8.0
2	.	14.6±1.0	56.7±4.4	28.7±5.1
3	.	10.0±1.6	52.1±3.0	37.9±1.4
4	5.0	11.7±2.0	48.9±1.9	39.4±3.8
5	14.3	23.0±2.6	44.9±7.9	32.1±10.3
6	9.4	28.4±2.9	42.0±8.6	29.6±8.3
7	8.0	17.3±6.7	36.0±11.4	46.7±9.9
8	1.8	2.6±1.3	54.0±2.3	43.4±2.1
9	6.4	20.6±2.0	51.4±5.3	28.0±3.9
10	7.4	40.0±3.6	10.7±1.3	49.3±2.1
11	4.0	25.8±1.4	48.9±3.1	25.3±3.4
12	5.6	19.9±1.3	55.5±2.1	24.6±3.4
13	6.2	31.0±1.2	54.3±5.0	14.7±4.0
14	10.4	17.7±2.7	64.8±4.0	18.0±3.7
15	3.4	19.9±0.4	49.1±1.6	30.7±0.4
16	.	10.3±0.3	53.3±1.7	36.9±1.8
17a(dry)	.	11.9±0.3	56.6±0.2	31.5±0.1
17b(wet 1)	.	24.8±0.4	56.4±1.0	18.8±0.6
17b(wet 2)	.	21.6±2.2	56.8±0.5	21.6±1.8
18	24.0	49.6±1.4	43.1±1.1	7.3±2.4
19	18.6	11.0±3.2	57.9±0.6	31.1±3.4
20	5.4	12.6±1.4	38.9±0.3	48.5±1.2
21	10.2	18.9±1.3	36.2±0.2	44.9±1.4
22	6.4	8.1±2.5	50.0±2.6	41.9±3.9
23	.	9.3 .	63.8 .	26.9 .

2.1.3.3 Acoustical results

The results of the acoustical measurements and analyses are represented on pp. 40-60. They include examples of the performance of the optimization routine, a comparison of the influence of the choice of the model, the plane wave reflection coefficients of most measurements, the specific impedances of all measurements and the acoustically derived specific flow resistances of some measurements. The plane wave reflection coefficients

are included because they provide an easy answer to the question of how much of the sound energy is absorbed by the ground. The impedances are given because they are the only acoustical soil parameters that are independent of the geometry of the measuring set-up.

Figure 2.3 (pp. 40-42). Typical performance of the optimization routine demonstrated for 11 pure tone frequencies of measurement 5 (barren plain). The crosses represent the sound pressure levels relative to the free field measured at the 30 microphone positions on the inclined track.

Tables 2.5-2.7 (pp. 43-45). The influence of the choice of the outdoor sound model on the specific impedances found for measurements 1-3.

Figures 2.4-2.25 (pp. 46-51). The measured plane wave reflection coefficients of the outdoor surfaces of measurements 5, 6 and 12-22 as a function of frequency (200-1600 Hz).

Figures 2.26-2.54 (pp. 52-59). The measured normalised specific impedances of the outdoor surfaces of measurements 1-23 as a function of frequency (200-1600 Hz).

Table 2.8 (p. 60). Acoustically derived specific flow resistances of the outdoor surfaces of some measurements.

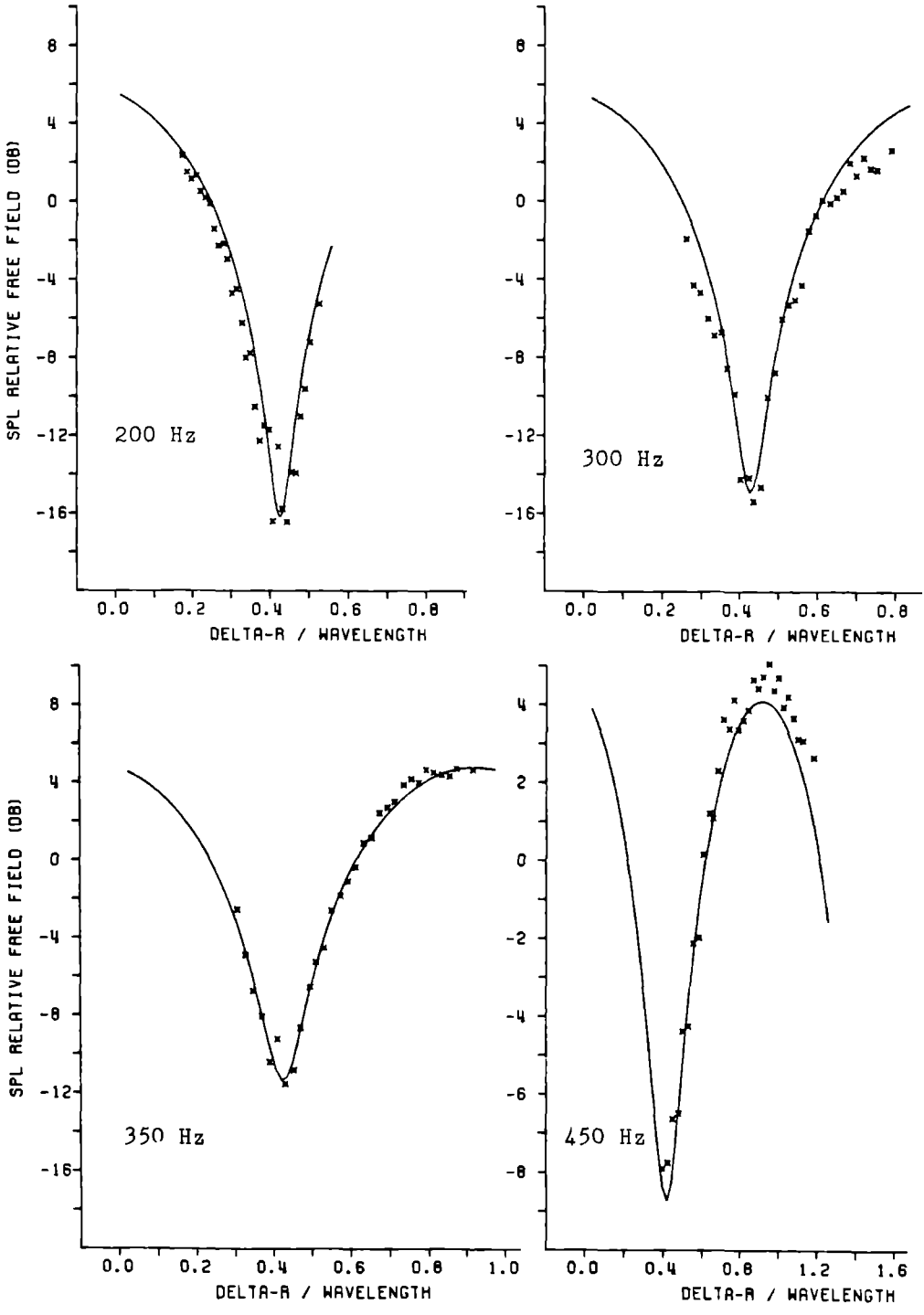
SPL RELATIVE FREE FIELD (DB)
200 Hz
DELTA-R / WAVELENGTH
300 Hz
DELTA-R / WAVELENGTH
350 Hz
DELTA-R / WAVELENGTH
450 Hz
DELTA-R / WAVELENGTH

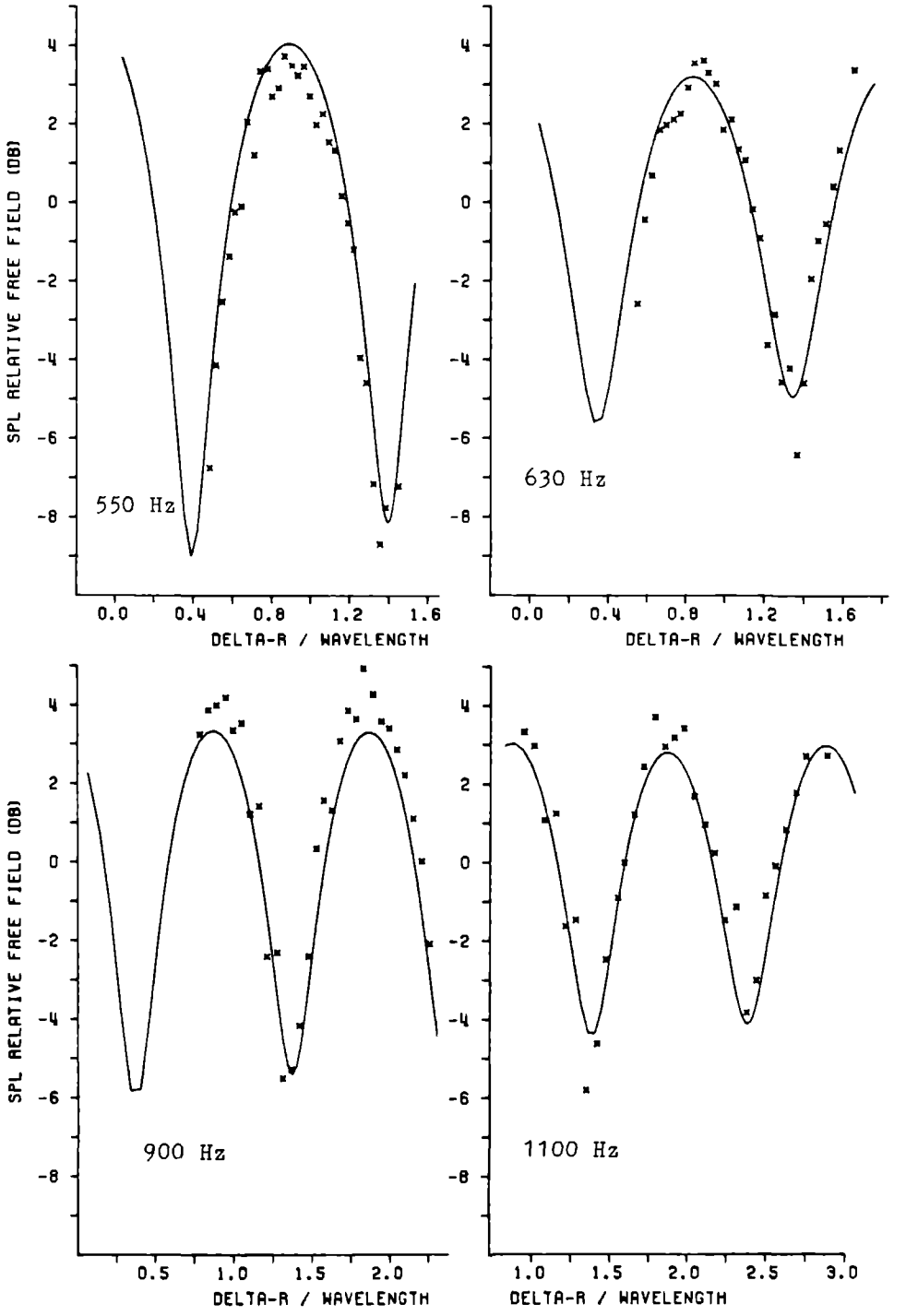
SPL RELATIVE FREE FIELD (DB)
550 Hz
630 Hz
900 Hz
1100 Hz
DELTA-R / WAVELENGTH

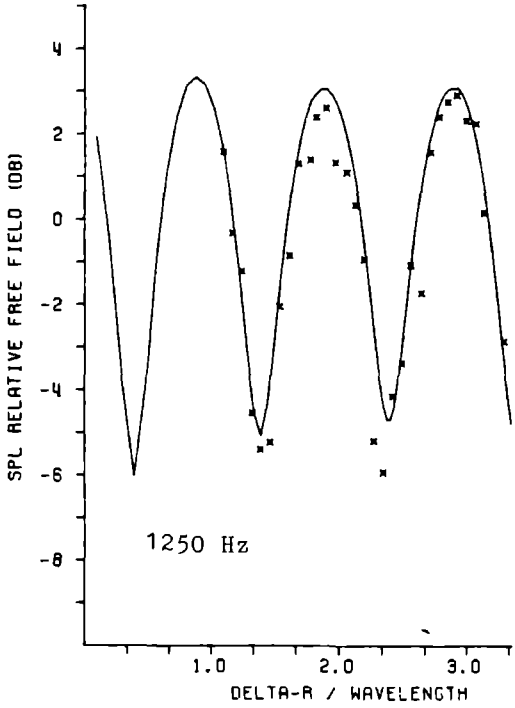
SPL RELATIVE FREE FIELD (DB)
4
2
0
-2
-4
-6
-8
1250 Hz
1.0
2.0
3.0
DELTA-R / WAVELENGTH

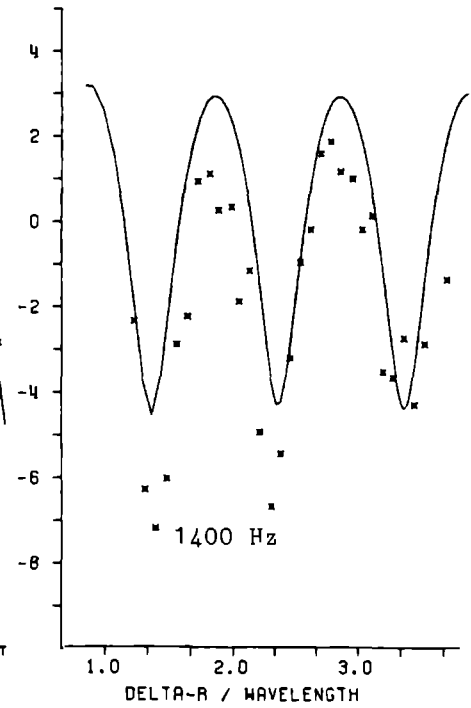
4
2
0
-2
-4
-6
-8
1400 Hz
1.0
2.0
3.0
DELTA-R / WAVELENGTH

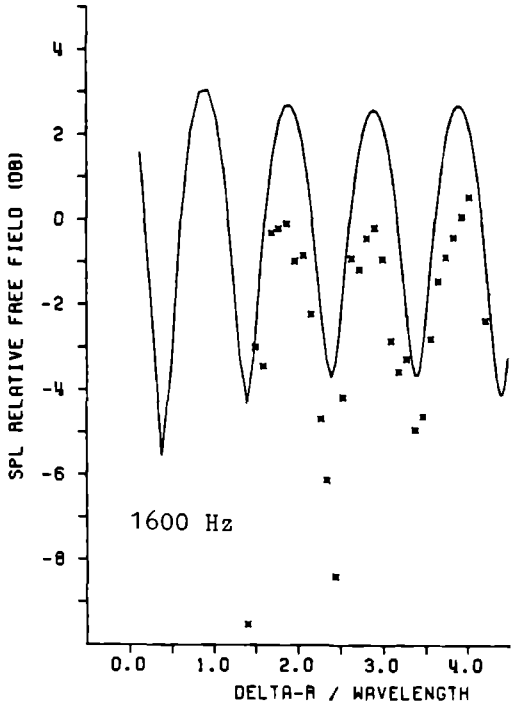
SPL RELATIVE FREE FIELD (DB)
4
2
0
-2
-4
-6
-8
1600 Hz
0.0
1.0
2.0
3.0
4.0
DELTA-R / WAVELENGTH

Table 2.5 A comparison of the specific impedances of measurement 1 (Querco Carpinetum forest floor) found by using five models. ΔL^2_{av} is the averaged square difference between model and measured sound pressure levels, per microphone.

Freq.	Plane waves			Ingard			Brekhovskikh			Thomasson			Ingard-Chessel		
	Re	Im	ΔL^2_{av}	Re	Im	ΔL^2_{av}	Re	Im	ΔL^2_{av}	Re	Im	ΔL^2_{av}	Re	Im	ΔL^2_{av}
200	1.70	4.12	1.28	2.46	3.73	1.27	2.51	4.01	1.18	2.44	3.77	1.26	2.43	3.72	1.27
250	1.57	3.99	8.83	2.21	3.63	8.31	2.21	3.90	7.86	2.19	3.66	8.29	2.19	3.62	8.36
300	2.01	3.10	2.87	2.42	2.83	2.49	2.45	2.95	2.64	2.41	2.86	2.56	2.41	2.82	2.51
315	2.03	2.35	0.78	2.32	2.12	0.75	2.33	2.18	0.74	2.31	2.15	0.75	2.32	2.12	0.75
350	1.91	1.53	7.14	2.09	1.39	6.89	2.09	1.40	6.94	2.08	1.41	6.92	2.09	1.38	6.88
400	2.13	1.68	0.96	2.28	1.51	1.02	2.28	1.54	1.00	2.27	1.53	1.01	2.27	1.51	1.02
450	2.18	1.54	3.28	2.27	1.40	3.38	2.27	1.42	3.35	2.26	1.42	3.37	2.26	1.40	3.38
500	1.62	1.32	1.44	1.69	1.26	1.52	1.69	1.27	1.51	1.68	1.27	1.51	1.68	1.26	1.52
550	1.70	1.40	3.93	1.77	1.34	3.98	1.76	1.35	3.97	1.76	1.35	3.97	1.76	1.34	3.98
600	2.12	1.44	6.28	2.19	1.36	6.35	2.19	1.36	6.34	2.18	1.37	6.34	2.18	1.36	6.35
630	1.78	0.69	6.91	1.82	0.63	6.89	1.81	0.63	6.89	1.81	0.64	6.89	1.81	0.63	6.89
700	1.57	0.73	17.21	1.60	0.70	17.70	1.60	0.70	17.17	1.59	0.71	17.17	1.59	0.69	17.17
800	2.09	0.61	1.84	2.12	0.56	1.82	2.11	0.56	1.82	2.11	0.57	1.82	2.11	0.56	1.82
900	1.72	0.28	5.30	1.74	0.25	5.30	1.73	0.24	5.30	1.73	0.25	5.30	1.73	0.24	5.10
1000	2.74	-0.39	1.37	2.73	-0.40	1.38	2.72	-0.45	1.38	2.72	-0.45	1.38	2.72	-0.45	1.38
1100	2.23	-0.57	4.86	2.22	-0.62	4.88	2.21	-0.62	4.88	2.21	-0.61	4.88	2.21	-0.62	4.88
1200	2.24	-0.21	2.28	2.24	-0.26	2.28	2.23	-0.26	2.28	2.23	-0.25	2.28	2.23	-0.26	2.28
1250	3.40	0.39	4.09	3.42	0.31	4.08	3.41	0.31	4.08	3.41	0.32	4.08	3.41	0.31	4.08
1300	2.77	-1.05	4.96	2.76	-1.10	4.96	2.74	-1.10	4.96	2.74	-1.09	4.96	2.74	-1.10	4.96
1400	3.28	-0.43	6.06	3.28	-0.49	6.04	3.26	-0.49	6.04	3.26	-0.48	6.04	3.26	-0.49	6.04
1500	3.16	-0.47	1.66	3.16	-0.53	1.66	3.15	-0.53	1.66	3.15	-0.52	1.66	3.15	-0.52	1.66
1600	4.18	0.09	1.05	4.19	0.01	1.06	4.18	0.01	1.06	4.18	-0.02	1.06	4.18	-0.01	1.06
Averaged over all frequencies			4.29			4.25			4.22			4.25			4.24

Table 2.6 A comparison of the specific impedances of measurement 2 (lawn, experimental garden) found by using five models. ΔL^2_{av} is the averaged square difference between model and measured sound pressure levels, per microphone.

Freq.	Plane waves			Ingard			Brekhovskikh			Thomasson			Ingard-Chessel		
	Re	Im	ΔL^2_{av}	Re	Im	ΔL^2_{av}	Re	Im	ΔL^2_{av}	Re	Im	ΔL^2_{av}	Re	Im	ΔL^2_{av}
200	12.09	5.53	0.53	12.56	3.62	0.53	13.33	3.43	0.56	12.52	3.68	0.53	12.50	3.62	0.53
250	18.40	9.60	5.79	18.92	6.36	5.67	19.69	6.40	5.44	18.87	6.46	5.67	18.86	6.35	5.67
300	14.14	18.42	5.39	16.15	15.48	5.30	17.02	16.08	5.17	16.07	15.54	5.30	16.09	15.44	5.30
315	16.79	12.69	0.95	17.77	9.97	0.90	18.67	10.21	0.85	17.71	10.04	0.90	17.71	9.95	0.90
350	12.18	11.08	0.64	13.25	9.24	0.67	13.87	9.49	0.69	13.19	9.29	0.67	13.20	9.22	0.67
400	9.48	9.56	0.71	10.46	8.23	0.77	10.83	8.45	0.77	10.41	8.27	0.77	10.41	8.21	0.77
500	7.62	8.49	1.34	8.45	7.51	1.38	8.54	7.72	1.34	8.40	7.54	1.38	8.42	7.49	1.38
550	11.00	7.10	0.96	11.39	6.23	0.98	11.50	6.35	0.97	11.36	6.25	0.98	11.36	6.21	0.98
600	10.62	6.21	2.15	11.05	5.62	2.21	11.14	5.63	2.24	11.02	5.64	2.21	11.03	5.61	2.21
630	9.62	6.44	1.12	10.04	6.12	1.14	10.09	6.13	1.14	10.00	6.12	1.14	10.02	6.09	1.14
700	8.02	2.38	0.79	8.14	1.97	0.81	8.16	1.98	0.81	8.12	1.99	0.81	8.12	1.96	0.81
800	8.60	4.80	0.76	8.85	4.39	0.76	8.87	4.40	0.76	8.82	4.40	0.76	8.83	4.37	0.76
900	9.06	7.55	1.73	9.41	7.12	1.74	9.63	7.15	1.73	9.38	7.13	1.74	9.40	7.10	1.74
1000	12.61	8.58	1.67	12.89	8.11	1.63	12.92	8.14	1.63	12.85	8.11	1.63	12.80	8.08	1.63
1100	10.01	9.41	2.32	10.38	9.05	2.31	10.38	9.07	2.30	10.34	9.05	2.31	10.36	9.02	2.31
1200	9.84	7.25	2.28	10.10	6.93	2.26	10.11	6.94	2.27	10.07	6.99	2.26	10.08	6.91	2.26
1250	5.94	9.30	2.66	6.30	9.11	2.70	6.29	9.13	2.67	6.27	9.11	2.70	6.29	9.09	2.67
1300	3.93	8.96	1.93	4.28	8.88	1.97	4.27	8.89	1.97	4.26	8.87	1.97	4.28	8.86	1.97
1400	3.15	8.47	3.17	3.41	8.41	3.14	3.40	8.42	3.14	3.39	8.40	3.14	3.40	8.40	3.14
1500	4.37	6.59	1.92	4.55	6.52	1.90	4.57	6.52	1.91	4.56	6.51	1.91	4.57	6.51	1.90
1600	5.40	6.53	1.65	5.62	6.42	.	5.61	6.41	1.66	5.60	6.41	1.66	5.61	6.40	.
Averaged over all frequencies			1.93			1.94			1.91			1.92			1.94

Table 2.7 A comparison of the specific impedances of measurement 3 (barren sandy plain, experimental garden) found by using five models. ΔL^2_{av} is the averaged square difference between model and measured sound pressure levels, per microphone.

Freq.	Plane waves			Ingard			Brekhovskikh			Thomasson			Ingard-Chessel		
	Re	Im	ΔL^2_{av}	Re	Im	ΔL^2_{av}	Re	Im	ΔL^2_{av}	Re	Im	ΔL^2_{av}	Re	Im	ΔL^2_{av}
200	32.14	11.60	0.64	32.63	6.62	0.64	31.45	5.99	0.60	32.56	6.76	0.64	32.52	6.62	0.64
250	43.21	28.84	3.40	45.42	21.01	3.40	47.55	21.03	3.31	45.28	21.19	3.40	45.28	20.97	3.40
300	18.15	21.94	1.72	20.40	18.40	1.69	21.60	19.03	1.63	20.31	18.48	1.69	20.33	18.35	1.69
315	17.21	28.20	0.98	20.27	24.71	0.98	21.70	25.71	0.98	20.15	24.77	0.98	20.19	24.64	0.98
350	11.91	21.22	0.95	14.29	18.92	0.96	15.19	19.67	0.96	14.21	18.96	0.96	14.24	18.87	0.96
400	7.64	15.17	1.35	9.39	13.87	1.43	9.85	14.38	1.45	9.33	13.90	1.43	9.35	13.83	1.43
450	10.94	16.31	1.01	12.63	14.69	1.05	13.15	15.11	1.04	12.56	14.72	1.04	12.59	14.65	1.04
500	14.60	12.01	1.82	15.65	10.10	1.84	16.02	10.29	1.81	15.59	10.15	1.84	15.60	10.08	1.84
550	15.92	6.20	2.19	16.16	5.10	2.11	16.55	5.12	2.14	16.13	5.13	2.12	16.11	5.08	2.11
600	18.13	8.78	2.97	18.76	7.75	3.00	19.05	7.75	3.02	18.70	7.77	3.00	18.71	7.72	3.00
630	13.89	7.15	2.00	14.31	6.32	2.00	14.40	6.33	2.00	14.26	6.34	2.00	14.27	6.29	2.00
700	12.98	8.96	1.87	13.48	8.24	1.89	13.54	8.27	1.89	13.43	8.25	1.89	13.45	8.21	1.89
800	17.88	17.05	2.34	18.78	16.06	2.35	18.87	16.13	2.35	18.72	16.06	2.35	18.76	5.99	2.35
900	7.34	11.39	4.08	7.89	10.93	4.05	7.88	11.00	4.04	7.85	10.93	4.05	7.88	10.90	4.05
1000	12.05	9.70	4.26	12.39	9.23	4.23	12.42	9.27	4.22	12.35	9.23	4.23	12.37	9.20	4.22
1100	12.29	3.25	5.32	12.40	2.86	5.29	12.41	2.86	5.29	12.37	2.87	5.29	12.37	2.85	5.28
1200	17.08	6.77	5.97	17.32	6.06	5.96	17.34	6.06	5.96	17.28	6.07	5.96	17.28	6.03	5.96
1250	19.65	25.51	1.97	20.70	24.62	1.97	20.73	24.67	1.97	20.63	24.59	1.97	20.68	24.53	1.97
1300	5.22	15.12	7.72	5.87	15.03	7.76	5.86	15.03	7.76	5.84	15.01	7.75	5.87	15.00	7.76
1400	15.04	7.31	8.46	1.74	7.34	8.39	1.72	7.34	8.40	1.72	7.33	8.39	17.31	7.33	8.39
1500	5.89	9.24	6.93	6.17	9.07	6.92	6.15	9.08	6.91	6.14	9.06	6.92	6.15	9.05	6.92
1600	2.63	6.52	10.29	2.85	6.48	10.29	2.83	6.48	10.28	2.83	6.47	10.29	2.84	6.47	10.29
Averaged over all frequencies			3.56			3.56			3.55			3.56			3.55

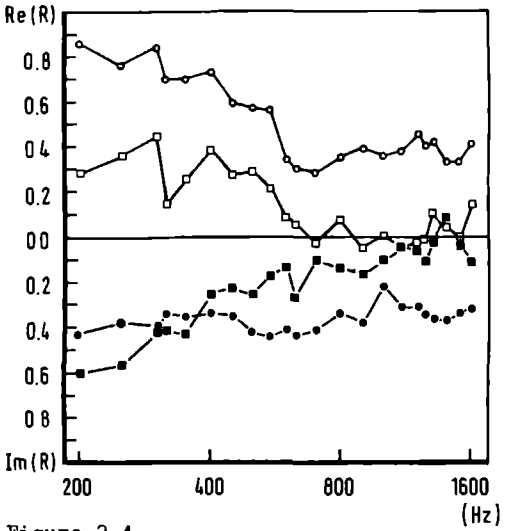

Figure 2.4
Measurements 5 and 6
Bare plain (circles)
Mixed deciduous forest (squares)

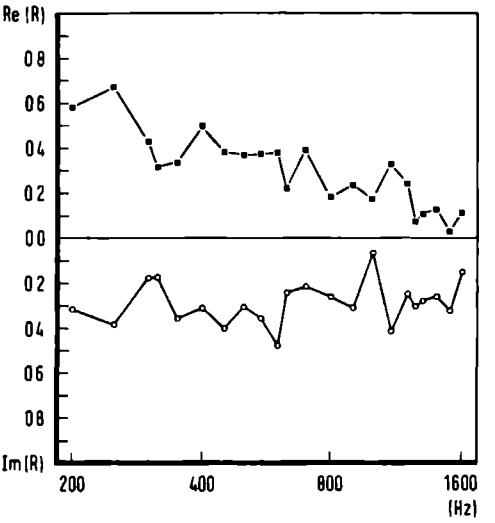

Figure 2.5
Measurement 12
Mixed deciduous forest

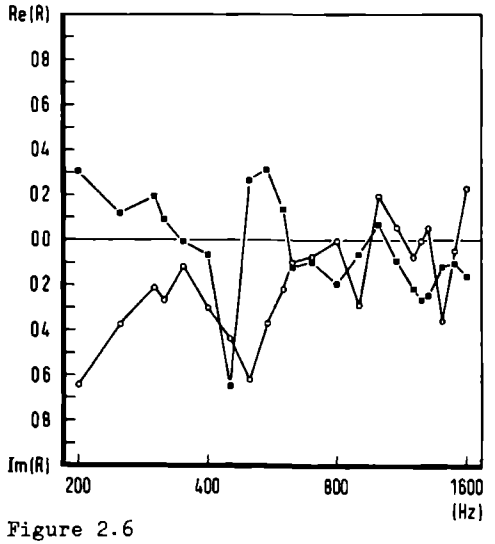

Figure 2.6
Measurement 13a
Beech-forest, with litter layer

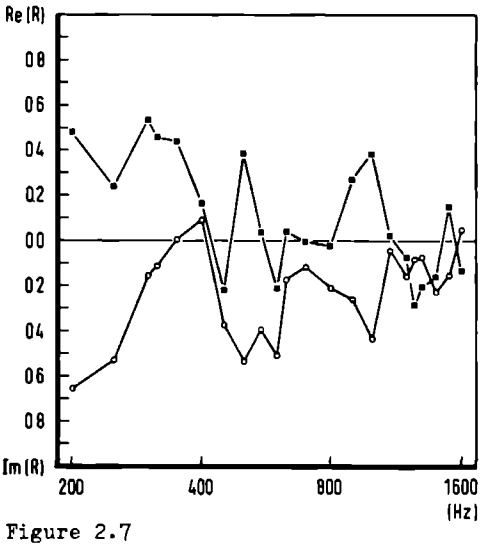

Figure 2.7
Measurement 13b
Beech-forest, without litter layer

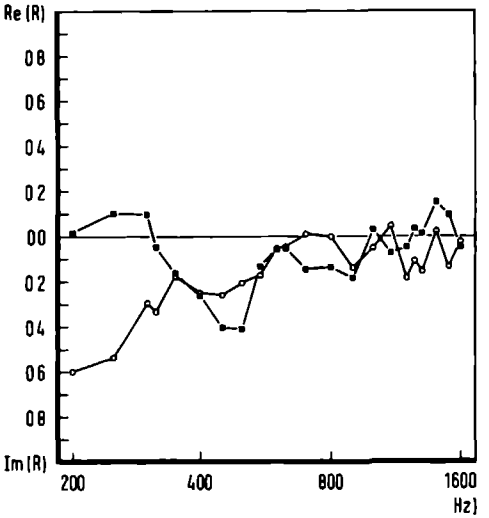

Figure 2.8
Measurement 14
Mixed deciduous forest

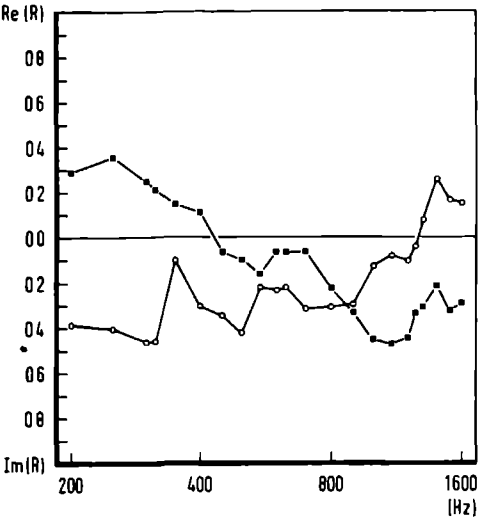

Figure 2.9
Measurement 15a
Pine-forest with litter layer

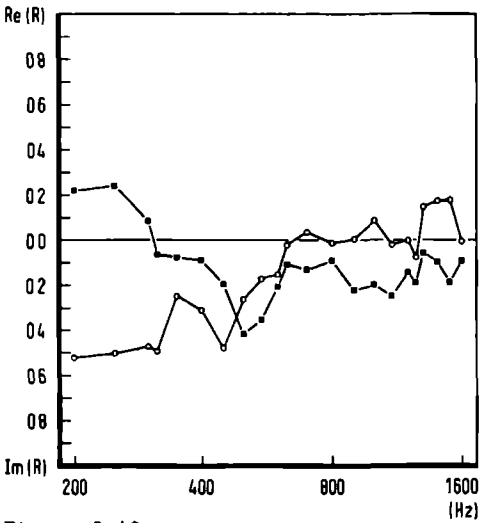

Figure 2.10
Measurement 15b
Pine-forest without litter layer

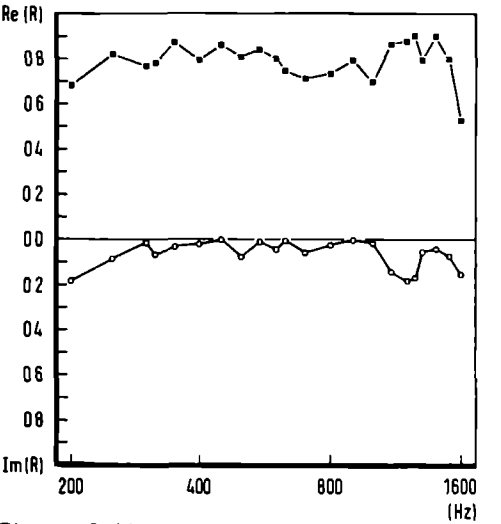

Figure 2.11
Measurement 16a
Barren field, normal angle

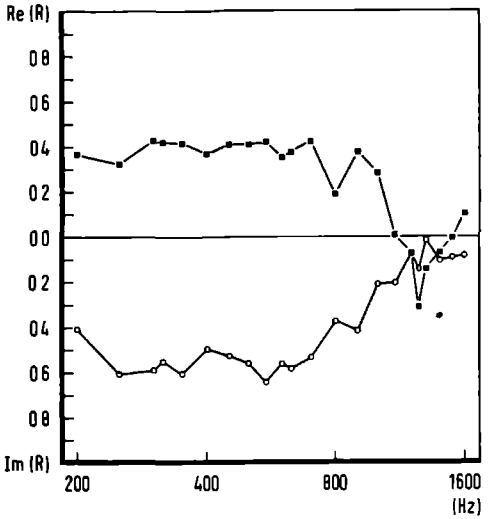

Figure 2.12
Measurement 16b
Barren field, deviating angle

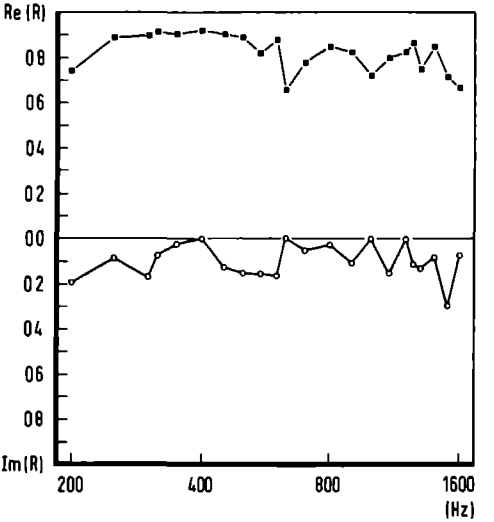

Figure 2.13
Measurement 17a
Barren field. dry

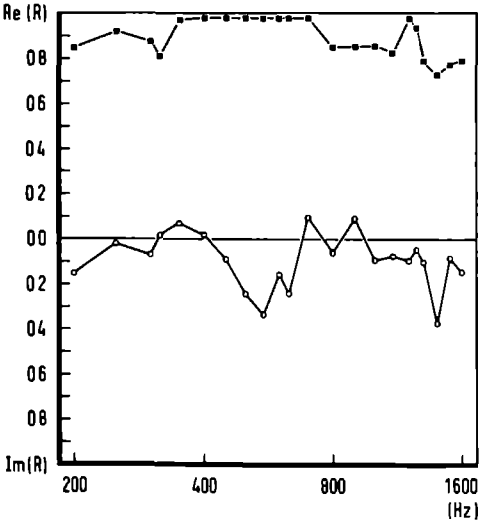

Figure 2.14
Measurement 17b
Barren field, wet 1

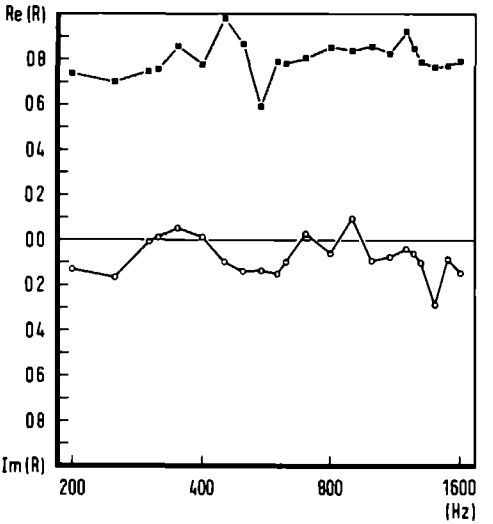

Figure 2.15
Measurement 17c
Barren field, wet 2

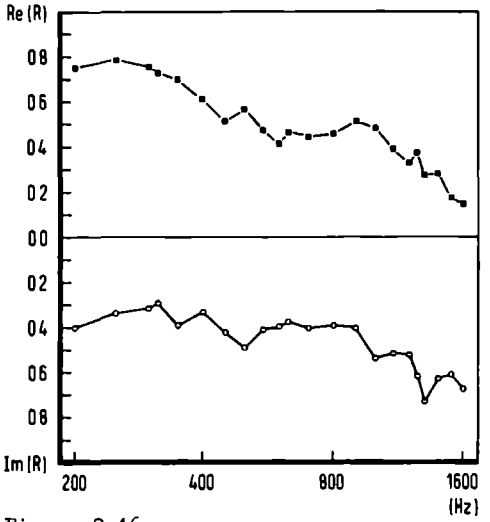

Figure 2.16
Measurement 18
Meadow, 30 microphones

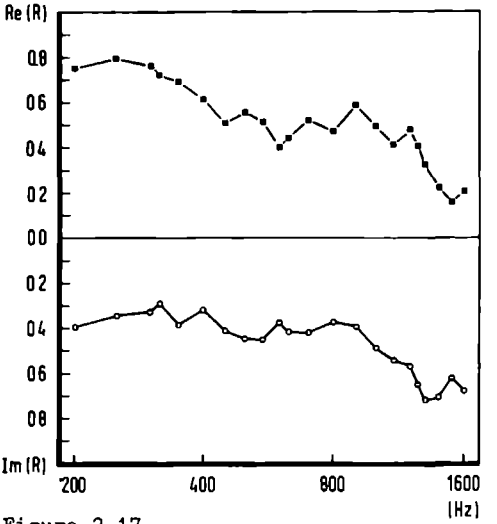

Figure 2.17
Measurement 18
Meadow, 15 microphones

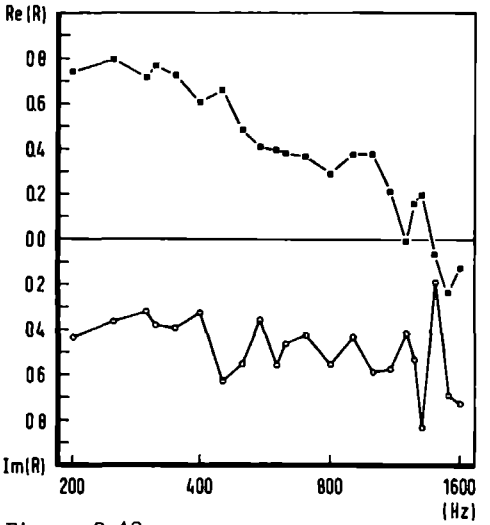

Figure 2.18
Measurement 18
Meadow, 5 microphones

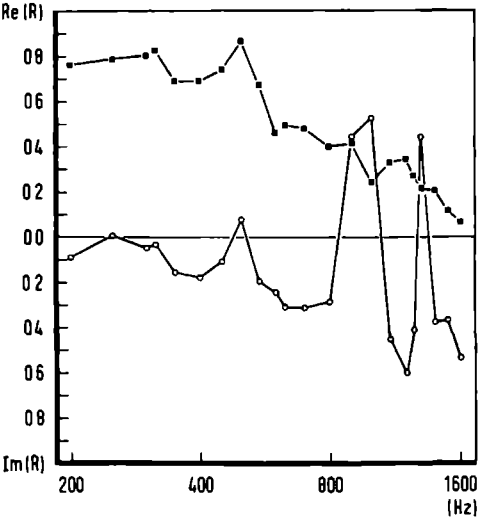

Figure 2.19
Measurement 19
Sand dunes

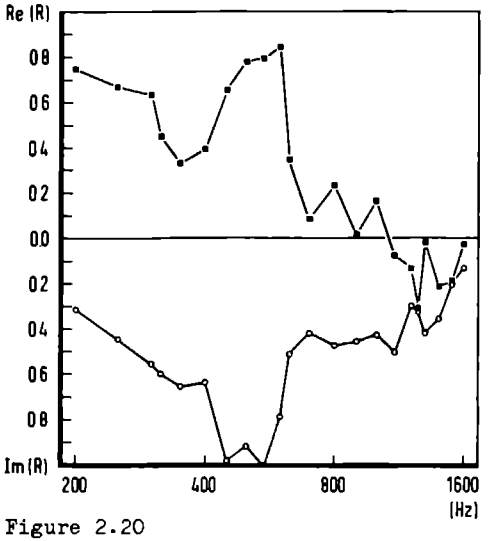

Figure 2.20
Measurement 20a
Fir-wood with needle layer

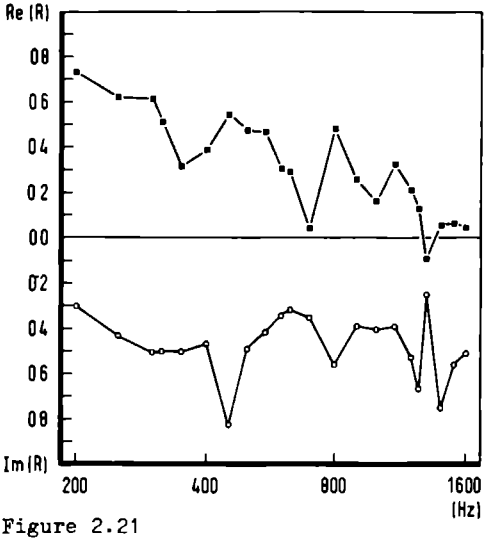

Figure 2.21
Measurement 20b
Fir-wood without needle layer

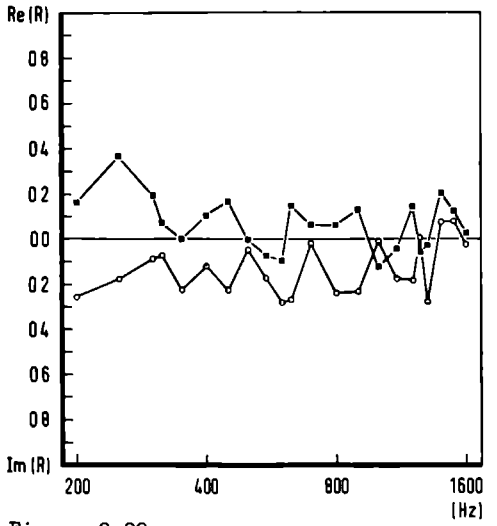

Figure 2.22
Measurement 21a
Deciduous forest with layer of leaves

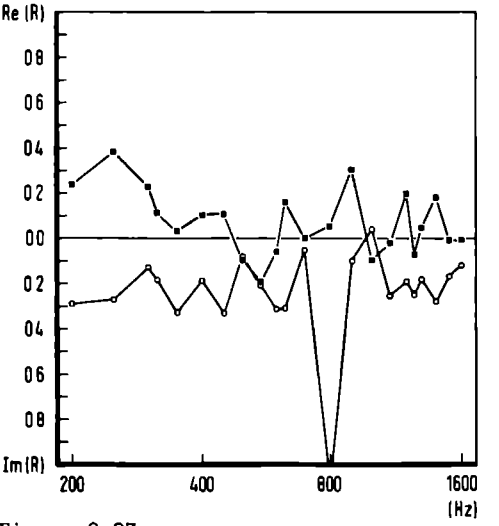

Figure 2.23
Measurement 21b
Deciduous forest without this layer

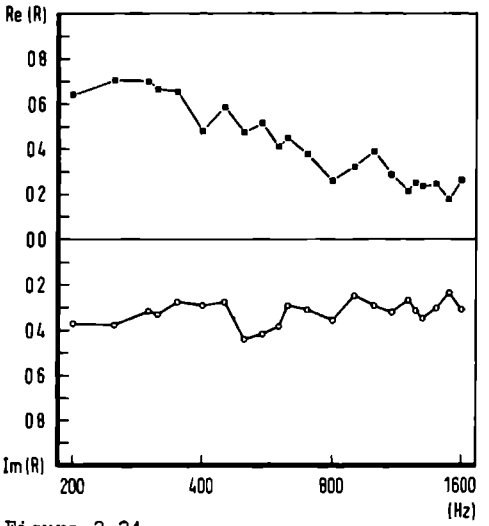

Figure 2.24
Measurement 22a
Lawn, normal angle

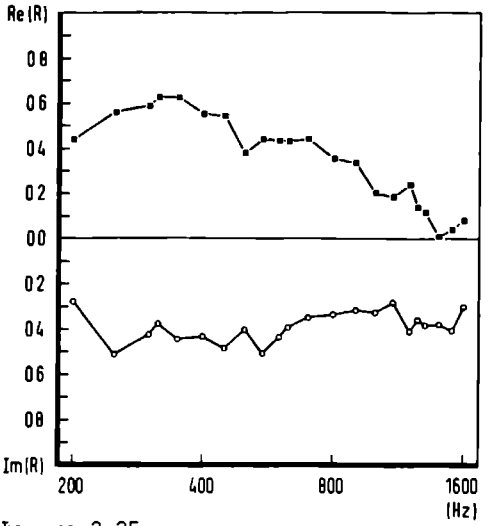

Figure 2.25
Measurement 22b
Lawn, deviating angle

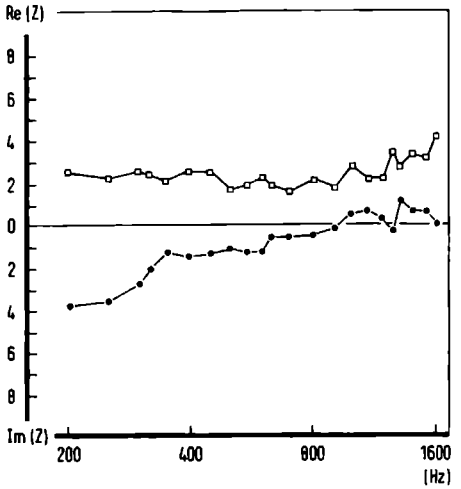

Figure 2.26
Measurement 1
Querco-Carpinetum

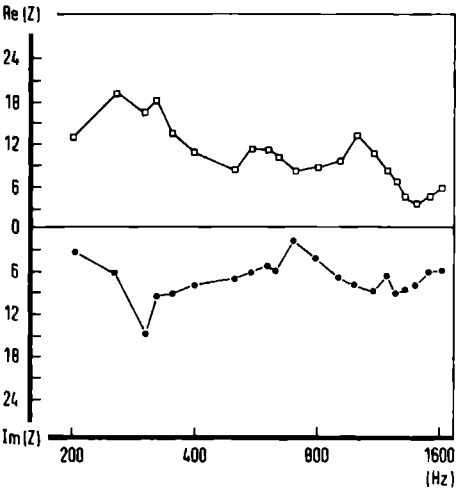

Figure 2.27
Measurement 2
Lawn

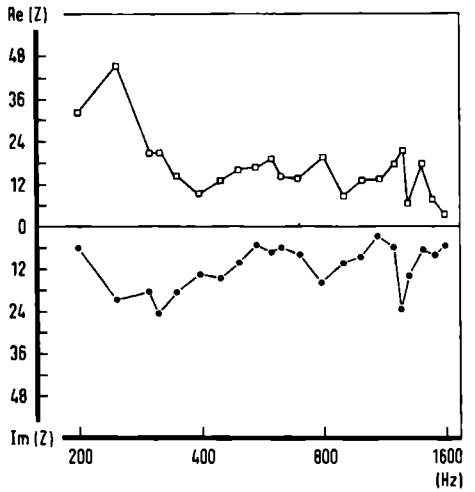

Figure 2.28
Measurement 3
Barren sandy plain

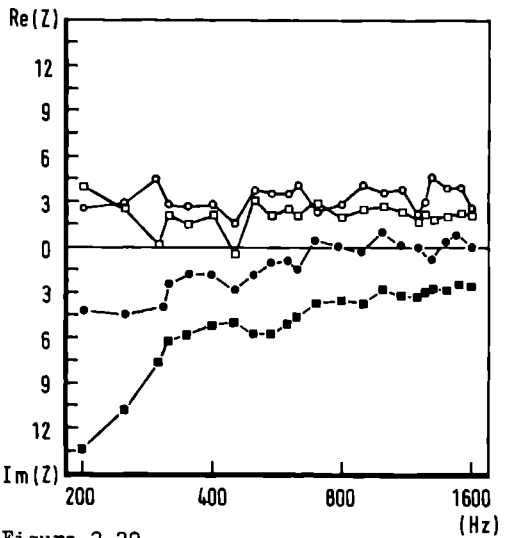

Figure 2.29
Measurements 4 and 5
Mixed forest (circles)
Bare plain (squares)

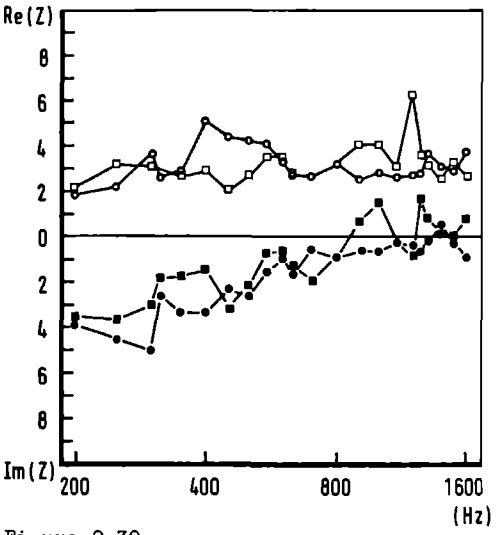

Figure 2.30
Measurements 6 and 7
Mixed forest (circles)
Mixed forest (squares)

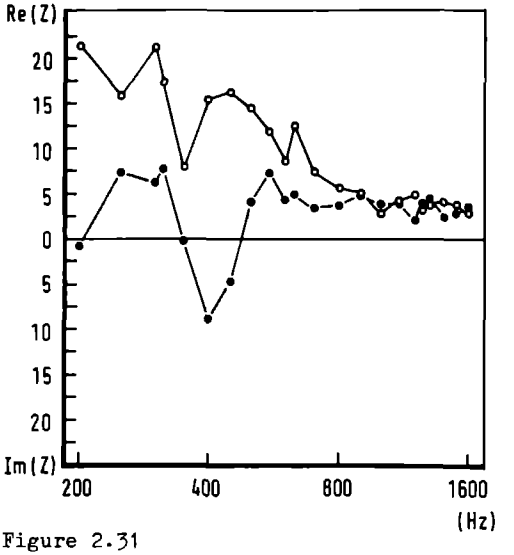

Figure 2.31
Measurement 8
Shifting sand

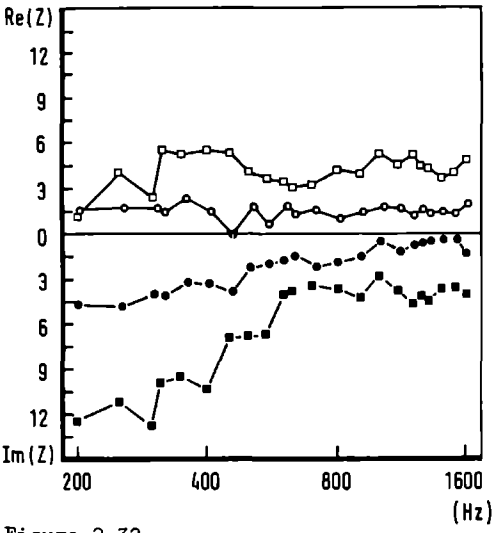

Figure 2.32
Measurements 9 and 10
Meadow (squares)
Spruce fir forest (circles)

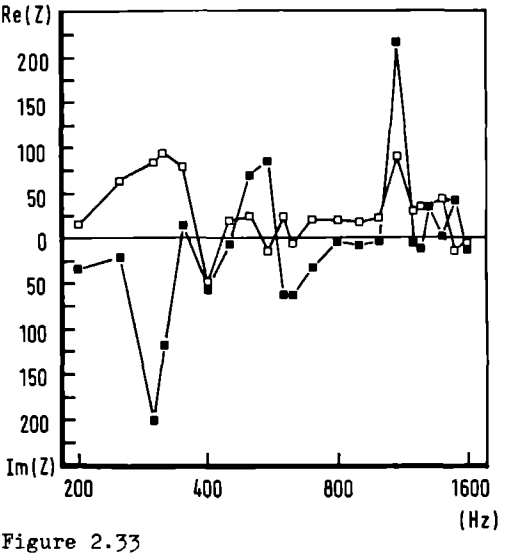

Figure 2.33
Measurement 11
Barren sandy plain

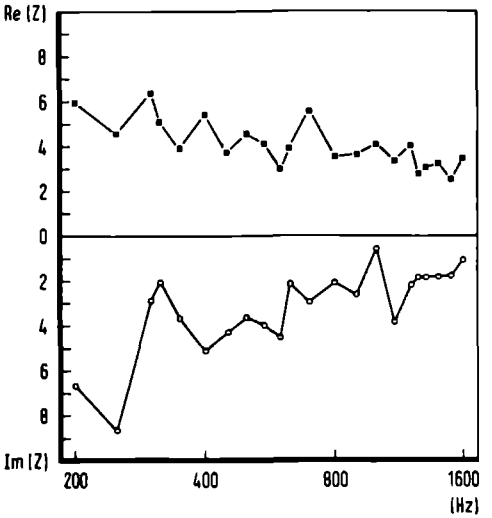

Figure 2.34
Measurement 12
Mixed deciduous forest

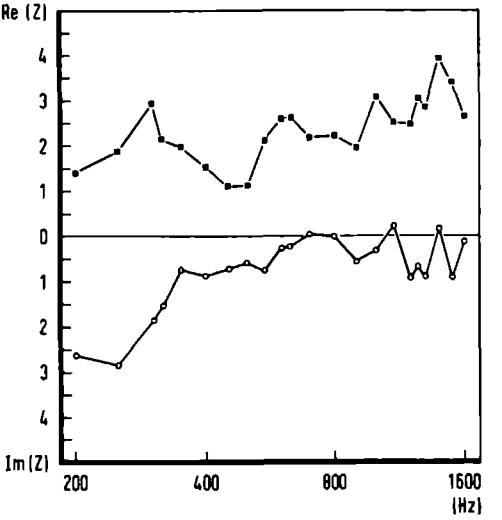

Figure 2.35
Measurement 14
Mixed deciduous forest

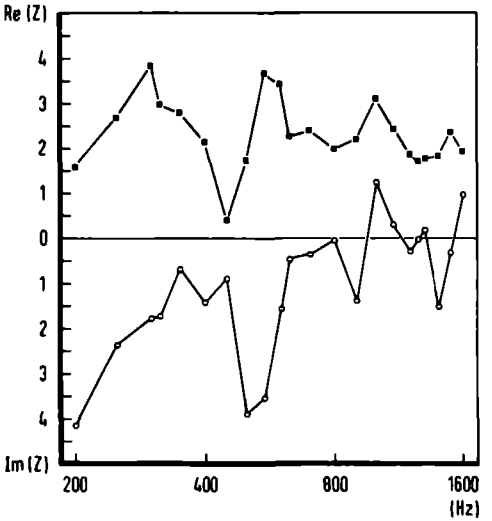

Figure 2.36
Measurement 13a
Beech-forest with layer of leaves

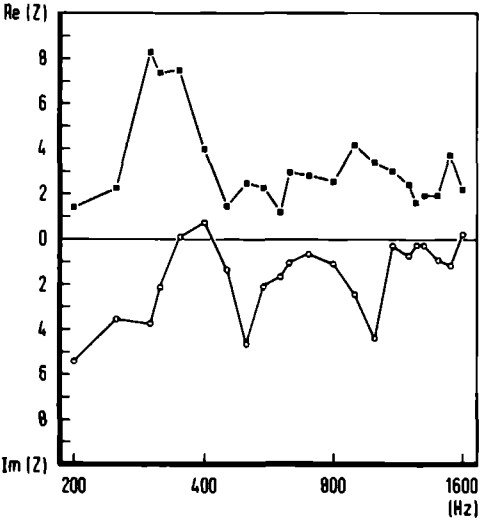

Figure 2.37
Measurement 13b
Beech-forest without this layer

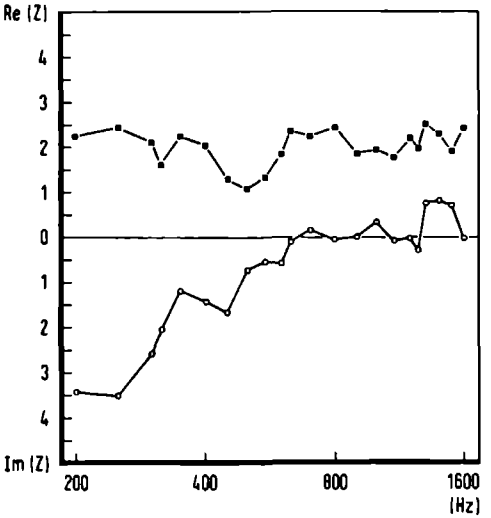

Figure 2.38
Measurement 15a
Pine-forest with needle layer

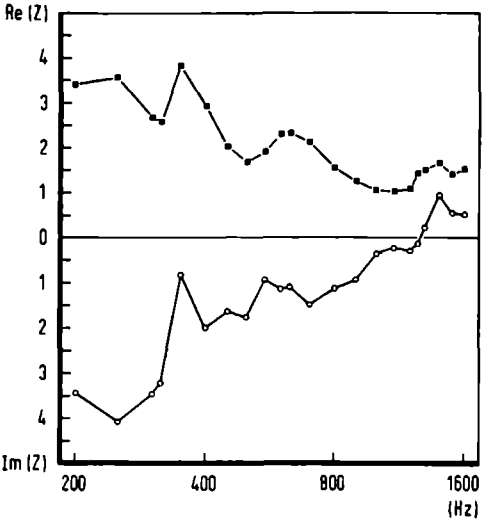

Figure 2.39
Measurement 15b
Pine-forest without needle layer

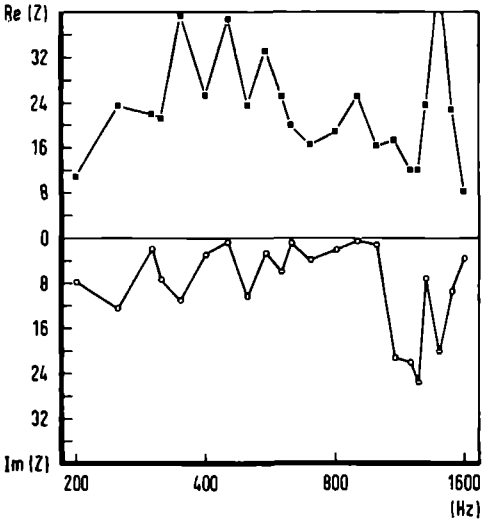

Figure 2.40
Measurement 16a
Barren sandy plain, normal angle

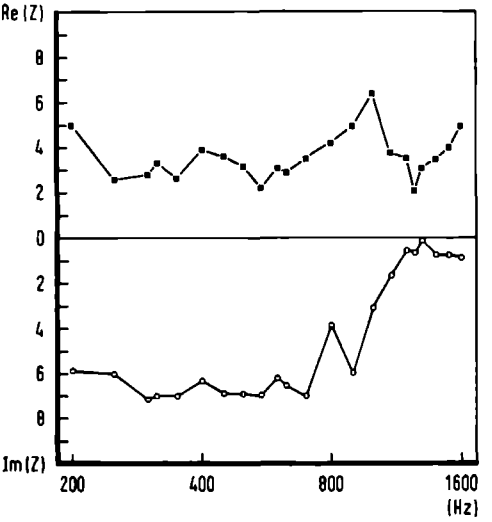

Figure 2.41
Measurement 16b
Barren sandy plain, deviating angle

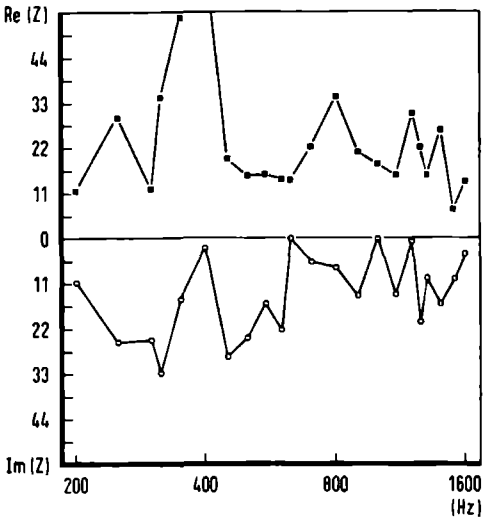

Figure 2.42
Measurement 17a
Barren sandy plain. dry

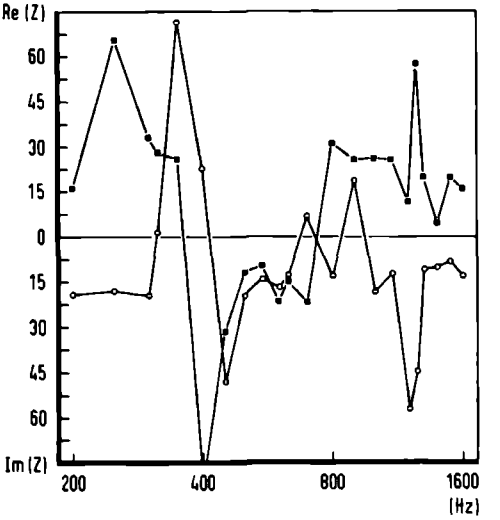

Figure 2.43
Measurement 17b
Barren sandy plain. wet 1

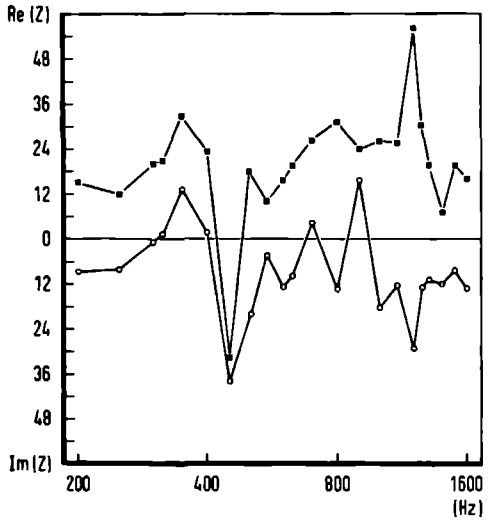

Figure 2.44
Measurement 17c
Barren sandy plain. wet 2

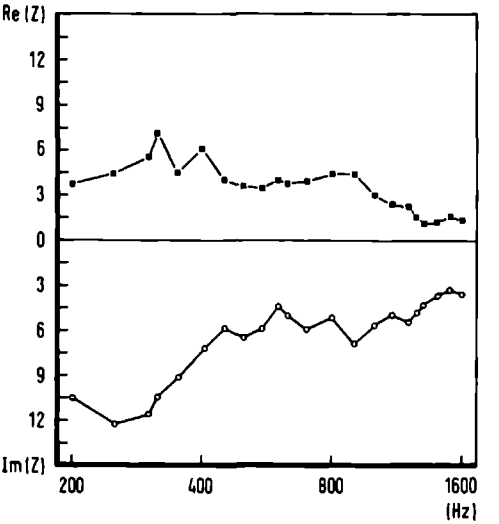

Figure 2.45
Measurement 18
Meadow, 30 microphones

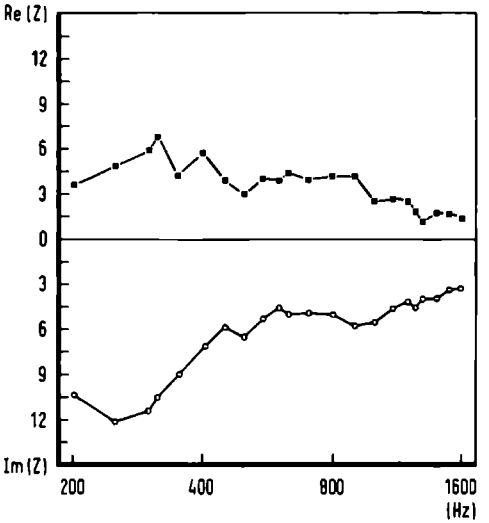

Figure 2.46
Measurement 18
Meadow, 15 microphones

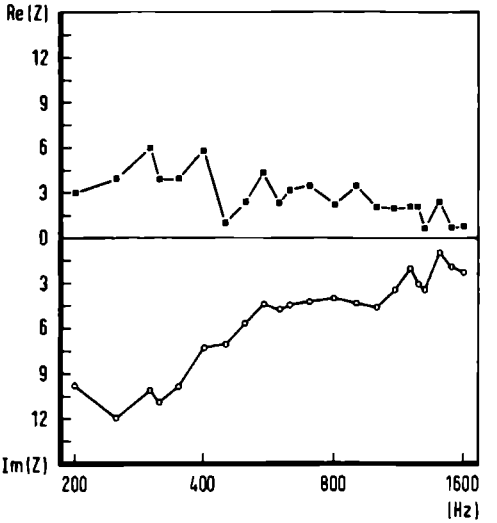

Figure 2.47
Measurement 18
Meadow, 5 microphones

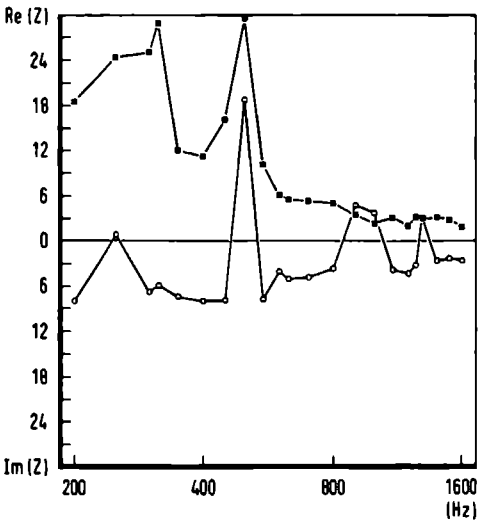

Figure 2.48
Measurement 19
Sand dunes

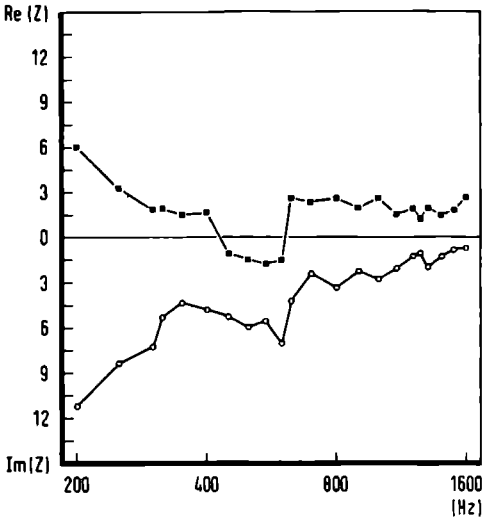

Figure 2.49
Measurement 20a
Fir-wood with needle layer

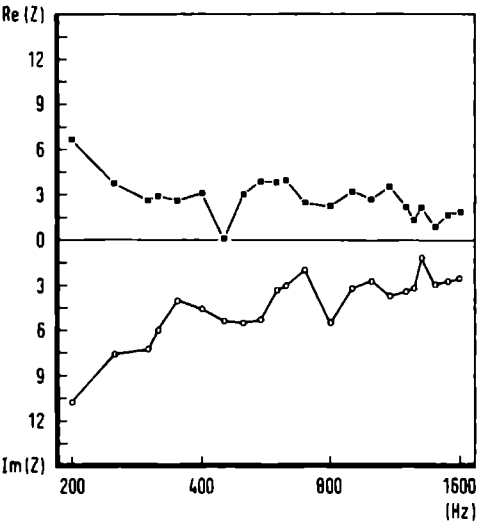

Figure 2.50
Measurement 20b
Fir wood without needle layer

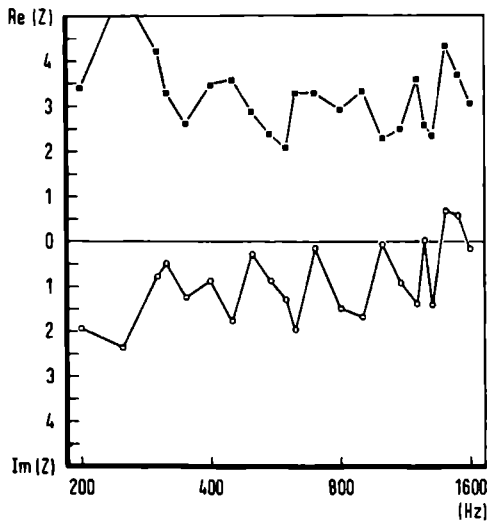

Figure 2.51
Measurement 21a
Deciduous forest with layer of leaves

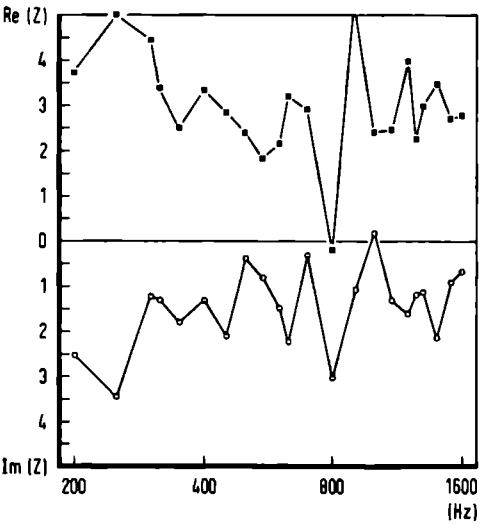

Figure 2.52
Measurement 21b
Deciduous forest without this layer

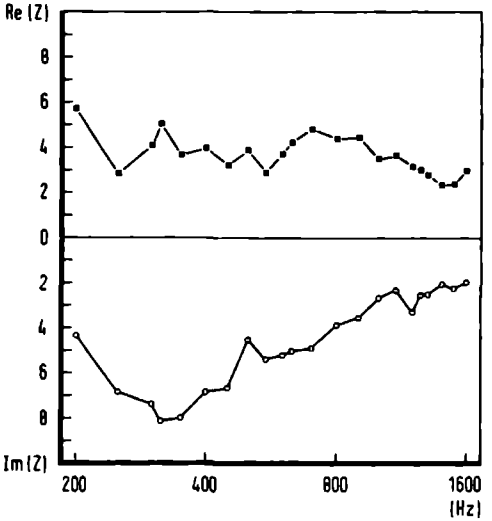

Figure 2.53
Measurement 22
Lawn

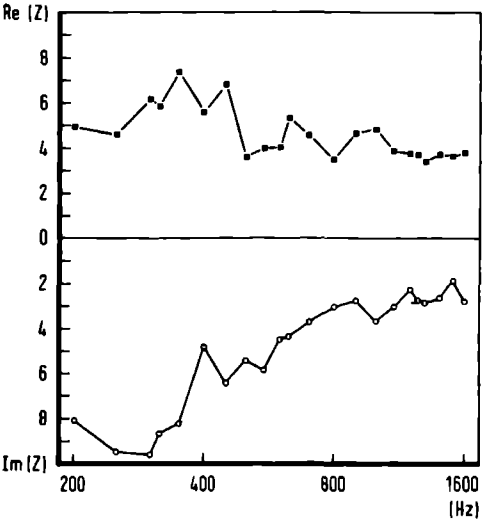

Figure 2.54
Measurement 22b
Lawn, deviating angle

Table 2.8 Results of fitting R_s on the measured interference patterns. For measurements 1-3 the plane wave model was used, for 4-11 no fits were performed and for 12-23 the Ingard-Chessel model was used. Porosity assumed to be 1.0, fit started at $R_s = 10^5$. The fitting procedure failed for measurements 14, 15a-b, 17b, 19, 20a, 21a-b.

measurement number	10^{-3} R_s	sum of squares
1	31.0	2587
2	506.0	1934
3	832.0	2875
12	118.2	3090
13a	34.5	1941
13b	69.9	2220
16a	2137.1	3592
16b	153.4	93551
17a	1410.2	2846
18a	204.4	2711
18b	213.1	1382
18c	168.5	474
20b	121.1	5178
22a	174.0	1190
22b	148.7	1082
23	315.0	1588

2.1.4 Discussion

2.1.4.1 Performance of the optimization

In general, the performance of the optimization was good, i.e. the averaged difference between model and measured sound pressure levels was in most cases 2 dB or less per measuring position. This coincides well with the expected inaccuracy in measuring sound pressure levels caused by the inaccurate placement of microphones on the track. This is well illustrated by fig. 2.3 in which a characteristic example is given of the optimization performance. Because a small variation in the specific impedance results in large changes in the sound pressure levels at the microphones situated at the steep slopes of the negative interference dips, the programme will always try to fit a line through these deep negative interference dips. This will sometimes result in a bad fit at the positions situated at the positive interference dips: see for example figs. 2.3b,d and g. Optimization with respect to the specific flow resistance will fail when the real measured parts of the normalised impedance become smaller than 1 or when the imaginary parts become negative (see table 2.8).

Choice of the model. First we tested the optimization routine for five models: plane waves, Ingard, Brekhovskikh, Thomasson and Ingard-Chessel. Tables 2.1-2.3 show that choice of the model hardly affects the impedances found or the averaged squared difference between model and measured sound pressure levels: differences occur only in the second digit after the decimal point. Therefore, we concluded that choice of the model is of no consequence and we chose the model of Ingard-Chessel for further analyses.

Number of microphones. The influence of the number of microphones was tested by analyzing measurement 18 (meadow) in three different ways. First, the normal way, with all 30 microphones (figs. 2.16 and 2.45); then with only the odd microphones (figs. 2.17 and 2.46) and finally with only every sixth microphone (figs. 2.18 and 2.47). So, 30, 15 and 5 microphones were used respectively. The graphs show that both the reflection coefficients and the impedances are hardly influenced by the lower number of microphones: the scatter is only slightly increased with five microphones. The flow resistance is also hardly affected by the halving of the number of microphones (see table 2.8). It is concluded that 15 microphones suffice. From measurement 18 onwards, 15 positions were used instead of 30.

More than 6 dB amplification. Above some hard surfaces the interference maxima exceeded +6 dB. In these cases the programme calculated negative real and imaginary parts of the reflection coefficients and impedances and their frequency characteristics were very irregular. See for example figs. 2.6, 2.7, 2.9, 2.10, 2.31, 2.33 and 2.43. This is a major handicap that makes the programme unsuitable for hard surfaces.

2.1.4.2 General behaviour of acoustic soil parameters

Dependency of the reflection coefficient on frequency. On the basis of figs 2.4-2.25 a rough acoustic classification of outdoor surfaces can be made:

1) Acoustically soft surfaces
The real and imaginary parts of the reflection coefficient are always smaller than 0.5, they sometimes change their sign, the values show a large scatter, and they are relatively independent of frequency.
These surfaces include those of a mixed forest (measurement 6), beech-forest (measurement 13), pine-forest (measurement 15) and an elm-forest (measurement 21).

2) Acoustically intermediate surfaces
The real part of the reflection coefficient starts at 0.6-0.8 at 200 Hz, then gradually decreases with frequency, reaching values of 0.0-0.4 at 1600 Hz. The imaginary part starts at 0.4 and decreases (more slowly than the real part) to 0.1-0.3 at 1600 Hz. This indicates that with increasing frequency more sound is absorbed and that the reflected sound is increasingly delayed.
These surfaces include a barren sandy plain (measurement 5), mixed deciduous forest (measurement 12), meadow (measurement 18), fir-wood (measurement 20) and a lawn (measurement 22).

3) Acoustically hard surfaces
The real part of the reflection coefficient lies between 0.7 and 1.0 and the imaginary part between 0.0 and 0.2 for all frequencies. This means that almost all sound is reflected and with zero phase shift.
This was observed for a barren sandy plain only (measurements 16 and 17).

Dependency of specific impedance on frequency. It is not easy to make an acoustic classification of outdoor surfaces based on the measured specific impedances because of the large scatter in the results. This scatter is the largest above hard surfaces (barren sandy plain, measurements 16 and 17). Above soft surfaces the real part of the normalised impedance is generally quite constant (1.0-4.0), between 200 and 1600 Hz. The imaginary part can start from 4.0-12.0 at 200 Hz and decrease to 0.0-4.0 at 1600 Hz. As will be shown later, this flat real and sloping imaginary behaviour can only be explained by assuming a layered floor.
Acoustically derived specific flow resistances. These show a large range of values: from 31×10^3 for a mixed forest floor to 2.1×10^6 for a barren sandy plain (table 2.8). It is clear that barren surfaces are the hardest and deciduous forest floors the softest.

2.1.4.3 Layered character of outdoor surfaces

The measured impedances are specific acoustical impedances - they give the ratio of sound pressure and air particle velocity just inside the soil. They are not characteristic impedances, which give the ratio of sound pressure and air particle velocity in an unbounded, infinitely extended medium. This is important because the formulae of Delany and Bazley give only a relation between the characteristic impedance and the flow resistivity. If we try, therefore, to extract values for flow resistivities for the soil surfaces of our measuring sites (see table 2.8), these will always be apparent flow resistivities based on the probably wrong assumption that the soil is a homogeneous, semi-infinite medium. In that case only will the specific impedance be equal to the characteristic impedance (see eq. 1.18). If we assume a one layer structure on a hard background this specific impedance will also be influenced by the thickness of the layer.
The calculation of flow resistivities from measured impedances will sometimes be difficult because real parts of the normalized specific impedances can become smaller than 1 whereas this is not possible according to eq. 1.19 (see e.g. fig. 2.32). Because we do not know anything about the layer structure at our measuring sites, this inclined track method will not contribute to a solution of the problem of the validity of the formulae of Delany and Bazley for ground surfaces. Indoor experiments should be performed on soil layers with a well-defined thickness (see section 2.2) in combination with measurements of flow resistivity (see chapter 3) to solve this problem.

2.1.4.4 Influence of angle of incidence

To test the hypothesis of local reaction (i.e. specific impedance independent of the angle of sound incidence), we performed two measurements with different angles: measurement 16 (barren sand) and measurement 22 (lawn). In measurements 16a and 22a the positions of the microphones were as described in table 2.1, resulting in an angle of incidence of 70°. In measurement 16b the microphones were positioned in such a way that the path length difference between direct and reflected sound increased 0.02 m per microphone. The source height was 1.25 m, the angle of incidence 76°. In measurement 22b the source height was 1.83 m, resulting in angles of incidence varying from 71 to 74.5° from the first to the last position. The results (figs 2.11-2.12, 2.24-2.25, 2.40-2.41, 2.53-2.54) show no significant differences between impedances with the normal and with the deviating angle. To test the hypothesis, the deviation of the angle probably has to be larger. This is not possible with the inclined track method, however, because the interference pattern cannot be sampled adequately with large angles of incidence. Most investigators seem to find the local reaction assumption a reasonable one [33, 99].

2.1.4.5 Influence of soil water content

It is to be expected that a soil will become acoustically harder if the air in the pores is replaced by water. In one experiment (17, barren sandy plain) we measured the interference pattern above a dry soil and above the same soil immediately after irrigation. The dry soil had a water content of 12 %, the wet soil 25 % at the beginning and 22 % at the end of the measurement. While reflection coefficients (figs 2.13-2.15) show that the wet soil is indeed harder than the dry soil, the impedances show such a large scatter that a comparison is difficult. The same sandy plain was measured several times (measurements 3, 11, 16 and 17). The water contents of 3, 16 and 17a were all approximately 10 %, those of 11 and 17b and c were 25 %. Again, the scatter interfered with a good comparison.
Frank found that sound absorption was "adequate" immediately following rain, that it increased after a couple of days of drying and decreased as the days numbered on without rain [44]. At 0.5 kHz he measured an increase of the absorption coefficient from 0.32 (bare soil) to 0.48 (with 5-7 cm dry grass), and from 0.68 (bare soil) to 0.86 (with leaves in a deciduous forest).
The influence of water content on flow resistivity was investigated by Dickinson and Doak [33]. They state that a small increase in water content (up to 8-10 %) leads to an opening up of the pores and consequently to a decrease in flow resistivity. Perhaps this can explain why shifting sand (with only 2 % water) gives such high impedances. Above 10 % an increase in water content will lead to a rapid increase in flow resistivity. For organic material containing soils the sound absorption is maximal for the dry situation.

2.1.~~4.6~~ Influence of organic layer

The influence of an organic layer on impedance was studied in two cases: a forest floor and a grass-cover.
In measurement 14, the forest floor covered with ivy, the interference patterns for frequencies above 500 Hz were found to show more scatter than was expected. This could have been by the 3-10 cm large ivy leaves causing a sound scatter.
A number of forest floor impedances were measured with an intact litter layer and then after removal of this layer. By litter layer we mean the layer of twigs and leaves or needles and not the humus layer. In measurement 13 (beech-tree forest) the reflection coefficient of the intact floor (fig. 2.6) very much resembled that of the floor without litter layer (fig. 2.7). The intact floor, however, seemed to be somewhat softer. This difference is clearly visible in the impedance graphs of the intact (fig. 2.36) and the denuded floor (fig. 2.37), especially for frequencies below 400 Hz. Flow resistivity for the intact floor was significantly lower than

that for the denuded floor, respectively 34.5×10^3 and 69.9×10^3, see table 2.8.
In measurement 15 (pine-forest) the reflection coefficient also seemed to decrease as a result of the removal of the litter layer (figs 2.9-2.10). Again the impedance graphs show a more pronounced softer intact floor (figs. 2.36-2.37). As in measurement 13, the removal of the layer results in a more flat frequency behaviour of the real part of the impedance. These flat real parts and decreasing imaginary parts are typical for intact forest floors and can be explained by eq. 1.18.
In measurement 20 (fir-wood) removal of the needle layer results in lower reflection coefficients for frequencies above 600 Hz (figs 2.20-2.21). No significant difference is found in the impedance (figs 2.49-2.50).
The intact elm-tree forest floor (measurement 21) was not significantly softer than the floor without leaves (figs 2.22-2.23,2.51-2.52).
In conclusion, it can be stated that only in the cases of beech forest and pine forest did the litter layer influence the acoustic properties of the floor. The minor effect of the litter layer and a more dramatic effect of the humus layer (see fig. 2.55) has also been demonstrated by Talaske [115].

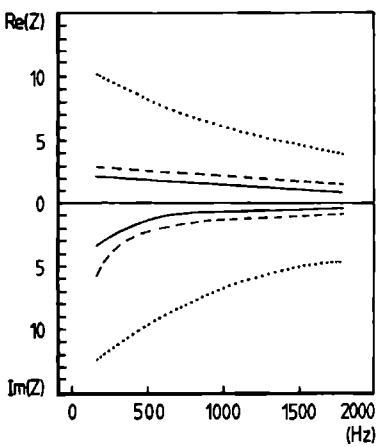

Figure 2.55. A schematical representation of the influence of organic layers on the specific impedance of the floor of a stand of mixed hardwoods comprising 39 % oak (Quercus sp.), 35 % other mixed hardwoods (birch, maple, cherry, sassafras) and 26 % white pine (Pinus strobus L.) (after Talaske [115]). The full curve represents an intact floor (with litter and humus layers); the dashed curve is the impedance after removal of the 1.9 cm thick litter layer; the dotted curve gives the impedance of the bare A-layer (a sandy loam with 63 % sand, 34 % silt and 3 % clay) after removal of the 3.4 cm humus layer.

The influence of a grass-cover on sound reflection by the soil surface can be deduced from measurements recorded in the experimental garden on two adjacent test sites of the same soil type, one without any vegetation (measurements 3, 11, 16 and 17) and one with a grass-lawn (measurements 2 and 9). The impedances of the barren sandy plain (figs 2.28, 2.33, 2.40 and 2.42) are approximately twice as large as those of the grass-covered surface (figs 2.27 and 2.32). Comparison is somewhat difficult because the impedances of the barren plain show large frequency fluctuations although the real part of the grass-covered plain seems to be more flat (fig. 2.32). The flow resistivities for the barren site were very much higher than those for the grass-covered site (table 2.8).
These measurements indicate that a grass-cover has a pronounced effect on the acoustic properties of an outdoor surface. It is even so that the impedance is totally determined by this cover, and that it is uninfluenced by the soil-physical characteristics of the underlying mineral soil. This is clearly demonstrated by a comparison of the impedances of a meadow on a silty clay soil (fig. 2.45) with those of a lawn on a sandy soil (fig. 2.53). The mineral soil of the meadow was very much more compact than that of the lawn (7.3 and 41.9 vol % air, resp.). Still, the impedances were very similar, as were the flow resistivities: 204.4×10^3 for the meadow and 174.0×10^3 for the lawn. Since the grass of the meadow was very much higher than of the lawn it can also be concluded from these measurements that the height of the grass is of no importance.

2.1.4.7 Comparison with values from the literature

Dickinson and Doak [32] were the first to measure accurately the impedances of natural surfaces. They found that there is a slight increase in the sound absorption of sand when a little moisture is present. They also found that when vegetable roots are present in the soil the sound absorption is greater than when they are absent. The normalized specific impedance measured for a range of frequencies from 200-1000 Hz was found to vary considerably for different ground surfaces: for example, from 3+3i for a soft grass patch to 7+17i for an area of rock covered with chippings. The frequency behaviour of the real and the imaginary parts found by these investigators is essentially the same as what we have found: a relatively constant real part and a decreasing imaginary part (see e.g. fig. 2.38).
At the Pennsylvania State University important results were obtained under the guidance of Reethof and McDaniel [47, 44, 115]. Frank measured the absorption coefficients of 47 sites by means of an impedance tube. He found values from 0.2 (for 125 Hz) to 0.8-0.9 (for 2 kHz). As the absorption coefficient is equal to 1 minus the squared magnitude of the plane wave reflection coefficient, these values match reflection coefficient amplitudes of 0.9 (for 125 Hz) and 0.3-0.4 (for 2 kHz). From figs 2.4-2.25 it can be seen that we find the same tendency. Similar results were obtained with a

short pulse method in laboratory experiments with layers of dried sand (see section 2.2). Thus, above 1-2 kHz nearly all incident sound is absorbed. Frank also provides some interesting sound absorption values for a moss-covered loam soil. Results from our experiments on a moss-covered ground (measurement 4) compare favourably with those of his (table 2.9).
Important results were obtained by Talaske [115] who , by means of an impedance tube, carefully determined the surface impedances of two forest floors: a red pine stand and a mixed hardwood stand. He found that the layered nature of a forest floor gives a typical frequency dependence of the impedance:the real parts of the impedances are almost independent of frequency. Our results seem to confirm his findings.

Table 2.9. Comparison of the absorption coefficients of moss-covered ground measured by Frank [44] and by our laboratory, with an impedance tube and the inclined track, respectively.

frequency	impedance tube	inclined track
125	0.35	-
200	-	0.42
250	0.90	0.47
500	0.75	0.80
1000	0.90	0.95
1600	-	0.91
2000	0.98	-

Our results also agree with the measurements of Glaretas [47] who found an imaginary part of the normalized impedance of 25 for 250 Hz and 10 for 1kHz and a more or less stable real part of approximately 5 for a grass-covered surface. Glaretas used a new experimental method a free field two-microphone method, consisting of measuring the sound pressure field by two microphones located on the same vertical axes and by calculating the transfer function of the two signals by FFT.
Thomasson also measured acoustic properties of outdoor surfaces, barren fields and grass-lands but not forest floors [120]. He expressed these in the form of the parameters A, B, C and D. We determined these in one case only (deciduous forest, measurement 1): A = 0.45, B = 10.72, C = 3915 and D = 462 with a sum of squares of 1582.

The experimental results described in this section indicate that the major action of vegetation on soil surfaces consists of the development of an acoustically relevant and detectable layered structure. This means that the only way in which the correct frequency behaviour of the impedance can be achieved (i.e. constant real part and decreasing imaginary part) is by assuming a layered structure. If this is omitted the real part of the impedance will also decrease, resulting in a too high predicted sound pressure level at the first frequency for which a destructive interference appears [102]. Furthermore, given the fact that soils can be modeled as porous media [77], this would imply that at low frequencies the real and imaginary parts of the characteristic impedance are equal and relatively high and that the real part tends to one and the imaginary part to zero for high frequencies. If no layered structure were assumed the specific impedance would give the same behaviour. And, as our results show, this is not the case, so theories on the acoustics of porous materials can only be used when a certain layer thickness is taken into account.

2.2 Indoor measurements with a short sound pulse*

2.2.1 Introduction

In addition to the specific impedance measurements conducted outdoors, as described in the previous section, some specific impedance measurements of sand and peat-dust were performed indoors.As also mentioned in the previous chapter, these measurements are essential in checking the Delany and Bazley relations (eq. 1.19-1.20) for natural soils, and any other equations describing the acoustic behaviour of soils.
In order to calculate the specific impedance of the ground, we applied a pulse sound method at layers of ground with well-known thicknesses. A short pulse of sound is directed at a reflecting surface, and by comparing the amplitudes and the phases of the direct and reflected pulses, Z_s of the surface can be calculated. This method has already been applied in some form in room acoustics to determine the absorbing properties of building materials [14, 30, 70, 134]. Its advantages over interference methods are obvious: no choice of interference model has to be made, it is a non-destructive method and it allows indoor measurements on samples of ground with finite dimensions because it is possible to limit the area contributing to the reflection by making the pulse sufficiently short [16, 70].
The performance is described of a Digital Pulse Sound Processor developed by the Department of Electronics Research of the Catholic University of Nijmegen. The direct and reflected pulses are compared both in the time and the frequency domain (by means of DFT). The pulse method is tested and its limits of application are described. Impedance values are given for sharp sand, peat-dust, grass-sods and oak leaves.

2.2.2 Apparatus and experimental set-up

We measured the absorption of sound and its reflection by layers of sand, peat-dust and leaves on a hard backing in an anechoic room with an effective working area of 3.6 m by 4.0 m and a height of 1.9 m.
For this purpose a Pulse Sound Processor was designed that can produce sine packets of 1-15 sine periods of any frequency. The PSP can store in a digital memory both the emitted and reflected sound pulses, both of which can be displayed on an oscilloscope or level recorder afterwards (fig. 2.56). With the aid of a microprocessor programme, the amplitude and time differences between the direct and the reflected sound pulses were determined. From these, R and Z_s were calculated.

---

*Part of this section has already been published [51].

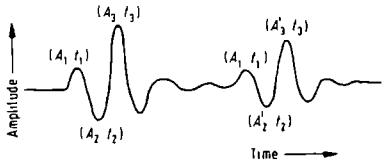

Figure 2.56 A schematical representation of the emitted sine pulse (left) and the reflected one (right).The frequency used was 1 kHz. The six points indicated were used in eqs. (2.21) and (2.22).

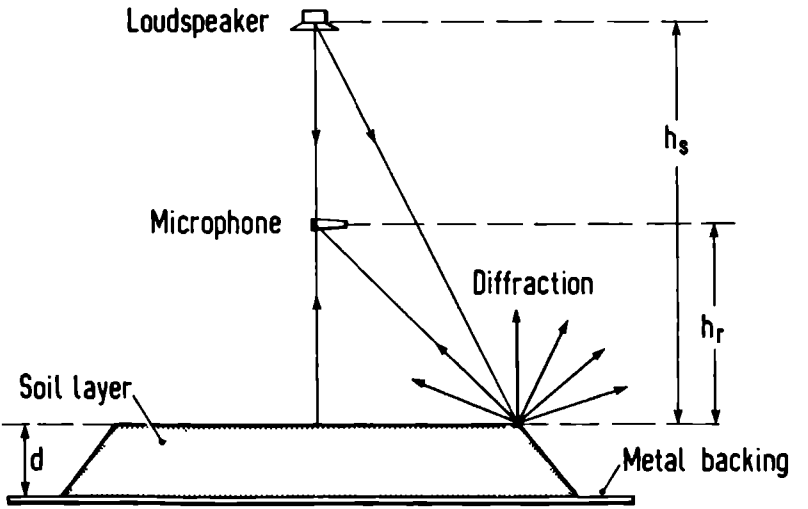

Figure 2.57 Experimental set-up for the pulse measurements on soil samples in the anechoic room.

The PSP contains a sampled sine of one period (128 time points with a resolution of 8 bits). By using a key-board, the frequency of the outgoing sine and the number of periods in the packet can be specified. The pulse was amplified by a Quad Power Amplifier and sent to a 2 inch high power dome squawker loudspeaker (Philips AD0210Sq). This speaker was placed one metre above, and directed straight down to, the reflecting surface.
The backing measured 1 by 2 m^2 or 2 by 2 m^2. In the first case movable edges were attached to the long sides to prevent the sand from falling off the plate. To avoid troublesome reflections no such edges were present at the short sides where the sand layer boundary was sloping. In the second case no such edges were used and all layer boundaries sloped.
A 1/2 inch electret microphone (GenRad 1961-9601), attached to a preamplifier (GenRad 1560-p42), was placed 0.5 m above the surface and exactly in the sound path (see fig. 2.57). The received signal was selectively amplified by an automatic scaling procedure of the PSP programme so as to achieve a maximum efficiency of the 8 bits sampling of the sound pulse amplitudes by an A/D-convertor (Computerlabs HAS 0802) with a sampling rate of 100 kHz. The sampling time of 10 μs has an accuracy of 10^{-5}. The A/D-convertor operates according to a successive approximation system. The digitized signal is stored in 5 kBytes RAM which allows 48.4 ms of real time to be recorded. The recording starts when the PSP emits a sound pulse or after a time lag from 0-655.35 ms. The 8 bits conversion allows an accuracy in the amplitude of 0.4 % on a linear scale and a S/N ratio of 59 dB. A schematic representation of the components of the PSP can be found in fig. 2.58.

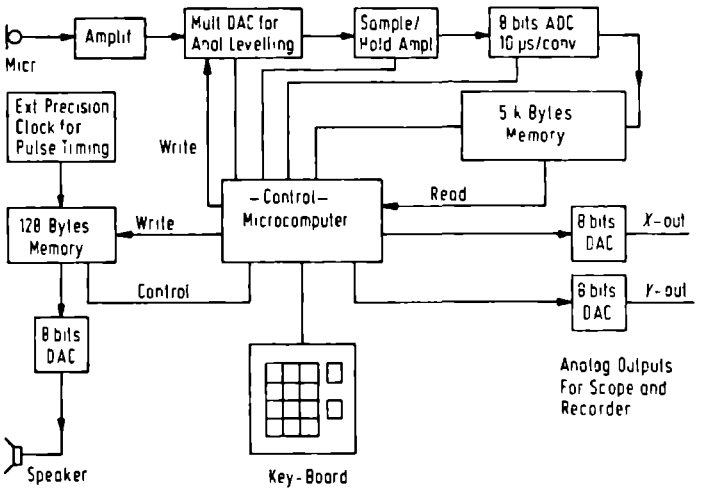

Figure 2.58 The components of the Pulse Sound Processor (PSP) for generating the sine pulses and for sampling and recording the direct and the reflected pulses.

2.2.3.1 In the time domain

The amplitudes and times of occurence of the first two maxima and the first minimum of both the direct and the reflected pulses were measured (fig. 2.56). From these the mean time delay t_r and amplitude decrease A_r were calculated according to:

$$t_r = \frac{1}{3} \sum_{n=1}^{3} (t'_n - t_n), \tag{2.21}$$

$$A_r = \frac{1}{3} \sum_{n=1}^{3} \frac{A'_n . B_n}{A_n . B'_n}. \tag{2.22}$$

The parameters B_n and B'_n are the amplitudes of the direct and reflected pulses in the case of the hard backing only; A_n and A'_n are the amplitudes in the situation where the plate is covered with absorbing material. By using eq. 2.22 we have eliminated the influence of the differences in the sound path lengths between direct and reflected pulses. It is also an approximate correction for the incomplete reflection caused by the finite dimensions of the plate.
From t_r we have calculated the phase ϕ of the reflection coefficient R by means of:

$$\phi = 2\pi f\{t_r - t_b + (r_2 - r_1) \times (1/c_{20} - 1/c_t)\} \tag{2.23}$$

with:
c_t : velocity of sound at t °C,
f : frequency of sine,
t_r, t_b : mean time differences between direct and reflected sines at a layer or hard backing,
r_2, r_1 : path lengths of reflected and direct pulses.
The velocity of sound is calculated from the temperature and relative humidity of the air by [63]:

$$c = [(273 + t)/273]^{1/2} \frac{331.6}{1} - 0.21 \times 10^{-4} p_w h \tag{2.24}$$

t : temperature of air in °C,
h : relative humidity of air in vol.%,
p_w : vapour pressure at t °C relative to the

barometric pressure.

The last term in eq. 2.23 corrects for the variation of phase caused by changes in the ambient air temperature.
A_r and ϕ are respectively the modulus and the argument of the complex acoustic reflection coefficient R_p from which Z_s was calculated according to eq. 1.6.

2.2.3.2 In the frequency domain

A sound pulse consisting of a limited number of sine periods contains more frequencies than a continuous signal. Some energy is also situated in the side-bands [110]. This phenomenon (called "leakage") is illustrated in figs. 2.59 and 2.60. During the pulse analysis in the time domain, only the center frequency was used but the efficiency of the measurement could be enhanced by including the side-band frequencies in the analysis of the reflection. This was done in a separate frequency analysis of the direct and the reflected pulses by means of Digital Fourier Transform (DFT)[110]. The experimental set-up of the pulse experiments (fig. 2.57) shows that the reflected pulse consists of two parts: a reflection from the center of the soil sample and a diffracted pulse from the edges of the sample [70,121]. This diffraction contribution has to be separated out because the results of the indoor experiments have to be comparable with the results of the outdoor impedance measurements. This can be achieved by using for the DFT only that particular part of the reflected pulse that arrives before the diffracted edge pulse starts to arrive at the microphone. The time difference T_e between the arrival of the reflected pulse and the arrival of the edge pulse is dependent on the geometry of the experiment (fig. 2.57) and the sound speed c:

$$T_e = \{(h_s^2 + b^2)^{1/2} + (h_r^2 + b^2)^{1/2} - (h_s + h_r)\}/c \qquad (2.25)$$

where b is the narrowest dimension of the reflecting area. This equation was used to calculate the required time window over the two pulses. A correction was applied for this pulse truncation by means of a deconvolution technique [110]. The cospectrum of the direct and the reflected pulses was also calculated. Only frequencies in the fourier spectra with a cross-correlation larger than 0.95 were taken into account.

2.2.4 Impedances of sand, peat, grass sod and oak leaf

These results of the measurements are represented in figs. 2.59-2.70. The impedance of a hard surface (a steel plate) is given as a reference (fig. 2.61). For this kind of surface, particle speed v is zero for any pressure on the surface, i.e. the impedance is infinite. The measured im-

pedance was high but finite.
The influence of layer thickness on the impedance of dry sand has already been published [51]. The results are summarized in figs. 2.62-2.65. The general impression of the reflection coefficient is a steady decrease of its real and imaginary parts. This is an indication for increasing sound absorption in the high frequency range. Thus, soil can be looked upon as a low-pass filter. For this reason, the sound levels in a narrow band of frequencies can be reduced to a large extend (15 to 20 dB) when, in an outdoor experiment, the direct and reflected waves are 180 ^{o} out of phase. It was concluded [51] that the sound absorption takes place in the upper 10 cm of sand because the specific impedances did not change when the sand layer thickness was increased from 9 to 15 cm. This also means that for layers thicker than 10 cm the measured Z_s equals Z_c.
To simulate a forest floor, the specific impedance of a 15 cm thick peat-dust layer was measured. The impedance found (fig. 2.66) shows that this kind of biological material has very large sound absorptive properties. This result compares well with the outdoor results. We also investigated the influence of the water content of the peat-dust on Z_s (figs. 2.66-2.68). The wetter the layer, the higher the impedance. This is caused by the reduced air content of wet peat-dust. The oscillations in the impedances at the high frequencies are probably caused by the layer character of the reflecting surface.
Two other layers of vegetation-produced organic material were measured: grass-sods and oak leaves (figs. 2.69-2.70). These layers also appear to be very absorptive.
The pulse method (in the frequency domain) was also used to measure the specific impedance of a layer of snow. The freshly fallen snow ((layer thickness of 11 cm) lay on a frozen grass-field. The air temperature was 0 ^{o}C, the relative humidity 30 %. The loudspeaker height was 1.528 m, the microphone height 0.478 m. The real part of the normalized specific impedance ranged from 1.39 (at 2900 Hz) to 1.47 (at 6300 Hz), its imaginary part from 0.03 (at 2900 Hz) to -0.04 (at 6300 Hz). This agrees well with the expected acoustically soft character of snow.
For some layers, the specific flow resistance was calculated from the measurements of the specific impedance. For this purpose eq. 1.18-1.20 were used in a curve-fitting procedure. The results are: $R_s = 18 \times 10^3$ for the layer of grass-sods, 18×10^3 for the layer of oak leaves, 60×10^3 for the dry peat-dust, 210×10^3 for the wet peat-dust, 146×10^3 for the wet peat-dust after drying overnight and 250×10^3 for the dry sand.

Figure 2.59 Time trace of the direct (left) and the reflected (right) pulse in the case of a low center frequency (1300 Hz) and the amplitude and phase spectrum of these pulses as obtained by DFT. Reflecting surface: wet peat-dust of 1x1 m^2 with a height of 0.15 m on a steel plate. Truncation of the pulse after one pulse cycle.

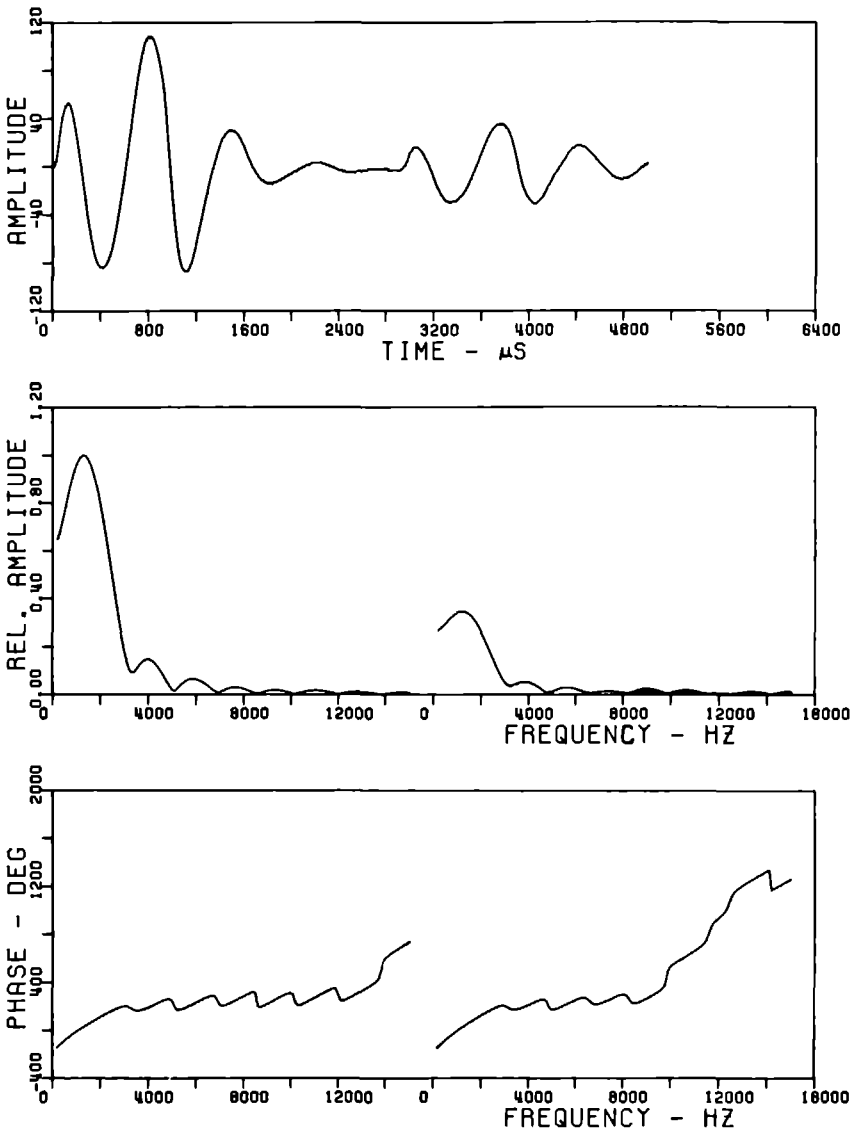

Figure 2.60 Same situation as in fig. 2.59, only with a center frequency of 3800 Hz.

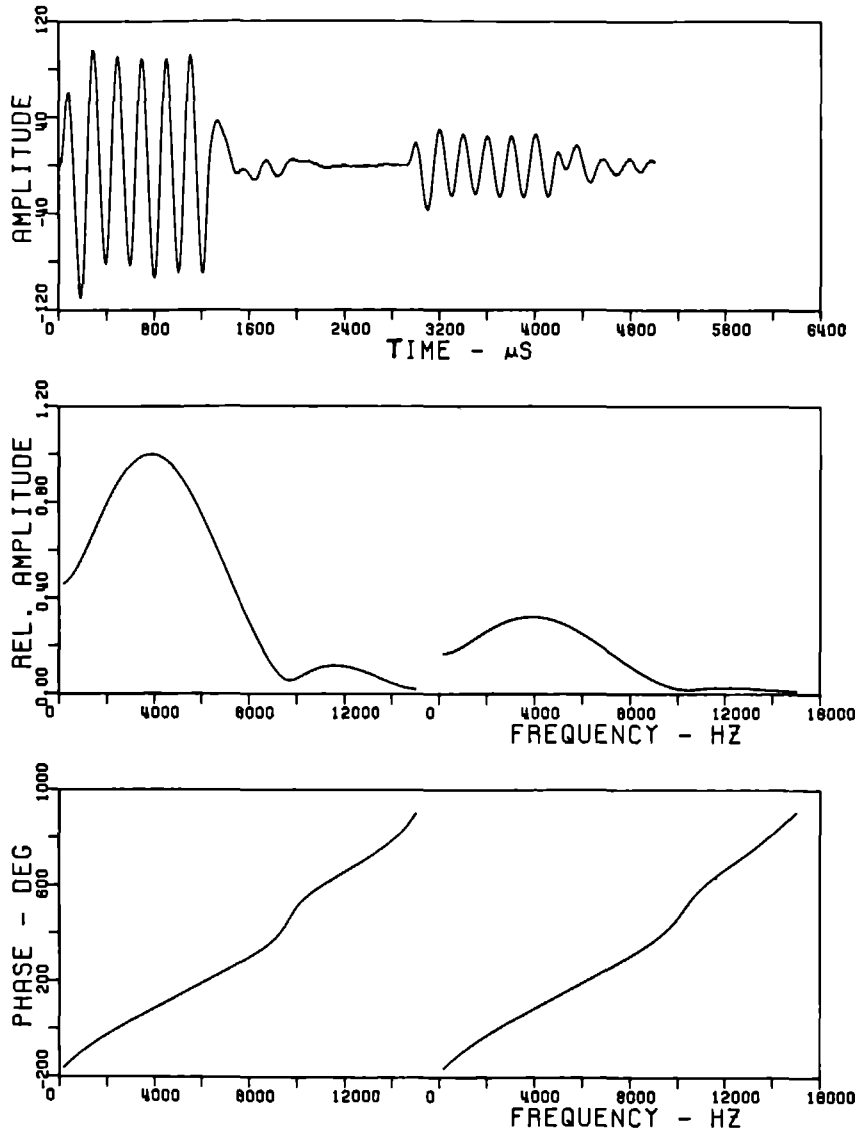

Figure 2.61 Normalized specific impedance of a 2x2 m^2 steel plate, measured with the frequency domain method. The pulse was truncated after one pulse cycle.

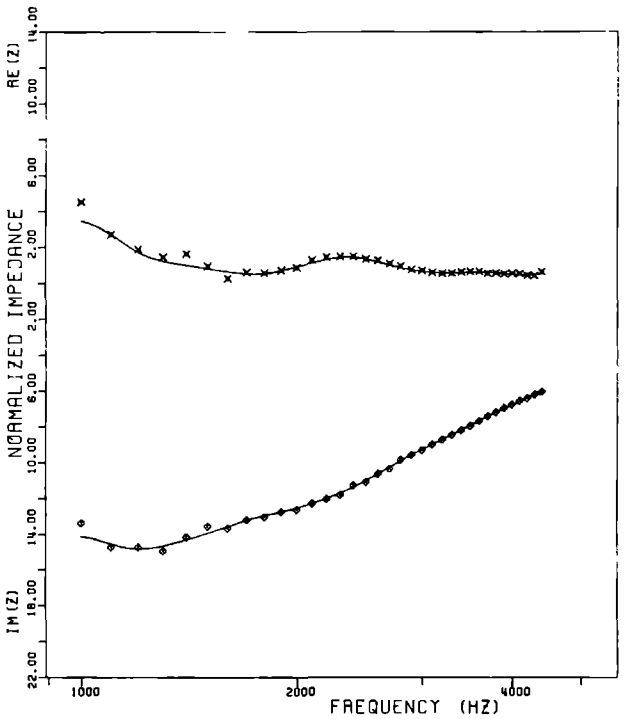

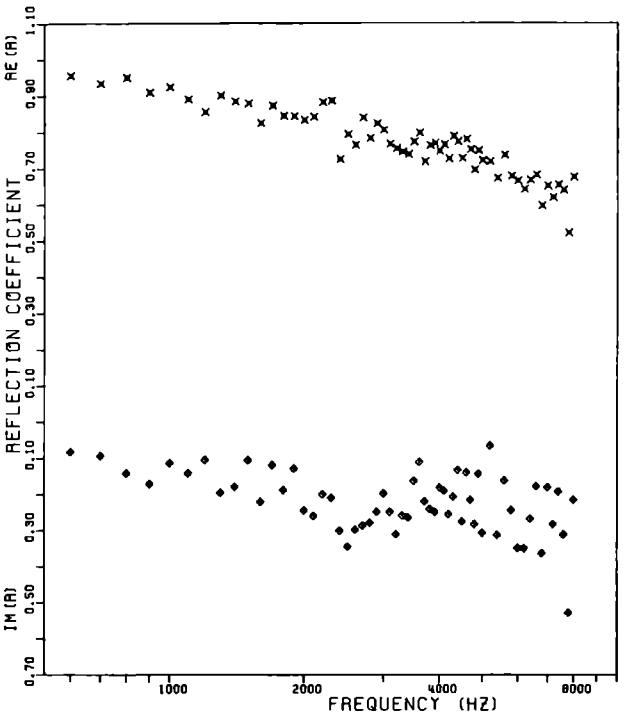

Figure 2.62 The reflection coefficient of a layer of dry sand (1x2 m^2, height 0.9 cm) on a steel plate (1x2 m^2), measured with the time domain method.

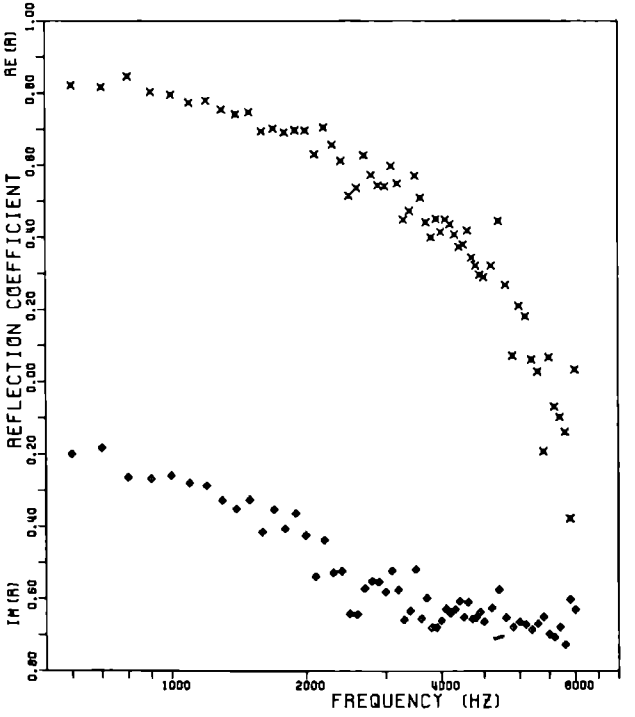

Figure 2.63 The reflection coefficient of a layer of dry sand of height 15.0 cm. See also fig. 2.62.

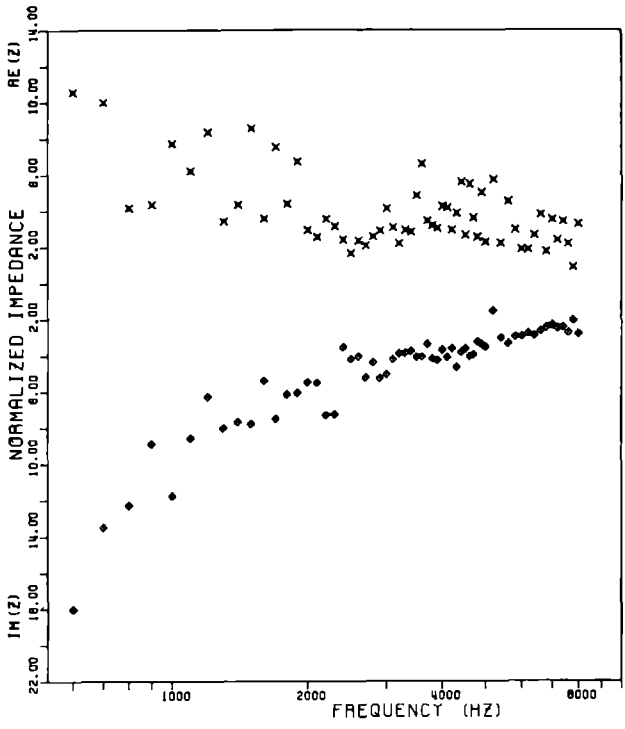

Figure 2.64 The normalized specific impedance of a layer of dry sand of height 0.9 cm. Calculated from the results of fig. 2.62.

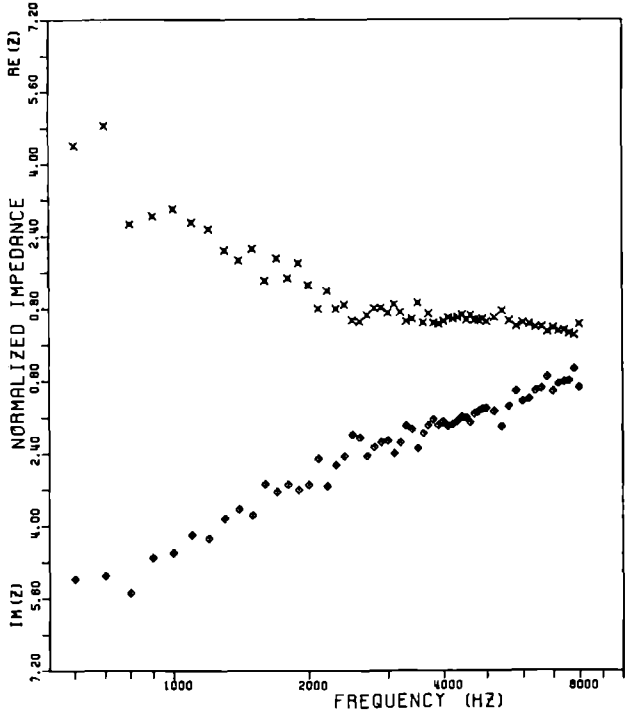

Figure 2.65 The normalized specific impedance of a layer of dry sand of height 15.0 cm. Calculated from the results of fig. 2.63.

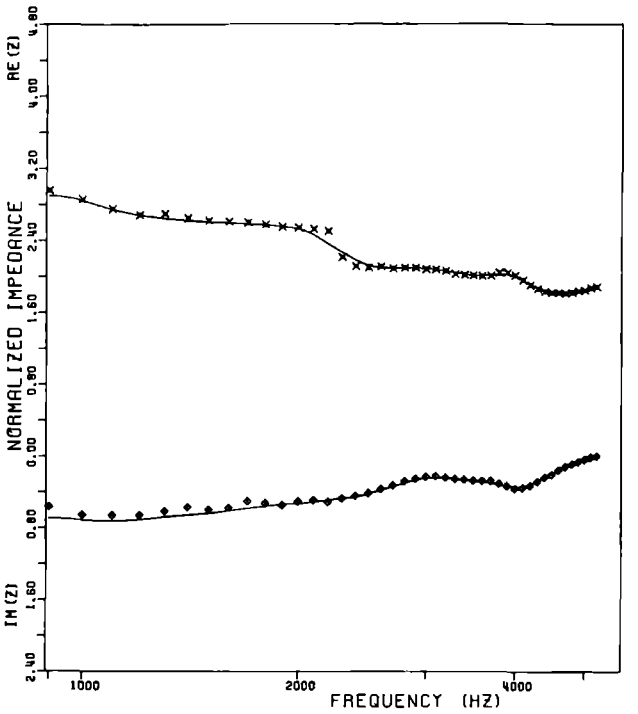

Figure 2.66 The normalized specific impedance of a layer of dry peat-dust (1.1x1.1 m^2, height of 0.15 m) on a steel plate (2x2 m^2), measured with the time domain method. Pulse was truncated according to eq. 2.25. Source height was 1.69 m, microphone height 0.50 m. The peat-dust contained 60.1 vol % air, 25.5 vol % water and 14.4 vol % solid matter.

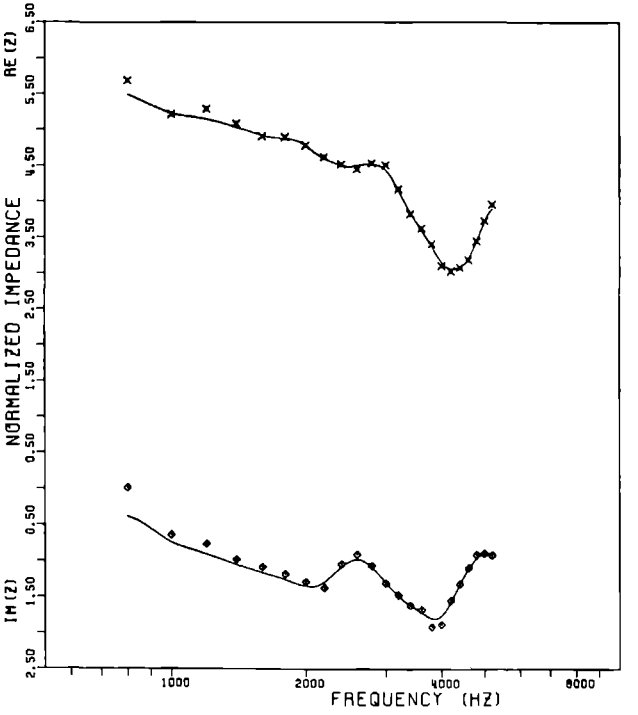

Figure 2.67 The normalized specific impedance of a layer of wet peat-dust. The peat-dust contained 53.2 vol % air, 33.4 vol % water and 13.4 vol % solid matter. The other conditions as in fig. 2.66.

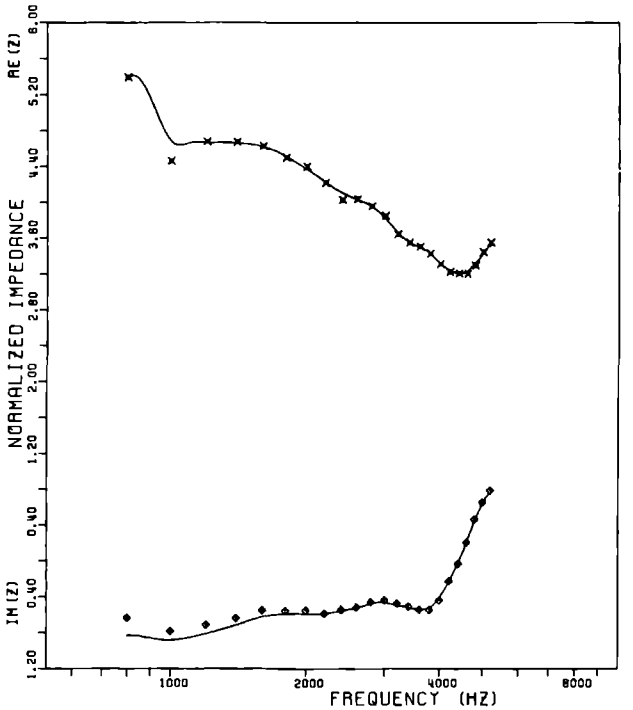

Figure 2.68 The normalized specific impedance of a layer of wet peat-dust after drying overnight. The peat-dust contained 55.7 vol % air, 30.9 vol % water and 13.4 vol % solid matter. The other conditions as in fig. 2.66.

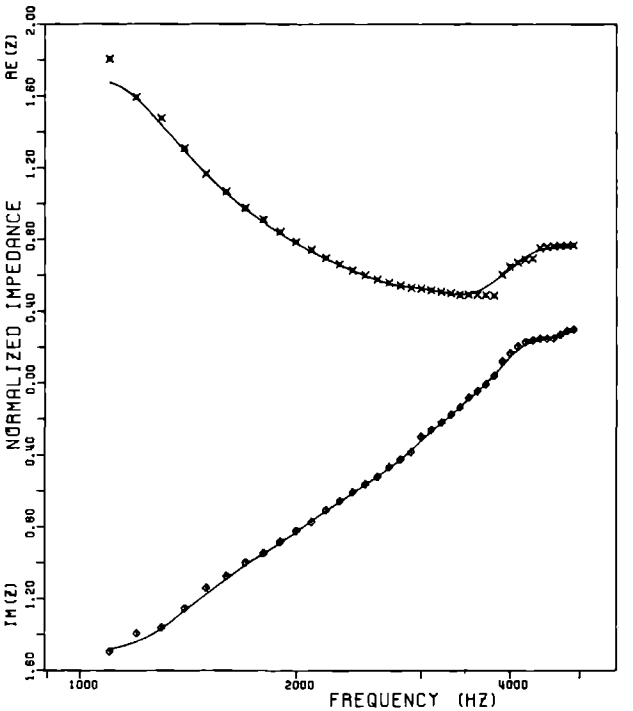

Figure 2.69 The normalized specific impedance of a layer of grass sods (1.0x1.0 m, height 0.09 m) on a steel plate (2x2 m^2) measured with the frequency domain method. Truncation of the pulses according to eq. 2.25. Source height, 1.758 m, microphone height, 0.51 m.

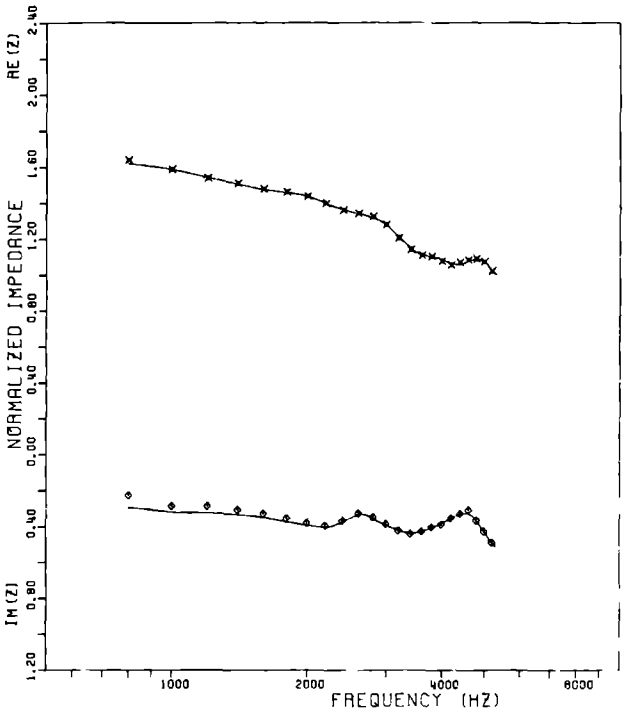

Figure 2.70 The normalized specific impedance of a layer of oak leaves (1.2×1.2 m^2, height 0.122 m) on a steel plate (2×2 m^2) measured with the frequency domain method. Truncation of the pulses according to eq. 2.25. Source height, 1.725 m, microphone height, 0.50 m.

2.2.5 Conclusion

The results obtained with the pulse measurement in the anechoic room confirm the outdoor results from the inclined track measurements: vegetation produced layers absorb much sound energy, especially above 2 kH; the influence of the underlying mineral soil is fully neglectable because of this vegetation influence; the absorption of sound takes place in the uppermost 10 cm of soil.

The pulse method proved to work sufficiently well but a number of sources of error limit the practical applicability of this method: errors in measuring the distances and heights of the speaker and the microphone, errors introduced by sampling the pulses and artefacts caused by the finite dimensions of the reflecting soil sample.

If we assume an incertitude in the path length difference between the direct and the reflected pulse of 1 cm, this will result in a variation of 30 μs in the arrival time between two pulses. The variation of the amplitude will be negligible.

Sampling the pulses with 100 kHz restricts the time resolution in the determination of t_r and t_b to 20 μs. At 500 Hz this introduces an error in

ϕ of 0.25 rad and this will increase linearly with frequency. The 8-bits conversion provides for a S/N-ratio of 59 dB. From eq. 2.22 it can be seen that A_r is very sensitive for round-off errors in A'_n and B'_n when the surface under investigation is very hard (A'_n nearly equals B'_n).

A major difficulty in the estimation of the specific impedance of an infinite ground surface from measurements on a finite soil sample is introduced by the refraction of sound. Sound with a wavelength smaller than two or three times the cross-section dimensions of an object with infinite impedance will not be reflected totally [16]. Since the smallest dimension of our samples is 1 m, this would mean that frequencies below 1 kHz would yield reflection coefficients that are systematically too low.

This pulse-sound method can contribute adequately to further investigations of the acoustic properties of soil surfaces. Its application in the measurements of impedances of natural soils will not be restricted by the finite dimensions of the soil sample and it can therefore be used to answer the many burning questions in this field of research.

Chapter 3

Measurements of specific flow resistances of soil samples

3.1 Introduction

The purpose of this chapter is to describe a flow resistance measuring device, to measure the R_s of soil samples, to check the condition of laminar flow (R_s independent of flow rate) and to compare measured R_s-values with acoustically derived ones. This latter experiment can be looked upon as being a test for the validity of the Delany and Bazley relations (eqs. 1.19 and 1.20).

This test is necessary because many investigators use these relations in models for outdoor sound propagation, especially in models for traffic noise propagation [5, 8, 35, 99]. They use R_s rather than Z_s because R_s can be derived from simple acoustical measurements with one microphone and for all frequencies at one time whereas the measurement of Z_s is difficult since it depends on the sound frequency. Directly measured R_s-values for soils are very rare [7].

Furthermore, the measurement of air flow resistance of soil samples can be relevant to agriculture. The first researcher in the Netherlands to note this was Janse [63]. The physical condition of soils is of practical importance of farmers. The growth of plants depends on a good gas-exchange in the soil and the porosity largely determines the water transport [13] and consequently the transport of dissolved nutrients. It is conceivable that physical properties of soils as acoustic impedance and flow resistivity could contribute considerably to the already existing large body of soil physical theory [2, 61, 94, 128].

Calculation of specific flow resistance

The international standard ISO/DIS 4638 [62] was used to calculate R_s, the specific flow resistance in Nsm^{-4}:

$$R_s = (\Delta p \cdot A)/(q_v \cdot l) \qquad (3.1)$$

with: Δp (Pa) as the pressure difference between the front edge and the rear edge of the soil sample, A (m^2) the cross-sectional area of the sample, l (m) its thickness and q_v (m^3/s) the air volume flow through the sample. In our case the relationship between Δp and the voltage U on the pressure gauge was described with: $\Delta p = (13.158)\ U$. With our standard sample thickness of l=0.05 m and diameter of 0.05 m, equation 3.1 reduces to:

$$R_s = 1\ 860\ 168(U/q_v') \quad Nsm^{-4} \qquad (3.2)$$

with q_v' in l/h.

Relation between air flow and sound pressure level

With increasing sound pressure levels the air molecules move faster. The correlation between pressure p and particle velocity u, is given by $p/u=Z_c$. By relating the pressure to $p_o=2\times10^{-5}$ Pa and using $Z_s=440\ kgm^{-2}s^{-1}$ for air, we obtain the following:

$$L_p = 20\ lg\ (p/p_o) = 20\ lg\ u + 146.87 \quad dB \qquad (3.3)$$

In the case of our sample tube this results in the following relation between L_p and the air flow q_v' through the sample:

$$L_p = 20\ lg\ q_v' + 69.88 \quad dB \qquad (3.4)$$

From this equation it can be seen that, if we want to know the behaviour of a material under the influence of sound with a level between 80 and 100 dB, we have to use flows between 3.2 and 32.1 l/h. A former German standard (DIN 52213, see [56]) advises us to measure at $u=5\times10^{-4}$ m/s (3.2 l/h).
Eq. 3.3 is only valid outside the soil sample. Inside it, the effective area will be smaller than the cross-sectional area of the sample: the porosity is not equal to 1. As a result of this, the particle velocity inside the pores, u_p, will be higher than the velocity u outside the sample. This is known as the relation of Dupuit [20]: u/u_p is equal to the porosity.

Description of the apparatus

On the basis of information from the literature [3, 14, 62, 69, 78], we designed a specific flow resistance measuring device especially suitable for measuring the values of Δp and q_v that are to be expected for soil samples.

A schematic representation of the flow resistance measuring device is given in fig. 3.1. The main part consists of a sample tube holder, through which air is sucked in by a jet-nozzle. The flow q_v is measured with a flow tube connected in series with the sample holder. The pressure difference over the soil sample is measured with a pressure gauge. The jet-nozzle was fed by pressurized air which was stabilized by a pressure tank.

The cylindrical sample tube holder (see fig. 3.2a) is constructed in such a way that the streamings profile in the tube before and after passage of the air through the sample is identical. Asymmetrical flow would result in a pressure difference because of the Venturi effect. No Venturi effect was measured: the pressure difference over the empty holder was zero for all flows applied.

The holder can be extended to contain more than one soil sample by attaching extra cylinders. Fig. 3.2a shows the holder with two cylinders, one of which contains a soil sample. This was done in order to extend the measuring range to those lower R_s-values expected with highly porous organic soil layers.

Special care was taken to prevent leakage of air between the soil sample and the inner wall of the sample holder and between the inner wall of the sample holder and the outer wall of the sample tube (see fig. 3.2b). The soil sample rested on a wire-mesh which offered negligible resistance to the air flow.

The pressure gauge (MKS Baratron, type 220B, MKS Instruments Inc., Burlington USA) measures the pressure difference by means of the change in distance between an immobile electrode and a movable metal diaphragm. Its measuring range is from 0-130 Pa; its sensitivity is 76 mV/Pa.

The voltmeter (Philips, PM2513A) has an accuracy of 2 mV, resulting in an accuracy in pressure of 25 mPa.

The flowmeter (Brooks Instruments rotameter) has a replacable tube. We used a low flow tube (measuring range 0-15 l/h, accuracy of 0.25 l/h) and a high flow tube (measuring range 0-150 l/h, accuracy of 2.2 l/h). Calibration graphs were used to derive the flow in l/h from the height of the float in mm.

Figure 3.1 A schematical representation of the components of the device for measuring specific flow resistances of soil samples.

1. flow meter;
2. sample tube holder;
3. pressure gauge;
4. voltmeter;
5. jet-nozzle;
6. flow control valve;
7. air buffer tank;
8. pressure regulator;
9. inlet of pressurized air

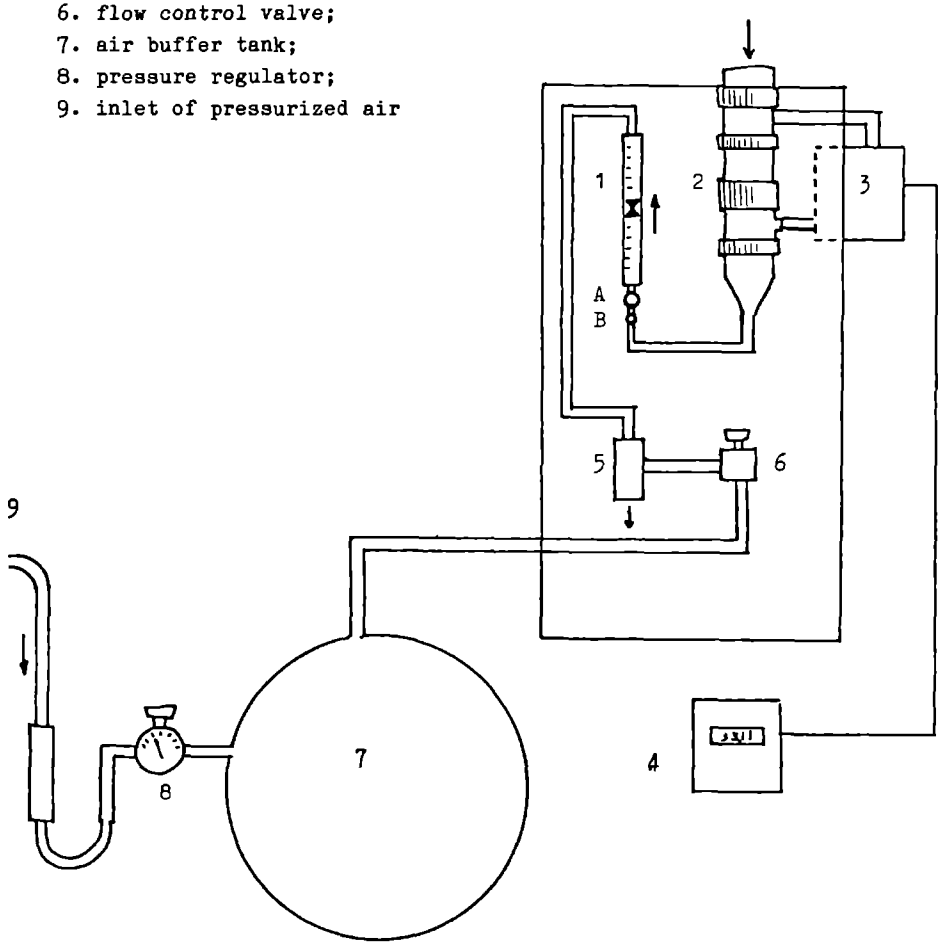

Figure 3.2. The sample tube holder (a) and a detail of the sealing up of the leaks between sample tube and holder (b). The black ellips is a rubber O-ring.

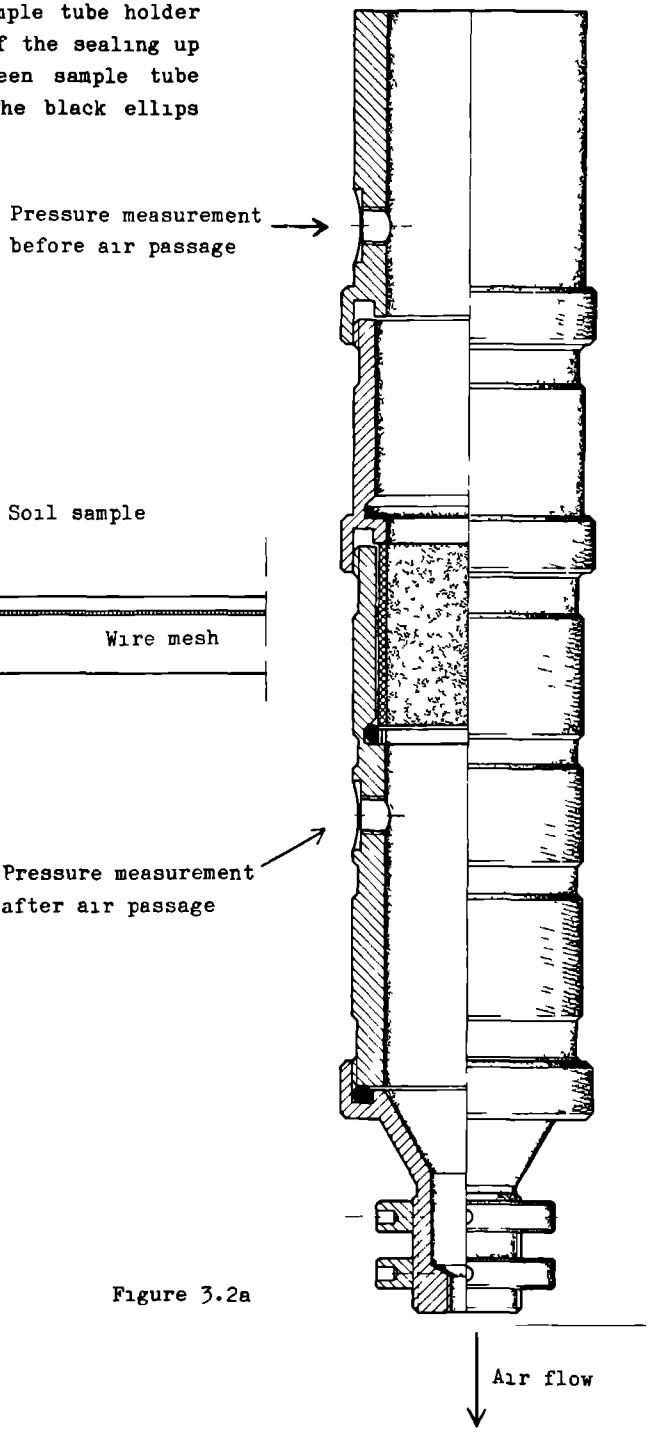

gure 3.2b

Figure 3.2a

3.3.1 Measured specific flow resistances

Specific flow resistances were measured of samples of five different materials: foam-plastic, wet peat mul, dry shifting sand, a grass-grown compact sandy soil and a barren sandy soil.

A sample of foam-plastic (l=0.05 m, weight=6.73 g), used as acoustical absorber in our anechoic room, was the first object to be measured (table 3.1). The results indicate that flow resistivities measured in the lower part of the measuring range tend to decrease with increasing flow rates. This was also found in the other materials. The discrepancy between measurement 2 and 3 was caused by the fact that in between these measurements, the sample of plastic-foam had been removed from the sample tube.

One sample of dry shifting sand was measured (see fig. 3.3). This was the same sand as used in the pulse measurements (sect. 2.2). The bulk density of the sample was 1608.8 kgm^{-3}, volume percentage of air was 27 %, of solid matter and water together 73 %.

Five samples of wet peat mul were measured (table 3.2). This material can be regarded as being similar to the organic layers encountered in forest floors. The results show a large variation between peat samples, both in R_s and in other physical characteristics. An increase in R_s of approximately 7 % with a decrease of flow from 31.2 to 18.0 l/h, however, is common to all samples: the correlation coefficient between the corresponding R_s-values of two samples is 0.99. This increase is not significant because of the S.D. of 20 %. The correlation of R_s at 62.4 l/h and the weights of the samples was better (correlation coefficient of 0.99) than the correlation of these values and the volume percentages of air (correlation coefficient of -0.81).

Five samples of compact natural grass-grown sandy soil were also measured (table 3.3). The 5 cm thick samples included an upper 1-3 cm zone that was densely rooted and covered by grass and moss. These results are an indication of the variability of R_s for soil samples, resulting in an S.D. of 25 % for four samples. All samples could be taken from the soil relatively undisturbed. However sample 3 was clearly falling apart and sample 5 contained a large stone (weight 54.9 g, total weight of the sample 150.0 g) that probably caused a relatively high flow resistivity.

Five samples of barren sandy soil at Wezep were also analysed (table 3.4). This soil contained no plant material, and it was very homogeneous, at least at first sight, but even in this ideal case the variability of the five samples was large: an S.D. of 20-25 % for n=5. The samples had such high resistances that they had to be halved in length to make measurements

of the pressure difference possible at the highest flow rates. This was possible since flow resistivities are independent of the length of a (homogeneous) sample.

As to the relation between R_s and q_v, the following: it has to be clear that the definition of R_s includes the necessary condition of laminar flow, i.e. an R_s independent of q_v. All measurements show a decreasing resistivity with increasing flow for the low flow rates, followed by quite stable resistivities for high flow values. The same phenomenon was measured elsewhere for plastic foam of polyether material and for cotton wool [56]. The authors do not try to explain this. Kilmer found just the reverse for fiber metal: an increase of R_s for increasing flows [69]. He attributes this to large errors in the measured pressure difference at low flow rates.

The flow resistivities found are in keeping with intuitively expected relative resistances. For the five materials tested, R_s increases in this order: wet peat mul (22 000); foam-plastic (60 000); dry shifting sand (240 000); barren sandy soil (366 000) and grass-grown compact sandy soil (530 000).

Other investigators also measured flow resistivities of soils and our results are of the same order of magnitude [7]. In this article, values for several types of sand are given: 61 200; 110 160; 306 000; 612 000 and even 958 800. For a natural grass-covered field a value of 300 000 was found.

Table 3.1 Three measurements on a foam-plastic sample. Both measurement 1 and 2 were performed with the high flow tube; measurement 3 was performed with the low flow tube.

	Measurement 1		Measurement 2		Measurement 3		
q_v'	U	R_s	U	R_s	q_v'	U	R_s
18.0	0.69	71 306	0.70	72 340	2.1	0.069	61 120
31.2	1.12	66 775	1.13	67 372	2.75	0.087	58 849
43.2	1.53	65 881	1.56	67 173	3.6	0.110	56 838
57.6	1.96	63 297	1.98	63 943	4.6	0.136	54 996
67.2	2.39	66 158	2.41	66 711	5.75	0.166	53 702
74.4	2.63	65 756	.	.	7.05	0.20	52 770
79.2	.	.	2.81	65 998	8.3	0.23	51 547
90.0	.	.	3.22	66 553	9.6	0.27	52 317
102.0	.	.	3.69	67 294	10.8	0.30	51 671
					12.0	0.335	51 930
					13.2	0.37	52 141

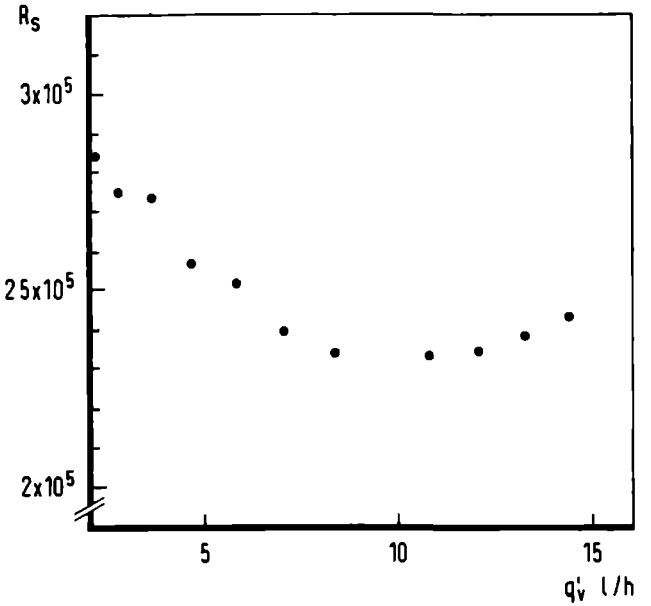

Figure 3.3 Measured R_s as a function of air flow through a sample of dry shifting sand.

Table 3.2 Flow resistivities and soil-physical characteristics of five samples of wet peat mul.

q_v'	R_s						
	sample 1	sample 2	sample 3	sample 4	sample 5	average	S.D.
18.0	18 602	18 602	27 903	27 903	24 802	23 562	4702
31.2	16 694	17 886	25 637	25 637	23 848	21 940	4328
43.2	16 793	17 654	25 836	25 405	23 252	21 788	4291
62.4	16 098	17 290	25 040	24 743	22 954	21 225	4233
Weight (g)	40.6	42.4	48.1	44.6	44.9	44.1	2.8
Air (vol %)	59.3	56.7	51.6	54.0	57.4	55.0	3.0
Water (vol %)	27.5	29.0	31.1	27.7	30.4	29.2	1.6
Solid (vol %)	13.2	14.3	17.3	18.3	12.2	15.1	2.6

Table 3.3 Flow resistivities and soil-physical characteristics of five samples of a grass-grown, compact sandy soil (in front of the Graalburcht).
The soil structure of sample 3 was clearly disturbed and this sample was therefore excluded when determining the average.

q'_v	R_s						
	sample 1	sample 2	sample 3	sample 4	sample 5	average	S.D.
14.8	594 500	472 583	169 678	300 392	486 409	463 471	121 618
21.8	680 071	552 077	194 550	344 728	554 637	532 878	138 934
29.6	716 406	572 504	205 498	357 580	580 046	556 634	148 267
36.6	.	594 136	211 937	365 427	602 268	520 610	134 454
weight (g)	143.6	124.2	120.8	127.2	150.0	133.2	12.9
air (vol %)	35.1	45.6	46.5	44.2	36.9	41.7	5.3
water (vol %)	5.8	5.5	5.6	4.9	4.0	5.2	0.7
solid (vol %)	59.1	48.9	47.9	50.9	59.1	53.2	5.5

Table 3.4 Measured flow resistivities as a function of air flow for five samples from the barren sandy soil at Wezep.

Flow	R_s (10^{+3} Nsm^{-4})						
l/h	Sample 1	Sample 2	Sample 3	Sample 4	Sample 5	Average	S.D.
24.6	501.6	277.3	231.6	392.3	386.2	357 ±	106
37.2	513.4	285.4	237.5	399.0	394.7	366 ±	108
49.8	513.0	286.4	237.3	395.3	396.2	366 ±	108
61.8	516.7	288.5	237.7	393.8	399.4	387 ±	85
73.2	.	289.6	238.8	404.0	402.0	334 ±	83
84.6	.	289.0	239.6	396.7	402.1	332 ±	81
95.4	.	290.0	238.5	401.0	.	310 ±	83
105.6	.	293.2	241.1	.	.	267 ±	37
110.4	.	293.1	239.4	.	.	266 ±	38
l (mm)	30	24	24	24	28		

3.3.2 Comparison of measured and acoustically derived resistivities

For a number of soil samples measured in the previous section, R_s was also derived from acoustical measurements of Z_c: the wet peat mul and dry shifting sand indoors with the pulse-method and the barren sandy soil with the inclined track method.

These measurements of layers of wet peat mul (section 2.2.4) with 30.9 vol % water gave as a result R_s=146 198 Nsm^{-4}; direct measurement of R_s resulted in 22 000.

Dry shifting sand (section 2.2.4) gave acoustically 250 754, whereas the direct measurement gave 240 000.

It is also interesting to look at table 2.8 which shows acoustically derived R_s-values for undisturbed outdoor surfaces. During these measurements we were not yet able to measure R_s directly on soil samples. We performed only one inclined track measurement (number 23, at Wezep) coupled with measurements of R_s of soil samples taken immediately after the completion of the acoustical measurement. The terrain at Wezep was a barren sandy soil (bulk density 1,700.3 kg/m^3, 26.9 vol % air, 9.3 vol % water and 63.8 vol % solid matter) without vegetation. The results of the measurements are represented in table 3.4

Both the measured impedances and the measured flow resistivities indicate that the bare sandy terrain at Wezep is acoustically relatively hard (see fig. 3.4). Furthermore, these measurements made it possible to test the validity of the empirical formulas of Delany and Bazley. These are often used to predict the frequency behaviour of the specific impedance of outdoor surfaces although they were based on measurements on material with a porosity of almost 1. From the results in chapter 2 it can be seen that this condition is not satisfied by soils. A second problem is that the impedance calculated from the flow resistivity is the characteristic impedance, while the impedances measured outside are specific impedances. These two impedances are only identical if the soil is assumed to be homogenous and unlayered. Since this rare condition is satisfied by the circumstances in Wezep, a comparison is allowed. Thus, on the basis of our measured R_s of 366 ± 108 × 10^3 Nms^{-4}, we calculated the range of $Z_c/\rho c$ and plotted this in figure 3.4 (the area between the dotted lines). The scatter of measured impedances lies reasonably well within the area of calculated impedances. We also checked the Delany and Bazley relations the other way round: by calculating a best fitting flow resistivity to the 19×20 measured sound pressure levels. The result of this fit (with a sum of squares of 1600, i.e. an average difference of 2 dB between measured and calculated levels) was R_s=315 × 10^3 Nsm^{-4}. The frequency behaviour of $Z_s/\rho c$ resulting from this flow resistivity is also rendered in fig. 3.4 (the full line). Again, the agreement is good. A similar flow resistivity was found by others [9].

In general it can be concluded that the Delany and Bazley relations are satisfied in the frequency range under consideration (200-1300 Hz), but it is difficult to say what will happen at lower frequencies.

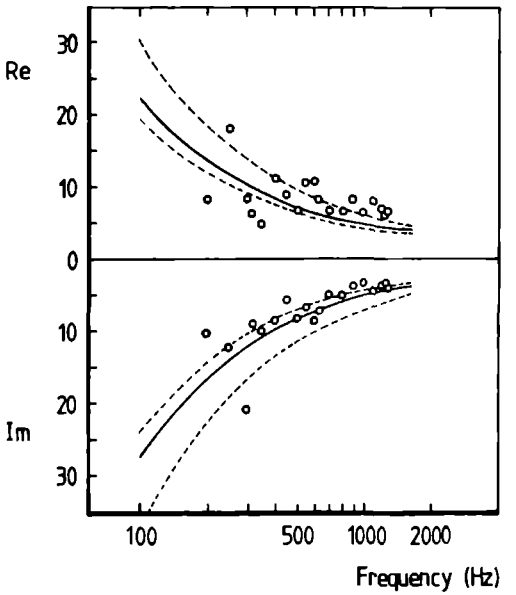

Figure 3.4 The specific impedances as calculated from the interference patterns (circles). The areas within the dotted lines correspond with the impedance ranges predicted by the formulae of Delany and Bazley on the basis of the measured flow resistivity of $366 \pm 108 \times 10^3$ Nsm^{-4}. The full lines represent the frequency behaviour of $Z_s/\rho c$ on the basis of $R_s = 315 \times 10^3$, the flow resistivity that gave the best fit to the measured interference patterns.

Chapter 4

Relative contributions of ground and vegetation to sound propagation

4.1 Introduction

For many years the question of the relative contributions of the elements that make up a forest to the total sound absorbing characteristics of forests have remained unanswered [8, 11, 40, 42, 79, 81, 132]. The major elements in a forest are the floor, trunks , twigs and leaves or needles. The floor is the principle element responsible for the sound interference patterns set up by the interaction of direct and ground reflected sound, living plant parts will influence sound by viscosity and thermal conductivity losses [8], by scattering [8, 82] and by movement of leaves [85]. These last factors depend linearly on the amount of biomass between the sound source and the receiver and if the amount of biomass is proportional to the distance (which is not often the case, by the way) , then the sound absorption through vegetation alone is expected to be proportional to the distance. This is the reason why attenuation through forests is often expressed in dB/100 m. Because of the very nature of the ground effect this factor, however, is not linearly dependent on distance and it is influenced by both source and receiver heights and by the horizontal distance. The purpose of this chapter is to extract this ground influence from sound propagation measurements thus obtaining the excess attenuations solely attributable to the vegetation. These values could then be expressed in dB/100 m.

As was seen in chapter 1.2, many models exist that describe pure tone sound pressure level above an impedance boundary. Most experimental results on the sound propagation through forests, however, are represented in the form of 1/3-octave or octave spectra. To be able to extract the ground influ-

ence from these measurements, a model was developed that calculates the 1/3-octave sound pressure level relative to the free field above an impedance boundary, in this case a forest floor. This model was used in the first place to investigate the theoretical influence on the ground contribution of experimentally relevant parameters as air temperature and humidity, heights of the sound source and receiver above the ground, the horizontal distance between source and receiver and of the acoustical soil parameters R_s and layer thickness. Secondly, the model was used to simulate some classical measurements of sound transmission in or through vegetation as reported in literature. We have tried to give indications of the relative contributions of ground and vegetation in these measurements.

4.2 The 1/3-octave model

A model was developed to calculate the 1/3-octave sound pressure levels relative to the free field of a sound source above an impedance boundary. The method used consisted of the calculation of the pure tone sound pressure levels according to the theory [23] presented in chapter 1.2. weighting these for 1/3-octave chararacteristics and summing these to get the 1/3-octave sound pressure levels.
To characterize the transmission through a 1/3-octave band with centre frequency f_c, we used the following equations for the transmission loss TL, i.e. the difference between input and output output sound pressure levels. The nominal lower and upper cutoff frequencies f_1 and f_2 are defined as [114]:

$$f_1 = 1/f_2 = 10^{-1/30} \times f_c \qquad (4.1a)$$

and for $f<f_1$ or $f>f_2$:

$$TL(f) = 10\lg A + B[C(f/f_c) - f_c/(Cf)]^6 \qquad (4.1b)$$

with TL(f) : transmission loss as a function of f

$A = 8/13$

$B = 2547.0$

$C = 10^{-1/60}$ if $f<f_1$ and

$= 10^{1/60}$ if $f>f_2$

For $f_1<f<f_2$, TL(f)=0 dB.

If $L_t(f)$ is the pure tone sound pressure level above an impedance surface, then L_c, the corresponding 1/3-octave sound pressure level above that surface, will be:

$$L_c = 10\ \lg\left\{\int_0^{\infty} 10^{[L_t(f)+TL(f)]/10}\ df\right\} \qquad (4.2)$$

We are mostly interested, however, in $L_{rf,c}$, the 1/3-octave sound pressure level relative to the free field. $L_{rf,c}$ is independent of the source strength and it excludes the influence of the attenuation over distance, therefore it is the most appropriate measure of the influence of the soil surface on the sound propagation. Furthermore, $L_{rf,c}$ has been measured for many surfaces, which makes possible a comparison of theoretical and experimental values.

If we define $L_{ft}(f)$ as the free field pure tone sound pressure level and L_{fc} as the free field 1/3-octave sound pressure level, $L_{rf,c}$ can be written as:

$$L_{rf,c} = L_c - L_{fc}$$

$$= 10\ \lg\left\{\frac{\int_0^{\infty} 10^{[B_t(f)+L_{ft}(f)+TL(f)]/10}\ df}{\int_0^{\infty} 10^{[L_{ft}(f)+TL(f)]/10}\ df}\right\} \qquad (4.3)$$

with $B_t(f) = L_t(f) - L_{ft}(f)$. The level $B_t(f)$ is the pure tone sound pressure level that can be calculated with equation 1.5. To come to a practically computable form, equation 4.3 has to be simplified. If $L_{ft}(f)$ is constant within the frequency limits of 1/3-octave band number c, 4.3 reduces to:

$$L_{rf,c} = 10\ \lg\left\{\frac{\int_0^{\infty} 10^{[B_t(f)+TL(f)]/10}\ df}{\int_0^{\infty} 10^{TL(f)/10}\ df}\right\} \qquad (4.4)$$

These integrals cannot be solved because of the intricate frequency dependence of B_t. They have to be approximated numerically:

$$L_{rf,c} = 10\ \lg\left\{\frac{\sum_{n=0}^{\infty} 10^{[B_t(f_n)+TL(f_n)]/10} \times \Delta f}{\sum_{n=0}^{\infty} 10^{TL(f_n)/10} \times \Delta f}\right\} \qquad (4.5)$$

with $f_n = n \times \Delta f$

This approximation is only possible if the variations in $B_t(f)$ and $TL(f)$ are small over the interval Δf. Because $TL(f)$ decreases rapidly beyond the frequency limits f_1 and f_2 (see equation 4.1b), the summation does not have to go from 0 to ∞ but from F_1 to F_2 ($F_1 < f_1$, $F_2 > f_2$, $F_2 = N \times \Delta f + F_1$):

$$L_{rf,c} = 10 \lg \left\{ \frac{\sum_{n=0}^{N} 10^{[B_t(F_1+n\Delta f)+TL(F_1+n\Delta f)]/10}}{\sum_{n=0}^{N} 10^{TL(F_1+n\Delta f)/10}} \right\} \qquad (4.6)$$

For our purpose we have set F_1 to $0.7f_c$ and F_2 to $(10/7)f_c$. This means that we included all frequencies around f_c where the filter attenuation was less than 30 dB. Equation 4.6 will give the 1/3-octave sound pressure level relative to the free field for band c if the pure tone sound pressure levels are known for all frequencies between F_1 and F_2. This equation represents then the ground attenuation component in 1/3-octave sound propagation spectra through forests. The attenuation by spherical spreading and the absorption by vegetation and air are separated out.

Influence of N on $L_{fr,c}$

Since the transmission characteristics of the model displays large dips, $L_{rf,c}$ will depend on N, the number of sample pure tones within the frequency band. Table 4.1 shows that the difference in dB between 2 samples per band and 30 samples per band can amount to as much as 4 dB, indicating that the comparison of pure tone models with 1/3-octave data [5, 101] can be quite dangerous. On the basis of table 4.1 we decided to include as a rule 60 pure tones for the calculation of $L_{rf,c}$. This amounts to a maximal error of 0.1 dB.

4.3 Results and discussion

The sound propagation through forests is influenced by many interrelated parameters. To facilitate the analysis of these parameters, a standard situation was selected. The values for the model parameters are listed in table 4.2. Unless stated otherwise, these values were used in the computations. The ground effect in these situations is plotted in fig. 4.1.

Table 4.1 Influence of the number of pure tones included in the calculation of $L_{rf,c}$. $R_s = 5 \times 10^4$ Nsm^{-4} and d=0.035 m, source and receiver heights were 1.22 m, their distance 48.0 m.

1/3-octave f_c(Hz)	Number of pure tones (N) 2	5	10	15	30	100
250	- 3.12	- 4.87	- 4.86	- 4.74	- 4.81	- 4.80
315	-18.40	-19.50	-18.96	-18.92	-18.94	-18.92
400	-17.90	-15.84	-15.69	-15.80	-15.74	-15.74
500	-10.00	-11.40	-10.04	- 9.97	-10.04	-10.00
630	- 6.91	- 6.16	- 6.11	- 6.15	- 6.13	- 6.13
800	- 3.71	- 3.12	- 3.09	- 3.12	- 3.10	- 3.10
1000	- 1.29	- 0.80	- 0.77	- 0.80	- 0.78	- 0.78
1250	0.76	1.19	1.21	1.18	1.20	1.20
1600	2.68	3.02	3.04	3.02	3.03	3.03
2000	4.07	4.32	4.34	4.32	4.33	4.33
2500	5.03	5.15	5.15	5.15	5.15	5.15
3150	5.28	5.16	5.14	5.15	5.14	5.14
4000	3.95	3.24	3.19	3.24	3.21	3.21
5000	- 1.09	- 3.24	- 3.26	- 3.12	- 3.20	- 3.19
6300	- 5.02	- 1.02	- 1.17	- 0.94	- 1.11	- 1.02
8000	4.47	4.92	4.90	4.88	4.89	4.89
10000	3.61	1.34	1.25	1.41	1.31	1.33

4.3.1 Variation of model parameters

The weather is the most hindering of all the uncontrollable experimental factors affecting outdoor sound propagation measurements. The influence of air temperature, humidity and pressure on the absorption of sound has already been sufficiently investigated (see chapter 1.2). Most researchers therefore correct their transmission spectra for air absorption.
Vertical gradients of temperature and wind velocity also influence the interference pattern because of the curvature of sound rays. As a result, the phase difference between direct and reflected rays changes, consequently shifting the frequencies at which positive or negative interference occurs. This effect cannot be corrected for because of incomplete theoretical and insufficient experimental material. In zero-gradient situations the interference patterns still depend on air temperature, humidity and pressure.

Table 4.2 The model parameters for the standard situation.

Model parameter	Value
Temperature	15 °C
Relative air humidity	80 %
Absolute air pressure	101.33 kPa
R_s	10^5 Nsm^{-4}
Layer thickness	∞
Source height	0.44 m or 1.20 m
Receiver height	1.5 m
Horizontal distance	36.4 m or 40.0 m

These influence the sound speed (see eqs. 2.4-2.5) and consequently the wave number $k=\omega/c$.
By varying air temperature we could calculate its influence on the ground effect. The effect was linear with temperature between 0 and 30°C and could therefore be expressed as dB/°C (see fig. 4.2). Only near the large interference dip was the temperature effect significant, but never more than 0.1 dB/°C. The effects of changes in humidity or pressure are even smaller. The effects of increasing source heights and increasing horizontal distances are represented in figs. 4.3 and 4.4. For very low source heights (<10 cm), high frequency sounds are strongly attenuated and the acoustic climate acts as a low-pass filter. For increasing source heights the ground effect is reduced, starting at the high frequencies. At a height of 6 m almost no interference patterns are visible above 1 kHz. The position of the first negative interference dip varies from 1250 Hz at a height of 0.11 m to 250 Hz at a height of 6 m.
Increasing the horizontal distance (fig. 4.4) has almost no effect on the position of the first negative interference dip, but it does have effect on the depth: -7 dB at 9.1 m and -27 dB at 291.2 m. The position of the second positive interference dip, however, changes drastically from 630 Hz at 9.1 m to 10 kHz at 291.2 m.

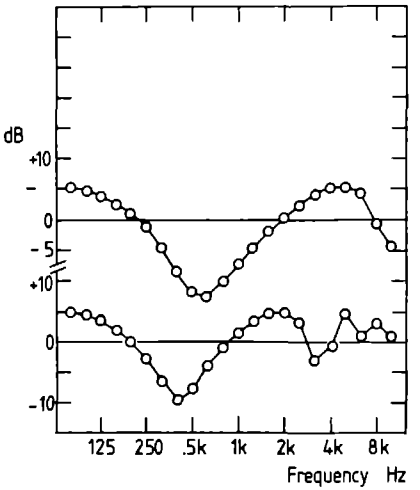

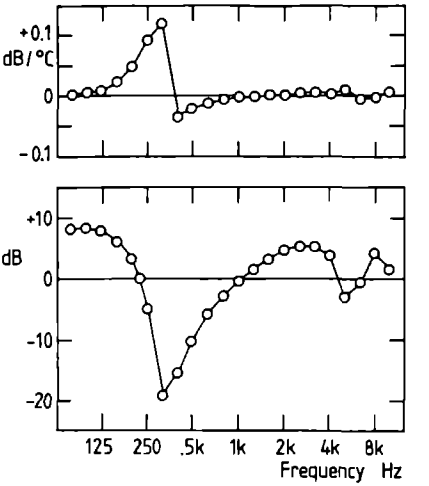

Figure 4.1. The ground effect for the standard situation. Source heights are 0.44 m (top) and 1.20 m (bottom). The distance is 36.4 m.

Figure 4.2 The effect of changing the air temperature (top) in the standard situation above a forest floor ($R_s = 5 \times 10^5$ Nsm^{-4}, layer thickness 0.035 m) on the ground effect (bottom). Source and receiver heights 1.22 m, horizontal distance 48 m.

The influence on the ground effect of the acoustical parameters of the forest floor, the specific flow resistivity R_s and the layer thickness d, is represented in figs. 4.5-4.8. The first important conclusion that can be drawn from these results is, that above 2 kHz the ground effect is not influenced by the acoustical characteristics of the forest floor . This means that for frequencies above 2 kHz a ground correction factor can be calculated solely on the basis of the geometry irrespective of the acoustical properties of the forest floor under consideration. Above 2 kHz the ground contribution to the total transmission spectrum of vegetation is independent of the sound absorbing qualities of the forest floor.
The second conclusion is that below 2 kHz R_s and d have a dramatic influence on sound propagation. With a half-infinite ground (fig. 4.5) the first destructive interference minimum shifts from 63 Hz at $R_s = 10^2$ Nsm^{-4} (snow) to 800 Hz at $R_s = 10^5$ Nsm^{-4} (very hard sand). For the R_s-values of forest floors the second interference maximum always occurs between 800 Hz and 2500 Hz. This sound amplification is probably identical to the sound window, referred to by several authors as a vegetation effect. This is influenced by the source receiver distance (fig. 4.4).

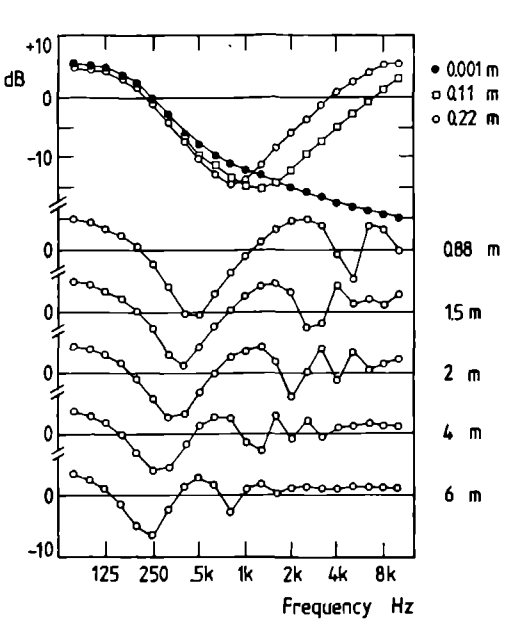

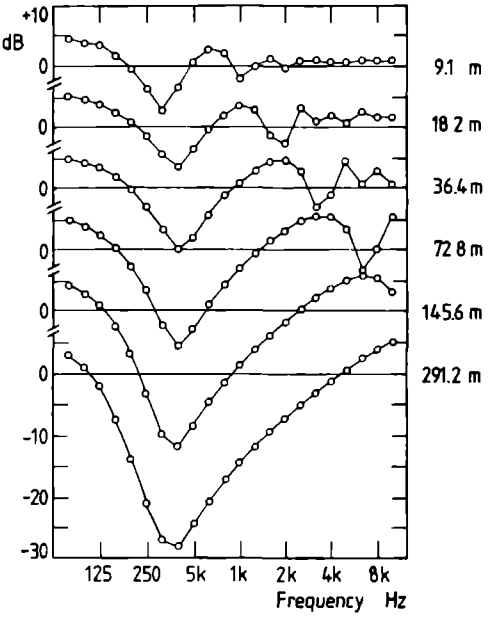

Top left: figure 4.3 The influence of varying the source height. The horizontal distance is 36.4 m.

Top right: figure 4.4 The influence of varying the horizontal distance. The source height is 1.2 m.

Page 105:

Top left: figure 4.5 The influence on the ground effect of varying R_s in the case of a semi-infinite ground. Source height 1.20 m, horizontal distance 36.4 m.

Top right: figure 4.6 The influence on the ground effect of varying layer thickness at constant R_s. Source height 0.44 m, horizontal distance 40.0 m.

Bottom left: figure 4.7 The influence on the ground effect of varying R_s at a constant layer thickness of 0.03 m. Source height 0.44 m, horizontal distance 40.0 m. The upper curve shows the ground effect for a semi-infinite ground.

Bottom right: figure 4.8 The influence on the ground effect of varying R_s at a constant layer thickness of 0.03 m. Source height 1.20 m, horizontal distance 40.0 m. The upper curve shows the ground effect for a semi-infinite ground.

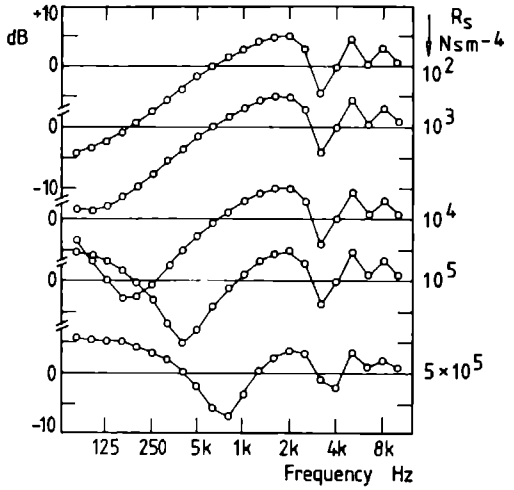
dB
+10
0
0
-10
0
0
0
-10
R_S
Nsm^{-4}
10^2
10^3
10^4
10^5
5×10^5
125 250 5k 1k 2k 4k 8k
Frequency Hz

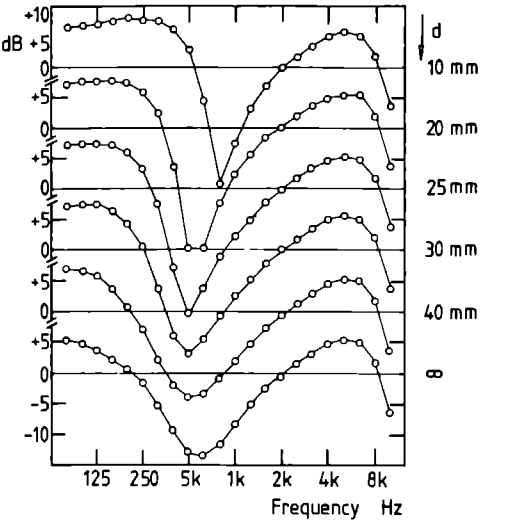
dB
+10
+5
0
+5
0
+5
0
+5
0
+5
0
-5
-10
d
10 mm
20 mm
25 mm
30 mm
40 mm
∞
125 250 5k 1k 2k 4k 8k
Frequency Hz

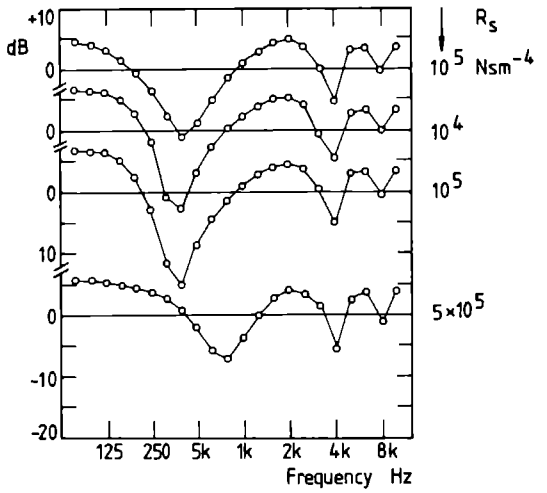
dB
+10
0
0
0
10
0
-10
-20
R_S
10^5 Nsm^{-4}
10^4
10^5
5×10^5
125 250 5k 1k 2k 4k 8k
Frequency Hz

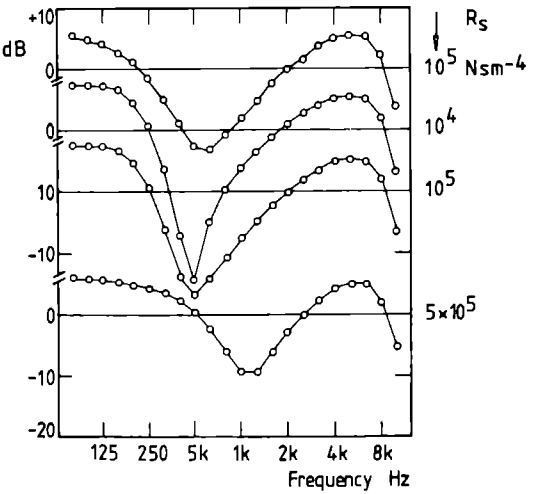
dB
+10
0
0
10
-10
0
-10
-20
R_S
10^5 Nsm^{-4}
10^4
10^5
5×10^5
125 250 5k 1k 2k 4k 8k
Frequency Hz

As expected, the first interference minimum shifts to lower frequencies for thicker layers of acoustical absorber (fig. 4.6): the ground becomes softer. A remarkable consequence of the application of a thin layer is the steepening of the slopes of the first interference minimum, especially of descending slope at the lower frequencies. It will be shown that this is also often measured in forests. The combined effect of varying R_s and d results in a shift of the first minimum to higher frequencies for increasing R_s (figs. 4.7 and 4.8).

4.3.2 Comparison with measurements

After having described the general performance of the model, a number of transmission measurements through forests are analysed with the purpose of elucidating the influence of the forest floor on these measurements.

The pioneering work of Eyring on jungle acoustics [42] is a good example of complete neglect of the influence of the forest floor on sound propagation. He worked for the American army and investigated sound propagation in Central-American jungles with application to guerilla-warfare. Eyring defined a terrain loss coefficient α as the ratio of sound pressure level difference between two points in a forest and the distance between these points. But, as stated in the introduction, the interference character of a sound field above a forest floor will inevitably result in non-linear changes with distance. After stating that the terrain loss was usually found to increase linearly with distance, Eyring concludes that measured non-linearities "seemed to be fortuitous in character and to suggest a non-uniformity of the terrain rather than a real departure from linear increase usually found." He overlooked the ground effect and calculated terrain losses based on a linear decrease of sound pressure level with distance.
Unfortunately, Eyring does not give the exact geometry of his experimental set-up. All he says is that the source and receivers were 1.50 m (6 ft) above the ground, that 2-4 microphones were used, 33 m (100 ft) or more apart, and up to 150 m (450 ft) separated from the source. These values were used to calculate the approximate influence of the ground on the terrain loss as defined by Eyring. We calculated the SPL relative to the free field for source-receiver separations of 75, 100, 125, and 150 m, at a temperature of 25 ^{o}C and a relative humidity of 80 % and for two floors, a hard one (with $R_s=2\times10^5$ Nsm^{-4}) and a soft one (with $R_s=5\times10^4$ Nsm^{-4}). The sound levels at every distance were subtracted from the levels of the next distance, and these values were averaged to get a terrain loss coefficient in dB/100 m. The results obtained are compared with measurements of Eyring in Fig. 4.9.

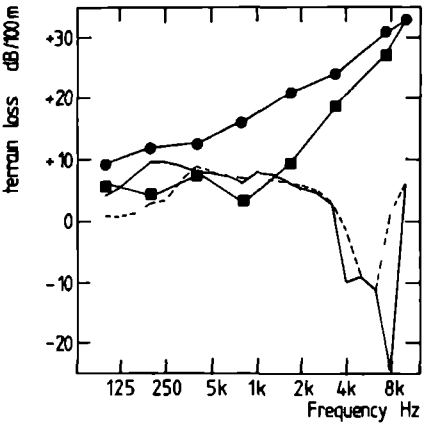

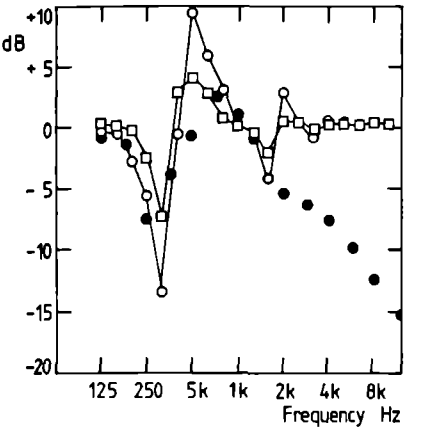

Figure 4.9 Comparison of terrain losses measured by Eyring [42] and calculated contributions of the forest floor to the terrain loss. Measurements were performed in two Central-American rain forests: las crucas No. 1 (squares) and las crucas No. 2 (circles). Calculations include a hard floor (full line) and a soft one (dashed line).

Figure 4.10 A comparison between the measurements of Beck [11] (filled circles) and two calculated excess attenuations, i.e. the SPL above the forest floor minus the SPL above a stubble-field; flow resistivity of the forest floor was 125×10^3 Nsm^{-4} (squares) and 280×10^3 Nsm^{-4} (open circles). In all cases the flow resistivity of the stubble-field was taken 50×10^3 Nsm^{-4}. The thickness of the layer was assumed to be infinite.

The terrain loss coefficient of Eyring includes the effects of vegetation, ground and air absorption; our calculated coefficients include only the ground effect. It was found that the measuring geometry of Eyring precludes the large negative interference dip below 1 kHz, common in outdoor measurements [40, 50, 79, 81, 85, 99]. Below 400 Hz the soft soil absorbs 5-7 dB more than the hard one, between 400 and 3150 Hz they both absorb 4-8 dB, and above 3150 Hz negative losses up to 26 dB can occur. Of course the model assumes the absence of any scatterers, so these values at high

frequencies do not really occur; the interference is reduced by the presence of trunks, branches and leaves, so they represent the largest influence of the floor. This comparison shows that up to approximately 2 kHz, the attenuations found by Eyring are caused by the forest floor and that at higher frequencies the forest floor could have reduced the terrain loss coefficient at the most by 26 dB.

In addition to neglecting the influence of the soil there are two other possible solutions for the problem of estimating the relative contributions of soil and vegetation: measuring the same track with and without vegetation and measuring a forest track and a nearby track without vegetation. The first solution is of course a very impracticable and unbotanical one because it entails the destruction of the vegetation. Besides, removal of the vegetation would inevitably alter the soil structure. As far as I know, only one experiment of this kind has been undertaken. This was done by Aylor [8], who measured the attenuation through a corn field before and after removal of the maize plants (Zea Mays L. var. Pa 290). In deciduous forests, however, it would be possible to measure in summer and winter, and these measurements could then be compared to yield the influence of the leaves. Although the soil surface structure also depends on the season, it was found, however, that the ground-influenced parts of 1/3-octave transmission spectra through forests were remarkably insensitive to seasonal influences [85].
The second solution, comparison of a track with vegetation and a nearby control track without vegetation, has been applied by several authors [11, 37, 40]. Embleton has measured the sound transmission through 4 types of forest and compared these with the transmission over a nearby terrain consisting of a light sandy soil covered with grass less than 15 cm long [40]. It is not possible to simulate his measurements with our model (his measuring procedures are not sufficiently described), but it is nevertheless clear that the negative excess attenuation he found for 625, 800 and 1000 Hz bands are due to the differences between the impedance of the forest soil and the sandy soil. This can be demonstrated by calculations on a similar measurement by Beck [11]. It is perhaps remarkable to note that at that time Embleton, who has now become one the greatest contributors to the field of outdoor sound propagation (cf. [99]), did not have the faintest idea of the soil influence and that he tried to explain his results in terms of resonant absorption by branches and trunks. An idea he abandoned in the same article.
Four years later the German investigator Beck presented similarly measured results, also without mentioning a possible influence of the softness of the soil [11]. We have simulated one of his measurements through a 10 m wide row of closed mixed vegetation. The source and receiver heights were 1.30 m, their distance was 15.5 m. Beck measured SPL differences between tracks through the stand and a track over a nearby stubble-field. We cal-

culated these differences for increasing differences in the flow resistivity of the two soils (see fig. 4.10). The temperature was 25 °C, the humidity 50 %. In all three cases this specific set-up yielded attenuation peaks in the 315, 1600 and 3150 Hz bands and negative attenuation peaks in the 500 and 2000 Hz bands. Up to 2 kHz these peaks also show up in the results of Beck. The peaks decrease with decreasing difference in flow resistivity. It is striking that this agreement between theory and experiment could only be attained by assuming that the forest floor was acoustically harder than the stubble-field! Generally, unplanted soil is more compact than the covering of a forest floor (see section 2.1). This comparison shows that below 2 kHz the results of Beck can be fully explained as soil artefacts and above 2 kHz as genuine excess attenuation values wholly attributable to the vegetation. In 1971 Cook and Haverbeke [24] represented the results of a very extensive investigation on the attenuation of traffic noise spectra by belts of trees. They were aware of the importance of the properties of the reflective surface and they compared the attenuation of truck noise over pavement, gravel, bare soil and plant grown soil. They found significant differences in the SPL summed over all bands which were used as correction factors in cases where the control track could not be located on the same surface through the belt as the measuring track.

Botanical Laboratory Nijmegen

For ten years now sound transmission characteristics of forests have been measured by the Department of Botany of the Catholic University of Nijmegen [79,85]. Here we will compare the results of some of these measurements with the results of simulations of the ground effect based on the measured impedances (see chapter 2.1) of the floors at these measuring-sites. This will give an indication of the ground contribution to the excess attenuation spectra. We will discuss a grass-field, a beechtree forest and a fir-tree forest.

Grass-field

The grass-field was chosen because it contained no other vegetation than short grasses and some heather-bells (Erica tetralix L.) having a maximum height of 5 cm [85]. The results of excess attenuation measurements over distances from 6 to 96 m are represented in figs. 4.11a and 4.12a, those of the simulations in figs. 4.11b and 4.12b. It is interesting to see that, although the attenuation measurements were done in June and August of 1978 and the impedance measurement, from which R_s and d were deduced, in September of 1980, the positions of the interference maxima and minima are accurately predicted for all source-receiver geometries in the attenuation measurement. The amplitudes also agree reasonably well, although the measurements give lower values (5 dB) for all frequencies. The simulation also shows that something must have gone wrong with the 96 m-measurement (dots)

in fig. 4.11a. Perhaps the loudspeaker was not accurately directed towards the last microphone or gradients spoiled the measurement. De Jong [67] has shown that the influence of gradients on sound propagation can be very dramatic, especially for frequencies >800 Hz and in down wind conditions. Another discrepancy between the simulation and the measurement is the small (2-3 dB) notch at 250 Hz in the descending slope of the first minimum. If it is not an error in the correction for the speaker characteristic, this could perhaps be the result of "grass-resonance absorption" [108]. This comparison shows that the model is quite realistic and that it can calculate the ground effect up to 96 m with reasonable accuracy.

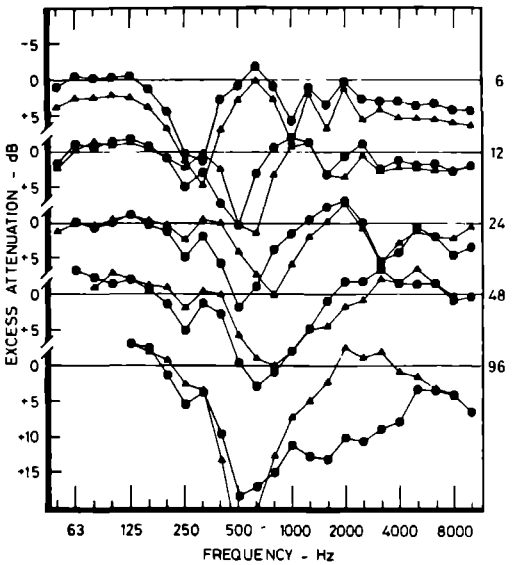

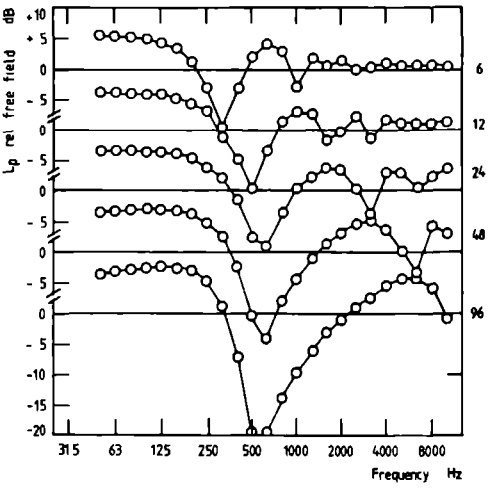

Figure 4.11a (left) Measured excess attenuation spectra, corrected for the 1/r-law and attenuation by air, at different distances between source and receiver (6, 12, 24, 48 and 96 m). Source and receiver heights 1.2 m. A positive attenuation is plotted downwards [85].

Figure 4.11b (right) Simulated ground effect spectra, calculated with eq. 4.6 for the situation of fig. 4.11a. Temperature 19.5 ^{o}C, rel. humidity 60 %, $R_s = 2.85 \times 10^{5}$ Nsm^{-4} and d=0.015 m.

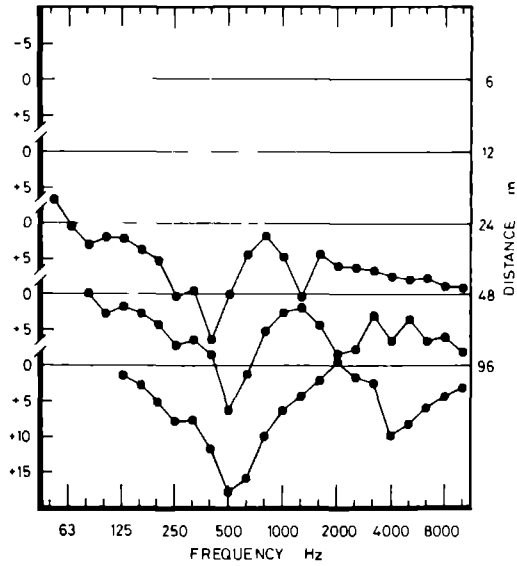

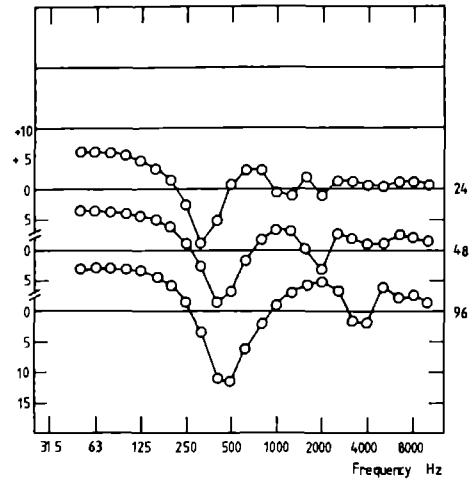

Figure 4.12a (left) As fig. 4.11a but with a receiver height of 3.9 m and only three distances (24, 48 and 96 m).

Figure 4.12b (right) Simulated ground effect spectra for the situation of fig. 4.12a. Same model parameters as in fig. 4.11b.

Beechtree forest

In this experiment an excess attenuation spectrum was measured in a beechtree forest and the impedance of the floor was measured on the same day and at the same spot. The beechtree forest is described in chapter 2.1. The impedance versus frequency characteristic (see fig. 2.36) was used to calculate an apparent R_s of 20×10^3 and d of ∞, which were subsequently used to predict the ground effect in the measured excess attenuation spectrum. Fig. 4.13 shows that the measured first minimum was situated at 200 Hz , while the predicted one was at 250 Hz. This means that the actual impedance of the floor was lower than the measured one. Although above 1 kHz the measurement shows only the small absorption of 2-3 dB, the simulation indicates that this is the result of a combined effect of the ground amplification of up to 5 dB and of the vegetational absorption, which consequently should have been 7-8 dB. Furthermore, the measured diffence between the second minimum (at 2500 Hz) and the second and third maximum (at 1600 and 5000 Hz) is approximately 5 dB, which is smaller than the predicted difference of 8-9 dB. This is probably due to a disturbance of

the phase relation of direct sound and the ground reflected sound as a result of the scattering from plant parts.
From fig. 4.11a (48 m) and fig. 4.13 it follows that the measured lower impedances of the forest floor (relative to those of the grass-field) result in a detectable shift of the first minimum from 630 Hz (grass-field) to 250 Hz (beechtree forest). This shift could adequately be predicted with the measured impedances and the model.

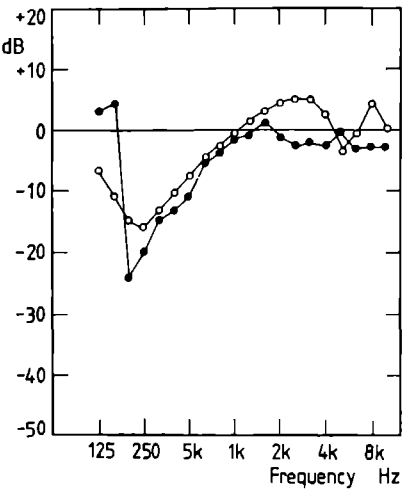

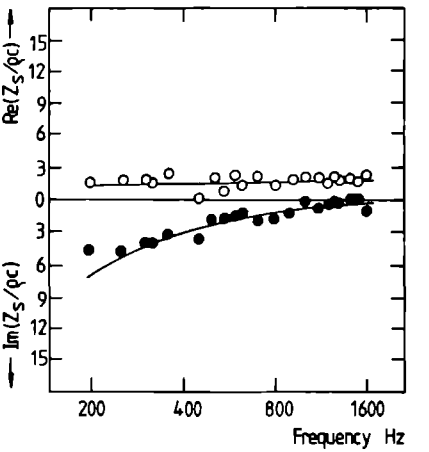

Figure 4.13 (left) Comparison of a measured excess attenuation (filled dots) and a calculated ground effect (open circles) for a beechtree forest. Source and receiver heights 1.22 m, horizontal distance 48 m, temperature 18 °C, rel. humidity 38 %. The measured impedance is represented in fig. 2.36.

Figure 4.14 (right) The measured normalized Z_s values for the fir-tree forest. The lines indicate the Z_s-values calculated with $R_s = 50 \times 10^3$ Nsm^{-4} and d=0.035 m.

Fir-tree forest

In August 1980 the impedance characteristics of a fir-tree forest were measured (see fig. 4.14). Two years later (in January 1982) the excess attenuation was measured in the same forest. This measurement was simulated with an apparent R_s and d calculated from the measured impedances (fig. 4.14). The results are represented in figs. 4.15-4.16. Again, the measurements and the calculations are in reasonable agreement. Above 2 kHz the interfence dips can be traced in the measurements and the ground again seems to reduce the sound absorption by some 5 dB.

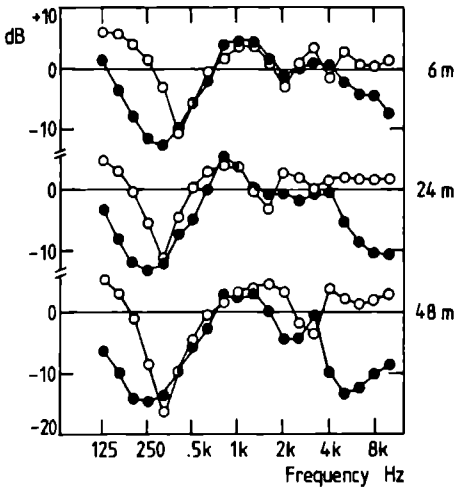

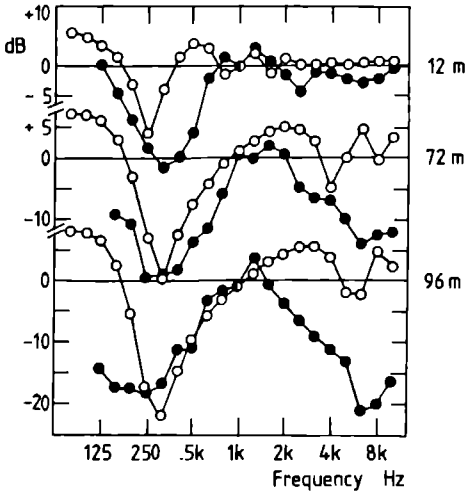

Figures 4.15a (left) and 4.15b (right) The measured excess attenuations in the fir-tree forest (filled circles) and the calculated ground effect (open circles), for horizontal distances of 6, 12, 24, 48, 72 and 96 m. Source height 0.72 m, microphone heights 3.90 m (except for 6 and 12 m with heights of 1.22 m), temperature 2.8 °C. rel. humidity 95 %, $R_s = 50 \times 10^3$ Nms^{-4}, d=0.035 m.

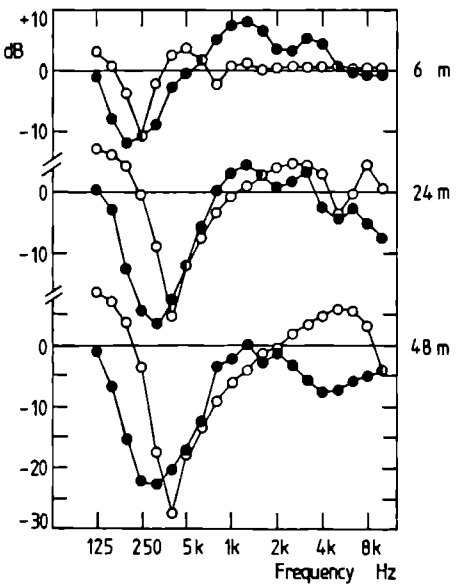

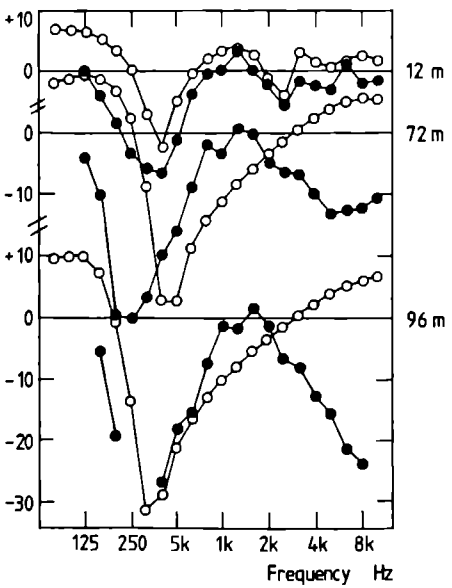

Figures 4.16a (left) and 4.16b (right) The same as in fig. 4.15 but with all microphones at heights of 0.60 m.

4.4 Conclusions

The above results prove that the relative contributions of both the forest floor and the vegetation to sound propagation through forests can easily be decribed as follows. Below 2 kHz, the vegetation has no influence and the excess attenuation is totally determined by the acoustical characteristics of the floor. Above 2 kHz, the floor does influence the excess attenuation, but this influence is independent of the acoustical properties of the forest floor. It can be predicted completely from the geometry of the experimental set-up in the propagation measurement. For most source-receiver distances this ground effect reduces the attenuating effect of the vegetation by 5-8 dB. This could perhaps explain the large attenuation coefficients of vegetation in an anechoic room [82] as compared with outdoor measurements [85]. Furthermore, this chapter shows that a measuring set-up in which a doubling of distances is applied [85] is not an efficient way to study the influence of vegetation on the sound propagation through forests: above 2 kHz the doubling of distances mainly introduces changes in the attenuation spectra because of the interference. It would be better to try to measure at a series of points located close together but at distances as large as practically feasible. As the spectrum above 2 kHZ is extremely sensitive to small variations in source and receiver heights at large distances (see fig. 4.3), it is apparent that errors in the measurement of these parameters can account for the often seen poor reproducibility at these high frequencies. This will specifically be the case in slightly sloping terrain.

Chapter 5

The influence of forest floors on traffic noise propagation

5.1 Introduction

For years a dispute has been going on between groups of investigators on the question: can forests be used effectively against traffic noise or not? Many reviews and bibliographies on this matter are available [83 (Dutch),87 (French), 68 (German), 74, 122, 125, 130]. Some of the results from the literature will be discussed in section 5.3.
In this chapter we will look more specifically at the influence of forest soil on the attenuation of traffic noise. A similar approach will be taken as that used by Attenborough [5]. He used impedances from the literature to predict the excess attenuation by the ground for a point source. Next, he integrated the results over an incoherent line source and over frequency of A-weighted spectra of cars and heavy trucks. Our approach is different on the following points. Firstly, we use the results of the measurements of soil impedances presented in chapter 2 to find typical attenuation spectra for layered forest floors. Most impedances used by Attenborough are too for the forest situation. Secondly, we include the effect of the diffraction of traffic noise at the impedance discontinuity at the transition from the road to the forest floor. Attenborough neglected this effect by assuming that the traffic was driving on the forest floor. Thirdly, we will calculate the ground attenuation of 1/3-octave bands by simulating these bands digitally. This is done in order to make possible a comparison with measurements of the influence of ground on the propagation of traffic noise. These results are often represented in the form of 1/3-octave excess attenuation spectra from which the influence on the A-weighted L_{eq}-level of traffic noise is deduced.

5.2 Theory of diffraction at the road edge

An exact solution exists for the diffraction of a sound wave at the edge of an infinitely thin layer with $Z_s = \infty$ [16]. In the case of traffic noise, diffracting at the impedance discontinuity between the road and the forest floor, the situation cannot be described exactly. This problem is similar to the diffraction of sound at wedges or screens. Jonasson showed that the solution to this type of diffraction is equivalent to the solution to the problem of an image source and receiver [65]. Other possible solutions are based on the compensation theorem [36], on the Kirchhoff-Huygen integration over a distribution of equivalent sources located in the vertical plane that intersects the ground along the border between the hard and the soft half-planes [36, 48, 101, 119] or on wavefield extrapolation [66, 67]. We used an approximation of the thin layer solution [16], as developed by De Jong [102]. According to this approximation the structure of the sound field depends on whether the reflection takes place on the hard or on the soft surface. If the point of reflection is located on the traffic road, the sound pressure field can be described as:

$$p/p_{ff} = 1 + (r_1/r_2)e^{ik(r_2-r_1)} \cdot Q_1 \qquad (5.1a)$$

$$+ (Q_2-Q_1)\frac{e^{-i\pi/4}}{\pi^{1/2}}(r_1/r_2)[F(\sqrt{k(r_3-r_1)})$$

$$+ F(\sqrt{k(r_3-r_2)})e^{ik(r_2-r_1)}].$$

$$F(z) = \int_z^\infty e^{iw^2}\,dw$$

The total sound pressure (p) results from three sound sources, i.e. the direct, the reflected and the diffracted sound and p_{ff} is the free field sound pressure, r_1 and r_2 are the path lengths of the direct and the reflected sound, r_3 is the path length of the diffracted sound (see fig. 5.1). Q_1 and Q_2 are the reflection factors in the case of reflection at an infinitely extended hard surface (Q_1) or soft surface (Q_2). In our case we made $Q_1 = 1$ for the asphalt ($Z_s = \infty$). Eq. 1.14 was used to calculate Q_2 for the forest soil. F(z) is the Fresnel-integral.

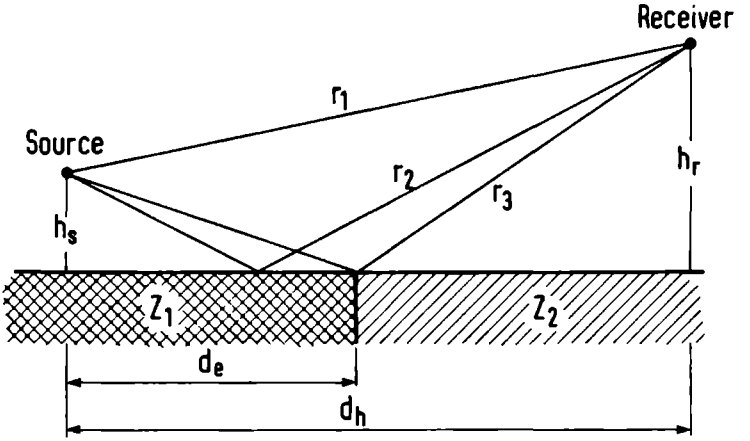

Figure 5.1. The geometry of the diffraction of sound at the edge of the road.

If the reflection takes place at the forest soil, the sound pressure field can be described with:

$$p/p_{ff} = 1 + (r_1/r_2)e^{ik(r_2-r_1)} \cdot Q_2 \qquad (5.1b)$$

$$+ (Q_2-Q_1)\frac{e^{-i\pi/4}}{\pi^{1/2}}(r_1/r_2)[F(\sqrt{k(r_3-r_1)})$$

$$- F(\sqrt{k(r_3-r_2)})e^{ik(r_2-r_1)}].$$

These equations are only valid for $Z_1 >> Z_2$, which is true in the case of an asphalt-forest floor discontinuity. Furthermore, they are only valid if the sound travels perpendicular (90^o) to the dividing line between the two impedance surfaces although Rasmussen showed that an angle of 10^o results in a maximum error of 0.5 dB and of 1 degree in 2 dB [102].
Equations 5.1a-b were used to calculate $B_t = 20\lg(p/p_{ff})$, which was subsequently used to calculate the 1/3-octave sound pressure levels relative to the free field, $L_{rf,c}$ (eq. 4.6). The predicted A-weighted 1/3-octave sound pressure level in band number c, $L_{p,c}$, is represented by:

$$L_{p,c} = L^{o}_{c} - 20\lg(r/r_0) + L_{rf,c}. \qquad (5.2)$$

In this equation, L^{o}_{c} is the A-weighted free field sound pressure level in 1/3-octave band c, measured at distance r_0. For our calculations we used the values from reference [126].
In the same way, the predicted A-weighted 1/3-octave band c free field sound pressure level, $L_{pff,c}$, is written as:

$$L_{pff,c} = L^{o}_{c} - 20\lg(r/r_0). \qquad (5.3)$$

By summing all 1/3-octave band levels from 50-20000 Hz, we eventually get the total predicted sound pressure level, L_{tot}, and the total predicted free field sound pressure level, $L_{tot,ff}$:

$$L_{tot} = 10\lg \sum_{c=1}^{24} 10^{L_{p,c}/10} \qquad (5.4a)$$

$$L_{tot,ff} = 10\lg \sum_{c=1}^{24} 10^{\{L^{o}_{c}-20\lg(r/r_0)\}/10} \qquad (5.4b)$$

The ground attenuation factor, A_g, is now defined as:

$$A_g = L_{tot} - L_{tot,ff} \qquad (5.5)$$

The value of A_g gives the influence of the ground on the total A-weighted sound pressure level of a point source emitting a traffic noise spectrum above a hard surface.

5.3 Results and discussion

In this section we will discuss the influence of our measured impedance characteristics of forest floors on the total L_{eq} (dB(A)) of car and heavy truck spectra emitted by a point source above a hard surface.
We have investigated the influence of various parameters on the edge effect in the 1/3-octave ground attenuation spectrum (figs 5.2-5.5) and on the total A_g of car and truck spectra (tables 5.1-5.7)
The edge effect is visible in the spectra as a superimposed Fresnel oscillation (figs 5.2-5.3). This oscillation is negligible for trucks (h_s=1.2 m). For cars (h_s=0.44 m) it causes the first interference dip (at 500 Hz) to be 10 dB shallower: the edge effect is most pronounced in the negative interference dip and especially for low source heights. It is almost independent of the distance between source and receiver (figs 5.4-5.5).

The effect of the edge on the A_g of a truck spectrum is independent of the distance of the truck from the edge (table 5.1). An increase in the distance of a car to the edge results in an increase in A_g of 1 dB(A) (tables 5.1 and 5.2). The influence of the edge effect on the A_g for trucks is negligible (table 5.3). This is caused by the source height of 1.2 m. An acoustically harder surface alongside the road (e.g. a grass-field in stead of a forest floor) causes only a very small (0.5 dB(A)) increase in the A_g of cars (tables 5.4 and 5.6) and of trucks (tables 5.5 and 5.7). This holds both for the situation with and without edges.
The ground attenuation of truck noise is much smaller than of car noise (see tables 5.6 and 5.7). This can be explained by the fact that truck noise contains more low-frequency noise, which is better attenuated than high-frequency noise, and by the fact that the sound emission points of trucks are located higher above the reflecting surface. These results support the suggestion made by Attenborough [5], that it is necessary to use different ground attenuation correction factors for cars and heavy trucks.

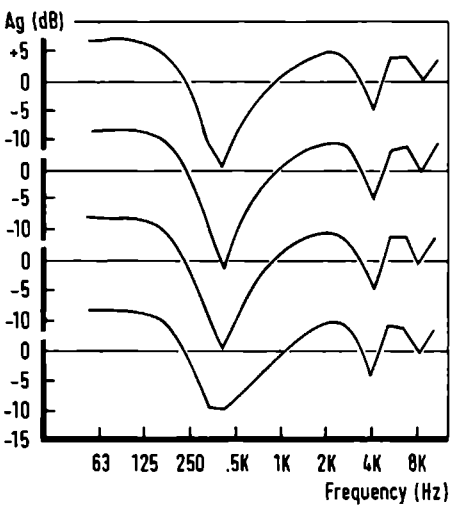

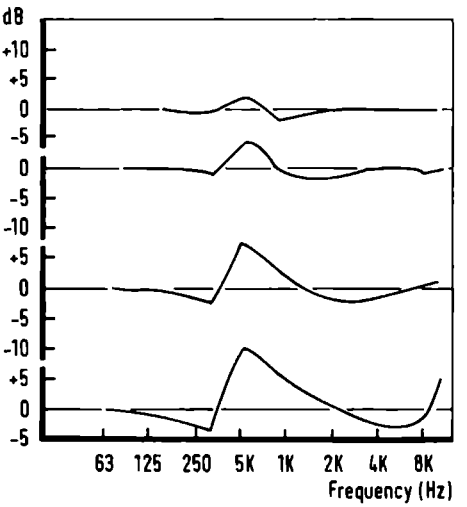

Left: Figure 5.2 The influence of d_e on the 1/3-octave ground attenuation spectrum with h_s=1.2 m, d_h=40.0 m. From top to bottom: no edge, d_e=2 m, 4 m and 8 m.

Right: Figure 5.3 The influence of d_e on the edge diffraction term in the 1/3-octave spectrum with h_s=0.44 m, d_h=40.0 m. This term was obtained by subtraction of sound pressure levels in the situation without edges from those in the situation with edges. From top to bottom: d_e=1 m, 2 m, 4 m and 8 m.

Table 5.1 Influence of d_e on A_g for a car (h_s=0.44 m) and a truck (h_s=1.20 m) spectrum emitting point source above a hard surface. Horizontal distance between line and receiver is 40.0 m.

A_g	d_e							
	No edge	0.5	1.0	2.0	3.0	4.0	6.0	8.0
Cars	-0.43	-0.44	-0.49	-0.15	0.39	0.71	0.69	0.16
Trucks	-0.52	0.53	0.51	0.50	0.51	0.51	0.51	0.71

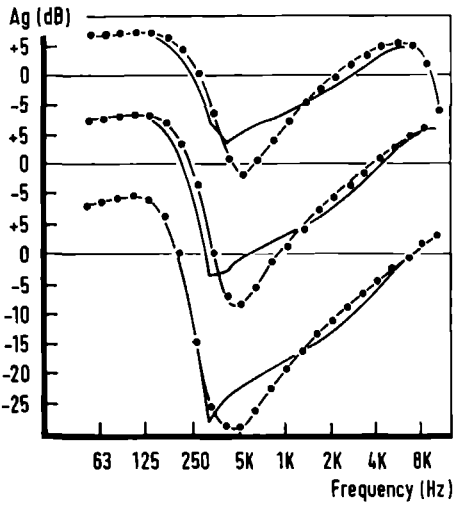

Left: figure 5.4 The influence of the horizontal distance between source and receiver on the 1/3-octave ground attenuation spectrum for a point source. Source height: 0.44 m; no edge (filled circles) or d_e=4.0 m. From top to bottom: d_h=40.0 m, 80.0 m and 160.0 m.

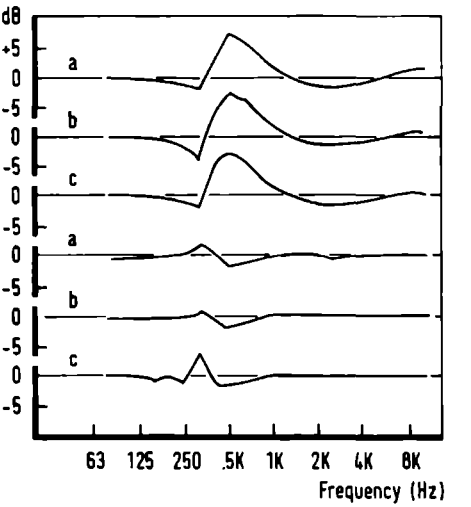

Right: figure 5.5 The influence of the horizontal distance between source and receiver on the diffraction term (d_e=4.0 m). Two source heights: 0.44 m (upper three curves) and 1.2 m (lower three curves). Three horizontal distances: 40.0 m (a), 80.0 m (b) and 160.0 m (c).

Table 5.2 The combined influence of horizontal distance (d_h) and distance to the edge (d_e) on the ground attenuation, A_g, for a car spectrum with h_s=0.44 m.

d_e	d_h			
	20	40	80	160
No edge	.	-0.43	3.94	9.37
1.0	-2.45	-0.49	3.90	9.33
2.0	-1.78	-0.15	4.14	9.55
4.0	.	0.71	4.79	10.14
6.0	-0.21	0.69	4.78	10.15
8.0	-1.34	0.16	4.38	9.81

Table 5.3 As table 5.2 but for a truck spectrum with h_s=1.2 m.

d_e	d_h			
	20	40	80	160
No edge	.	0.52	2.12	5.71
1.0	0.69	0.51	2.11	5.71
2.0	0.69	0.50	2.11	5.72
4.0	.	0.51	2.13	5.73
6.0	0.98	0.51	2.13	5.73
8.0	1.27	0.71	2.19	5.76

Table 5.4 The influence of varying R_s at constant d=0.03 m on A_g. Car spectrum used with h_s=0.44 m and d_e=4.0 m.

R_s	d_h					
	40 m		80 m		160 m	
	Edge	No edge	Edge	No edge	Edge	No edge
10^4	0.06	-1.23	4.26	3.31	9.68	8.82
$5 \cdot 10^4$	0.40	-0.80	4.52	3.63	9.88	9.07
10^5	0.71	-0.43	4.79	3.94	10.14	9.37
$5 \cdot 10^5$	1.25	0.48	4.71	4.16	9.38	8.87

Table 5.5 As table 5.4 but with a truck spectrum at h_s=1.20 m.

R_s	d_h					
	40 m		80 m		160 m	
	Edge	No edge	Edge	No edge	Edge	No edge
10^4	-0.37	-0.40	1.59	1.57	5.43	5.41
$5 \cdot 10^4$	0.03	-0.02	1.75	1.71	5.33	5.31
10^5	0.51	0.52	2.13	2.12	5.73	5.71
$5 \cdot 10^5$	-0.89	.	0.27	.	3.03	.

Table 5.6 The influence of varying layer thickness d and horizontal distance d_h with constant $R_s = 10^5$ Nsm^{-4}. Car spectrum used with h_s=0.44 m, no edge effect included.

d	d_h		
	40	80	160
0.01	-1.49	1.22	3.53
0.02	-0.57	3.83	9.19
0.025	-0.47	3.90	9.31
0.03	-0.43	3.94	9.37
0.04	-0.44	3.94	9.40
∞	-0.44	3.94	9.40

Table 5.7 As table 5.6 but for a truck spectrum at h_s=1.2 m.

d	d_h		
	40	80	160
0.01	-2.82	-2.91	-3.14
0.02	-0.20	1.12	3.97
0.025	0.31	1.84	5.28
0.03	0.52	2.12	5.71
0.04	0.61	2.25	5.94
∞	0.56	2.24	5.98

It is interesting to compare our results with the results of actual measurements of the influence of ground on traffic noise.

Hess [54] compared the attenuation of the sound of a Diesel engine over open terrain with its attenuation through a mixed forest. He found that the forest attenuated 7 dB more over 100 m. This attenuation includes both ground and vegetational absorption. Tables 5.5 and 5.7 show that the ground effect alone cannot account for more than 2 dB, the greater part of the measured absorption has to be attributed to the vegetational effect.

Scholes and Sargent [107] propose a ground effect correction factor of 4 dB(A) for a receiver located 1.5 m above the ground and at a distance of 120 m from the road. If we assume the presence of a grass-field along the road and look at tables 5.4 and 5.5, it can be concluded that this value fits our data well. Scholes and Sargent suggest, however, that the ground correction factor is independent of distance. Our results do not corroborate this.

The Dutch government has also investigated the influence of forests on the absorption of traffic noise [125]. The results are expressed in an absorption factor of 0.05-0.08 dB(A)/m. The author of the report is aware of the fact that this correction factor could be dependent of the distance.

Mitscherlich and Schölzke [89] found that at 120 m from the road a pine-forest attenuated 7 dB(A) , a deciduous forest 5 dB(A) and a field 3 dB(A) more than a meadow.

Huys et al. [57] measured the differences in L_{eq} in a mixed forest and above an open field. Both at a microphone height of 1 and 4 m and a distance of 96 m from the road edge, the L_{eq} in the forest was found to be 3.5 dB(A) lower than above the field.

Kragh [73, 74] measured the equivalent constant A-weighted sound pressure levels, L_{Aeq}, at a number of sites with belts of trees and bushes (widths between 3 and 25 m) and compared these with measurements above grass-covered ground. At a microphone height of 1.5 m he found in eight measurements the following excess attenuations behind the belts: 0.0, 0.0, 0.4, 0.6, 1.3, 2.6, 3.2 and 5.2 dB(A). He concludes that belts are not effective acoustically, although they might influence the environmental quality of residential areas due to nonacoustic, psychological factors.

Attenborough [5] gives the following predictions for the excess attenuation over grass-land at a microphone height of 1.5 m: 1.1 dB(A) at a distance of 18.2 m, 2.8 dB(A) at 36.4 m and 4.7 at 72.8 m. Our values are in reasonable agreement with these results.

The results of this chapter confirm the conclusions reached at by a number of other investigators [5, 122, 125]: given the pronounced sound influencing properties of the surface of the earth, care must be taken not to overestimate the sound-attenuating properties of a wooded area as opposed to those of a thinly-vegetated terrain [125].

Summary

The influence of organic soil layers on the propagation of sound through vegetations was investigated both theoretically and experimentally. A comparison was made between different existing models of outdoor sound propagation and between models describing the acoustical properties of soils. Specific acoustic impedances were measured as a function of sound frequency (between 200 and 1600 Hz) for several forest floors, grass-covered sandy plains and barren sandy plains. These impedances were derived from the sound interference patterns, measured with an inclined track array of microphones, on the basis of the Ingard-Chessel model. A good correlation was found between the frequency dependency of the specific impedance and the first interference dips in measured attenuation spectra. For forest floors this dependency differed from the dependency of the characteristic impedance, as predicted by the specific flow resistance, indicating that forest floors have an acoustically detectable layered structure. In an anechoic room the specific and characteristic impedances of layers of sand and of peat mul were measured with a pulse sound technique. A device was constructed with which the specific flow resistance of soil samples could be measured. The dependence of this parameter on air flow through the samples and its relation to soil impedance was investigated for peat mul and sand.

The results of the measurements were used to predict the influence of the soil on the propagation of sound through forests. Below *2* kHz, this influence appeared to be strongly dependent on the geometry of the sound source and receiver and on the impedance. Above 2 kHz, only the geometry was of importance. The 1/3-octave model was found to be appropriate as a ground correction factor in measurements aimed at the determination of the influence of living plant parts only on the propagation of sound through forests.

A traffic noise model was used to predict the influence of acoustic characteristics of soils and of the impedance discontinuity at the asphalt-soil boundary on the A-weighted immision Leq-levels of car and truck noise. The results of the calculations indicate that, notwithstanding the large differences in acoustic characteristics of forest floors and grass-fields, these levels are hardly influenced by the type of soil adjacent to the road.

Samenvatting

Van de twee factoren die de voortplanting van geluid door bossen beïnvloeden, namelijk de bovengrondse plantedelen en de organische bodemlaag, is de laatste onderzocht. Hiertoe werd een inventarisatie opgemaakt van bestaande modellen van geluidsvoortplanting in de buitenlucht en van modellen waarmee bodems akoestisch zijn te beschrijven. Aan de hand van het meest geschikte model en metingen in een aantal vegetatietypen werd de relatie tussen de specifieke akoestische impedantie en de geluidsfrequenties tussen 200 en 1600 Hz bepaald voor diverse bosbodems, grasvlaktes en zandvlaktes. De impedantie werd met het model van Ingard-Chessel berekend uit het interferentiepatroon dat gemeten werd met een schuin oplopende rij microfoons. Het impedantieverloop bleek goed gecorreleerd te zijn aan de positie van het eerste interferentie minimum in gemeten verzwakkingsspectra. Het verloop bleek voor bosbodems af te wijken van het door de specifieke stromingsweerstand gedicteerde verloop: bosbodems bleken akoestisch gelaagd te zijn. In een geluidsdode kamer werden met behulp van een geluidpulsmethode de specifieke en karakteristieke impedantie gemeten aan turfmolm en zandlagen. Een apparaat werd ontwikkeld om de specifieke stromingsweerstand van grondmonsters te meten. De relatie tussen deze parameter en de bodemimpedantie werd onderzocht bij turfmolm en zand. De resultaten van de metingen werden gebruikt om de bodeminvloed op de geluidsvoortplanting in bossen te voorspellen. Deze invloed bleek beneden 2 kHz sterk afhankelijk van de geometrie van de geluidsbron en -ontvanger en van de bodemimpedantie. Boven 2 kHz bleek alleen de geometrie invloed te hebben. Het ontwikkelde tertsbandenmodel bleek geschikt om als bodemcorrectiefactor gebruikt te worden voor de bepaling van de invloed van de levende bovengrondse plantedelen op de geluidsvoortplanting door bossen. Een verkeerslawaaimodel werd ontwikkeld waarin de invloed van de bodemimpedantie en de geluidsbreking aan de impedantiesprong tussen asfalt en bosbodems werden verwerkt. Berekeningen geven aan dat, ondanks het grote verschil tussen de verzwakkingsspectra boven bosbodems en boven grasvelden, de A-gewogen L_{eq}-niveau's van personenverkeer en vrachtverkeer niet erg sterk veranderen onder invloed van het soort bodem dat naast de weg ligt.

References

[1]
Ando Y and Kosaka K (1970), Effect of humidity on sound absorption of porous materials. Applied Acoustics 3 , 201-206.

[2]
Arya LM and Paris JF (1981), A physicoempirical model to predict the soil moisture characteristic from particle-size distribution and bulk density data. Soil Science Society of America Journal 45, 1023-1030.

[3]
ASTM Standard C 522. Standard test method for airflow resistance of acoustical materials.

[4]
Attenborough K, Hayek SI and Lawther JM (1980). Propagation of sound above a porous half-space. Journal of the Acoustical Society of America 68 (5). 1493-1501.

[5]
Attenborough K (1981), Predicted ground effect for highway noise. Journal of Sound and Vibration 81 , 3, 413-424.

[6]
Attenborough K (1982), Acoustical characteristics of porous materials. Physics Reports 82 (3), 177-225.

[7]
Attenborough K (1983). Acoustical characteristics of rigid fibrous absorbents and granular materials. Journal of the Acoustical Society of America 73 (3), 785-799.

[8]
Aylor D (1972). Noise reduction by vegetation and ground. Journal of the Acoustical Society of America 51, 197-205.

[9]
Bass HE and Bolen LN (1980), Coupling of airborne sound into the earth: frequency dependence. Journal of the Acoustical Society of America, 67 (5), 1502-1506.

[10]
Baumgartner A (1956), Untersuchungen über den Wärme- und Wasserhaushalt eines jungen Waldes. Berichte des deutschen Wetterdienstes, 28, Band 5.

[11]
Beck G (1967), Pflanzen als Mittel zur Lärmbekämpfung. Veroffentlichungsreihe des Instituts für Landschaftsbau und Gartenkunst der Technischen Universität Berlin, Vol. 12, Patzer-Verlag, Hannover-Berlin-Sarstedt.

[12]
Berenyi D (1967), Mikroklimatologie. Mikroklima der bodennahen Atmosphäre. Gustav Fischer Verlag, Stuttgart.

[13]
Beven K and Germann P (1982), Macropores and water flow in soils. Water Resources Research 18(5), 1311-1325.

[14]
Bies DA de and Hansen CH (1980), Flow resistance information for acoustical design. Applied Acoustics 13, 357-391.

[15]
Borthwick JO, Reethof G, McDaniel OH and Carlson DE (1979), Attenuation of highway noise by narrow forest belts. Report Noise Control Laboratory, Pennsylvania State University.

[16]
Bowman JJ, Senior TBA and Uslenghi PLE (1969), Electromagnetic and acoustic scattering by simple shapes. North-Holland Publishing Company, Amsterdam.

[17]
Brady NC (1974). The nature and properties of soils (8th ed.). Macmillan, New York.

[18]
Brekhovskikh LM (1969), Waves in layered media. Academic Press, New York (translated from the Russian).

[19]
Burns SH (1979), The absorption of sound by pine trees. Journal of the Acoustical Society of America, 65 (3), 658-661.

[20]
Carman PC (1956), Flow of gases through porous media. Academic Press, New York.

[21]
Chappuis C (1971), Un exemple de l'influence du milieu sur les émissions vocales des oiseaux: l'évolution des chants en forêt équatoriale. La Terre et la Vie 25, 183-202 (in French).

[22]
Chernov LA (1960), Wave propagation in a random medium. McGraw-Hill, New York (translated from the Russian).

[23]
Chessel CI (1977), Propagation of noise along a finite impedance boundary. Journal of the Acoustical Society of America, 62 (4), 825-834.

[24]
D.I. Cook and Haverbeke DF van (1971), Trees and shrubs for noise abatement. Research Bulletin No. 246, The Forest Service U.S. Dept. of Agriculture in cooperation with University of Nebraska College of Agriculture. The Agricultural Experiment Station.

[25]
Cunningham RG (1957), Jet pump theory and performance with fluids of high viscosity. Transactions of the ASME, Nov. 1957, 1807-1820.

[26]
Daigle GA, Piercy JE and Embleton TFW (1978), Effects of atmospheric turbulence on the interference of sound waves near a boundary. Journal of the Acoustical Society of America 64 (2), 622-630.

[27]
Daigle GA (1979), Effects of atmospheric turbulence on the interference of sound waves above a finite impedance boundary. Journal of the Acoustical Society of America 65 (1), 45-49.

[28]
Daigle GA (1980), Correlation of the phase and amplitude fluctuations between direct and ground reflected sound. Journal of the Acoustical Society of America 68 (1), 297-302.

[29]
Daigle GA, Embleton TFW, Piercy JE (1979), Some comments on the literature of propagation near boundaries of finite acoustical impedance. Journal of the Acoustical Society of America 66 , 918-919.

[30]
Davies JC, Mulholland, KA (1979), An impulse method of measuring normal impedance at oblique incidence. Journal of Sound and Vibration 67 , 135-149.

[31]
Delany ME and Bazley EN (1970), Acoustical properties of porous materials. Applied Acoustics 3, 105-116.

[32]
Dickinson PJ (1969), Free-field measurement of the normal acoustic impedance of ground surfaces. Thesis, University of Southampton.

[33]
Dickinson PJ and Doak PE (1970), Measurements of the normal acoustic impedance of ground surfaces. Journal of Sound and Vibration 13(3), 309-322.

[34]
Diggory IS and Oakes B (1980), Computer simulation model for the prediction of traffic noise level. Applied Acoustics 13 (1), 13-31.

[35]
Durnin J and Bertoni HL (1981), Acoustic propagation over ground having inhomogeneous surface. Journal of the Acoustical Society of America 70 , 852-859.

[36]
Dziedzic A and Barraud M (1979),
Propagation en milieux naturels semi-transparents. (Propagation through semi-transparent natural environments.)
Revue d'Acoustique No. 51, 239-242 (in French).

[37]
Donato RJ (1977), Impedance models for grass-covered ground,
Journal of the Acoustical Society of America 61 , 1449-1552.

[38]
Ehlers W, Grimme K, Baeumer K, Stülpnagel R,
Köpke U and Böhm W (1981), Flow resistance in soil
and plant during field growth of oats. Geoderma 25 , 1-12.

[39]
Eldred KM (1975), Assessment of community noise.
Journal of Sound and Vibration 43 ,137-146.

[40]
Embleton TFW (1963), Sound propagation in homogeneous deciduous and evergreen woods. Journal of the Acoustical Society of America 35, 1119-1125.

[41]
Embleton TFW (1966), Scattering by an array of cylinders as a function of surface impedance. Journal of the Acoustical Society of America, 40 , 667-670.

[42]
Eyring CF (1946), Jungle acoustics. Journal of the Acoustical Society of America 18, 257-273.

[43]
Foss RN (1979), Effects of wind and ground plane attenuation
on sound propagation near the ground, Journal of the Acoustical Society of America 66 (4), 1088-1092.

[44]
Frank L (1976), Tree bark and the forest floor as sound absorbing elements in a forest, Master Thesis, Pennsylvania State University.

[45]
Geiger R (1961), Das klima der bodennahen Luftschicht.
Vieweg Verlag, Braunschweig.

[46]
Gill PE and Murray W (1978), Algorithms for the solution of the non-linear least squares problem. SIAM Journal on Numerical Analysis, 15, 977-992.

[47]
Glaretas C (1981), A new method for measuring the acoustic impedance of the ground.
Thesis of the Pennsylvania State University.

[48]
Goethals H (1981), Reflektie van geluidsgolven aan een oppervlak met impedantiesprong (Reflection of sound waves at a surface with an impedance discontinuity). Master of Science Report, Laboratory for Acoustics and Heat Conduction, Katholieke Universiteit Leuven (in Flemish).

[49]
Harper EY and Labiance FM (1975), Scattering of sound from a point source by a rough surface progressing over an isovelocity ocean. Journal of the Acoustical Society of America 58 , 349-364.

[50]
Heijden LAM van der (1981), Impedance measurements of natural soils with an inclined track method. In: Peutz MA and Bruijn A de (eds), Proc. Inter-Noise 81 Amsterdam, 265-270.

[51]
Heijden LAM van der, Bie JGEM de and Groenewoud J (1982), A pulse method to measure the impedance of semi natural soils, Acustica 51 ,No. 3, 193-197.

[52]
Heijden LAM van der and Son RJJH van (1982), A note on the neglect of the doppler effect in the modelling of traffic flow as a line of stationary point sources. Journal of Sound and Vibration 85 (3), 442-444.

[53]
Heijden LAM van der, Claessen V and Cock N de (1983), Influence of vegetation on acoustic properties of soils. Oecologia (Berlin), 56 , 226-233.

[54]
Hess W (1961), Die Lärmdämmerung mit Hilfe von Grünpflanzen (Sound attenuation by means of plants). Zeitschrift für Präventivmedizin 6, 303-312 (in German).

[55]
Hole FD (1981), Effect of animals on soil. Geoderma 25 , 75-112.

[56]
Huszty D, Illenyi A and Vass Gy (1972), Equipment for measuring the flow resistance of porous and fibrous materials. Applied Acoustics 5, 1-14.

[57]
Huys L, Hulshof P and Walraven M (1980), De invloed van twee vegetaties op verkeerslawaai (The influence of two vegetations on traffic noise). Master of Science Report, Botanisch Laboratorium, Katholieke Universiteit Nijmegen (in Dutch).

[58]
Ingard U (1951), On the reflection of a spherical sound wave from an infinite plane. Journal of the Acoustical Society of America

23 , 329-335.

[59]
Isei T (1980), Absorptive noise barrier on finite impedance ground. Journal of the Acoustical Society of Japan (E) 1 , 1, 3-10.

[60]
Isei T, Embleton TFW and Piercy JF (1980), Noise reduction by barriers on finite impedance ground. Journal of the Acoustical Society of America 67 , 46-58.

[61]
Ismail SNA (1974), Micromorphometric soil porosity analysis. Doctoral thesis University of Utrecht.

[62]
ISO/DIS 4638. Cellular polimeric flexible materials. Test for air permeability.

[63]
Janse ARP (1969), Sound absorption at the soil surface. Thesis Agricultural University of Wageningen.

[64]
Jilka A and Leisler B (1974), Die einpassung dreier Rohrsängerarten (Acrocephalus schoenobaenus, A. scripaceues, A. arundinaceus) in ihre Lebensräume im bezug auf das Frequenzspektrum ihrer Reviergesänge. Journal of Ornithology 115, 192-212.

[65]
Jonasson HG (1972), Diffraction of wedges of finite acoustic impedance with applications to depressed roads. Journal of Sound and Vibration 25 , 577-585.

[66]
Jong BA de (1980), A new method for calculation of the influence of wind and temperature. In: Peutz MA, Bruijn A de (eds), Proc. Inter-Noise 81, Amsterdam, 261-264.

[67]
Jong BA de (1983), The influence of wind and temperature gradients on outdoor sound propagation. Development and Evaluation of a calculation method based on wavefield extrapolation. Thesis at the Technical University Delft, Delft University Press.

[68]
Kampfer M (1970), Noise control by methods of landuse planning, amenity plantings and forests. Bibliography No. 6 (revised, in German). Bundesanstalt für Vegetationskunde, Naturschutz und Landschaftspflege, Bad Godesberg, Fed. Rep. of Germany.

[69]
Kilmer RD (1974), Evaluation and prediction of the sound absorbing characteristics of composite acoustic absorbers for normally incident plane waves. Master thesis, Pennsylvania State University.

[70]
Kintzl Z (1975), Investigations of the sound absorption of wall sections by a pulse technique. Soviet Physics Acoustics 21 , 30-32.

[71]
Klein C, Cops A (1980), Angle dependence of the impedance of a porous layer. Acustica 44 , 258-264.

[72]
Komarov VS (1977), Adsorbenty i ih svojstva (Adsorbents and their properties), Minsk (in Russian).

[73]
Kragh J (1981), Road traffic noise attenuation by belts of trees. Journal of Sound and Vibration 74 (2), 235-241.

[74]
Kragh J (1982), Road traffic noise attenuation by belts of trees and bushes, Report no. 31, Danish Acoustical Laboratory, Lyngby, Denmark.

[75]
Lansing DL (1980), Some effects of motion and plane reflecting surfaces on the radiation from acoustic sources, Noise Control Engineering, Vol. 14, 2, 54-65.

[76]
Lee R (1978), Forest microclimatology, Columbia University Press, New York.

[77]
Leonard RW (1946), Simplified flow resistance measurements. Journal of the Acoustical Society of America 17(3), 240-241.

[78]
Leonard RW (1948), Simplified porosity measurements. Journal of the Acoustical Society of America 20(1), 39-41.

[79]
Linskens HF, Martens MJM, Hendriksen HJGM, Roestenberg-Sinnige AM, Brouwers WAJM, Staak ALHC van der and Strik-Jansen AMJ (1976), The acoustic climate of plant communities. Oecologia (Berlin) 23, 165-177.

[80]
Lozinskaja EA (1980), The solution of the system of equations describing the heat and water transfer in a plant canopy. In: Fizika počvennyh vod (Soil water physics), Akademija Nauk SSSR, Moscow (in Russian).

[81]
Martens MJM (1977), The influence of the soil on the acoustic climate of plant communities. In: Rathe EJ (ed), Proc. Inter-Noise 77, Zürich 1977, B593-B598.

[82]
Martens MJM (1980a), Foliage as a low-pass filter: experiments with model forests in an anechoic chamber.

Journal of the Acoustical Society of America 67, 66-72.

[83]
Martens MJM (1980b), Geluid en groen (Sound and vegetation). Doctoral thesis, Katholieke Universiteit Nijmegen (in Dutch and English).

[84]
Martens MJM and Michelsen A (1981), Absorption of acoustic energy by plant leaves. Journal of the Acoustical Society of America 69 (1), 303-306.

[85]
Martens MJM (1981), Noise abatement in plant monocultures and plant communities. Applied Acoustics 14, 167-189.

[86]
Michelsen A (1978), Sound reception in different environments. In: Ali MA (ed), Sensory Ecology, Plenum, New York, 345-373.

[87]
Migneron J-G (1980), Acoustique urbaine (Urban acoustics). Les presses de l'Université Laval, Québec, 306-316 (in French).

[88]
Miles JH (1975), Application of cepstral techniques to ground reflection effects in measured acoustic spectra, Journal of the Acoustical Society of America 61 (1), 35-38.

[89]
Mitscherlich G and Schölzke D (1977), Schalldämmerung durch Wald (Sound attenuation by forest). Allgemeine Forst und Jagdzeitung, 148 (7) (in German).

[90]
Moerkerken A (1975), De invloed van grondabsorptie op de geluidvoortplanting boven een bodem. (The influence of ground absorption on the propagation of sound over a soil.) ICG Report VL-DR-21-02, Ministerie van Volksgezondheid en Milieuhygiëne, Den Haag (in Dutch).

[91]
Moerkerken A and Toorn JD van der (1981), A simple computation method for noise of highways and city streets. In: Peutz MA, De Bruijn A (eds), Proc. Internoise 81, 1013-1018.

[92]
Morse PM (1976), Vibration and sound. American Institute of Physics. 468

[93]
Morton ES (1975), Ecological sources of selection on avian sounds. American Naturalist 109 , 17-34.

[94]
Motovilov JuG (1980), Rasčet osnovnoj gidrofizičeskoj harakteristiki počv po dannym o počvennogidrobiologičeskih konstantah. (Calculation of fundamental hydrophysical soil characteristics from the data of soil hydrology constants.)

Meteorologija i Gidrologija, no. 12, 93-101 (in Russian).

[95]
NAG Fortran Library Manual, Mark 8, Volume 4 (1981), NAG Central Office, Oxford, U.K.

[96]
NF T 56-127 Produits alveolaires à base de caoutchouc ou de matières plastiques. Détermination du comportement à l'écoulement de l'air (in French).

[97]
Oosting WA (1977), Berekeningsmethode wegverkeerslawaai voor zoneringsdoeleinden. Rapport VL-HR-22-01, Ministerie van Volksgezondheid en Milieuhygiene, Den Haag (in Dutch).

[98]
Pierce AD (1981), Acoustics. An introduction to its physical principles and applications, McGraw-Hill, New York.

[99]
Piercy JE, Embleton TFW and Sutherland LC (1977), Review of noise propagation in the atmosphere. Journal of the Acoustical Society of America 61 , 1403-1418.

[100]
Rajčev T and Dimitrov DN (1981), Diagnostika poristosti počv metodom Komarova (The diagnostics of soil porosity according to the method of Komarov). Počvoznanija i Agrohimija, XVI, 3, 56-61 (in Russian).

[101]
Rasmussen KB (1981), Sound propagation over grass covered ground. Journal of Sound and Vibration 78 (2), 247-255.

[102]
Rasmussen KB (1982), Sound propagation over level terrain. Report No. 33, Technical University of Denmark, Lyngby, Denmark.

[103]
Roberts JP, Kacelnik A and Hunter MJ Jr (1980), Some consequences of sound interference for birdsong. Acoustics Letters 3 (7), 141-146. 141-146.

[104]
Rosenberg NJ (1974) Microclimate:The biological environment. Wiley, New York.

[105]
Ruijgrok GJJ (1980), Experiments on the validity of ground effect predictions for static noise testing of propeller aircraft. Journal of Sound and Vibration, 72 ,4, 469-479.

[106]
Scheffer F and Schachtschabel P (1979), Lehrbuch der Bodenkunde (10th ed.). Ferdinand Enke Verlag, Stuttgart.

[107]
Scholes WE and Sargent JW (1972), Ground effect and motorway noise. Applied Accoustics (5), 145-148.

[108]
Severens PPJ (1983), Trillende plantedelen (Vibrating plant parts). Master of Science Report, Botanical Laboratory, Katholieke Universiteit Nijmegen (in Dutch).

[109]
Spomer LA (1980), Graphical prediction of porosity and water retention in sand-soil mixtures for drained turf sites. Canadian Journal of Soil Science, Vol. 60, no. 4, 787-791.

[110]
Stearns SD (1975), Digital signal analysis. Hayden Book Company, Rochelle Park, New Yersey.

[111]
Stoutjesdijk Ph (1975), On the range of micrometeorological differentiation in the vegetation. In: Dierschke H (ed), Berichte der Internationalen Symposien der Internationalen Vereinigung für Vegetationskunde. Vegetation und Klima, Rinteln, 1975.

[112]
Sutherland LC, Piercy JE, Bass HE and Evans LB (1974), Invited paper before the 88th meeting of the Acoustical Society of America, St. Louis, Missouri, 4-8 November 1974.

[113]
Sutherland LC (1975), Review of experimental data in support of a proposed new method for computing atmospheric absorption loss. DOT Report TST-75-87.

[114]
Sutherland LC and Bass HE (1979), Influence of atmospheric absorption on the propagation of bands of noise, Journal of the Acoustical Society of America 66 (3), 885-894.

[115]
Talaske RH (1980), The acoustic impedance of a layered forest floor. Report to USDA Forest Service submitted by Noise Control Laboratory, Pennsylvania State University.

[116]
Tatarskij VI (1971), The effects of the turbulent atmosphere on wave propagation. Keter, Jerusalem (translated from Russian).

[117]
Tatarskij VI (1979), K teorii rasprostranenija zvuka v stratifičirovannoj atmosfere (On the sound propagation in a stratified atmosphere), Fizika Atmosfery i Okeana, 15 , No. 11, 1140-1150 (in Russian).

[118]
Thomasson S-I (1976), Reflection of waves from a point source by an impedance boundary. Journal of the Acoustical Society of America 59 (4), 780-785.

[119]
Thomasson S-I (1977), Sound propagation above a layer with a large refraction index. Journal of the Acoustical Society of America 61 (3), 659-674.

[120]
Thomasson S-I (1979), Bestämning av markimpedansen (Estimation of ground impedance). Rapport R32:1979, Statens råd för byggnadsforskning, Stockholm (in Danish with English tables, legends and summary).

[121]
Thomasson S-I (1980), On the absorption coefficient, Acustica, 44, 265-273.

[122]
Tiplady PH (1981), Noise and its attenuation by vegetation - A review, Master of Science Report, Department of Horticulture, Wye College, University of London.

[123]
Tolstoy I (1981), Energy transmission into shadow zone by rough surface boundary wave. Journal of the Acoustical Society of America 69 (5), 1290-1298.

[124]
Tolstoy I (1982), Coherent sound scatter from a rough interface between arbitrary fluids with particular reference to roughness element shapes and corrugated surfaces. Journal of the Acoustical Society of America 72 (3), 960-972.

[125]
Toorn JD van der (1975), Geluiddemping door bossen (Sound attenuation by woods). Report VL-HR-06-01, Interdepartementale Commissie Geluidhinder, Ministerie van Verkeer en Waterstaat, Den Haag (in Dutch).

[126]
Toorn JD van der (1976), Geluidemissie door personenauto's en vrachtwagens op autosnelwegen (Sound emission by cars and trucks on highways). Report VL-HR-01-01, Interdepartementale Commissie Geluidhinder, Ministerie van Verkeer en Waterstaat, Den Haag (in Dutch).

[127]
Twersky V (1983), Reflection and scattering of sound by correlated rough surfaces. Journal of the Acoustical Society of America 73 , 85-94.

[128]
Vorobeva LA, Glebova GI, Gorshova EI et al. (1980), Fiziko-himičeskije metody issledovanija počv. (Physico-chemical research methods of soils.) Moscow University Press (in Russian).

[129]
Vries O de and Dechering FJA (1969), Grondonderzoek. Bedrijfslaboratorium voor grond- en gewasonderzoek, Mariendaal, Oosterbeek, the Netherlands (in Dutch).

[130]
Vulcan G and Gomersall A (1979), Traffic noise: a review and bibliography on surface transportation noise, 1964-1978, Bedford, IFS Publications.

[131]
Waser RM and Waser MS (1977), Experimental studies of primate vocalization: specializations for long-distance propagation. Zeitschrift für Tierpsychologie, 43, 239-263.

[132]
Wiener FM and Keast DN (1959), Experimental study of the propagation of sound over ground. Journal of the Acoustical Society of America 31, 724-733.

[134]
Westhoff V and Held AJ den (1969), Plantengemeenschappen in Nederland. Thieme & Cie, Zutphen (in Dutch).

[134]
Yuzawa M (1975), A method of obtaining the oblique incident sound absorption coefficient through on-the-spot measurements. Applied Acoustics 8 , 27-41.

[135]
Žantiev RD (1981), Bioakustika nasekomyh. (Bioacoustics of insects.) Moscow University Press, 168-175 (in Russian).

[136]
Zwikker C and Kosten CW (1949), Sound absorbing materials. Elsevier Press, Amsterdam.

Leo van der Heijden werd geboren op 22 mei 1955 te Vlijmen. Na het behalen van het diploma HBS-β aan het Dr. Moller College te Waalwijk in 1972 ging hij in datzelfde jaar Biologie studeren aan de Katholieke Universiteit te Nijmegen. Het kandidaatsexamen (richting B3) werd in 1978 afgelegd. Het doctoraalprogramma omvatte de hoofdvakken Algemene Botanie ('Metingen van de akoestische impedantie van diverse bodemtypen', onder leiding van prof. dr. H.F. Linskens) en Biofysica ('Visuo-motor neurons in the Internal Laminar Nuclei of the monkey', onder leiding van dr. J.A.M. van Gisbergen) en het bijvak Chemische Cytologie ('Invloed van een aantal factoren op de oppervlakteladingsdichtheid van de gistcelmembraan', onder leiding van drs. A.P.R. Theuvenet). Het doctoraalexamen werd afgelegd in april 1979 en per 15 april 1979 volgde een aanstelling voor 5/10 weektaak als wetenschappelijk medewerker aan het Botanisch Laboratorium van de Katholieke Universiteit te Nijmegen, waar tot mei 1983 het onderzoek voor dit proefschrift werd verricht. Van april 1980 tot april 1983 was hij tevens part-time werkzaam als redacteur bij het wetenschappelijk en technisch maandblad 'Natuur en Techniek' te Maastricht. Per 1 mei 1983 volgde zijn aanstelling als wetenschappelijk redactieadviseur bij het Pudoc (Centrum voor Landbouwpublikaties en Landbouwdocumentatie) te Wageningen.

Stellingen

1. Het wijdverbreide gebruik om geluidsverzwakking in bossen uit te drukken in aantal decibel per meter is door het a-lineaire karakter van het bodemeffect alleen toegestaan als voor dit effect gecorrigeerd is.

   Dit proefschrift

2. Door de combinatie van de specifieke spectrale samenstelling van verkeerslawaai en de absorptie-eigenschappen van bosbodems zal het totale niveau van verkeerslawaai langs een snelweg met daarnaast een bosbodem slechts 1-2 dB(A) lager zijn dan in het geval van een grasveld.

   Dit proefschrift

3. Het gebruik van de specifieke stromingsweerstand van grondmonsters als ingangsparameter voor de empirische formules van Delany en Bazley resulteert bij bosbodems niet in een adequate beschrijving van het verloop van de akoestische specifieke impedantie met de frequentie.

   Delany, M.E. and Bazley, E.N. (1971), Acoustical properties of fibrous absorbent materials. Applied Acoustics 3 , 105-116.

   Dit proefschrift

4. De moeilijk door geluidsschermen of vegetatie te dempen lage tonen in verkeerslawaai zouden effectief gereduceerd kunnen worden door middel van absorptie van oppervlaktegolven boven een aangepaste structuur in de bodem langs snelwegen.

   Heijden, L.A.M. van der en Martens, M.J.M. (1982), Traffic noise reduction by means of surface wave exclusion above parallel grooves in the road side. Applied Acoustics, 15 , 329-339.

5. De serene stilte in bossen wordt niet veroorzaakt door bijzondere geluidsdempende eigenschappen van vegetatie of bodem maar veeleer door het ontbreken van lawaaibronnen.

   Dit proefschrift

6. Buiten in het vrije veld heerst over het algemeen geen akoestisch vrij veld.

Dit proefschrift

7. Zoals Charles Darwin een einde maakte aan het beeld van een onveranderlijke stoffelijke wereld zo heeft de door Bahá'u'lláh verkondigde leer van de Progressieve Openbaring een einde gemaakt aan de statische opvatting van de geestelijke wereld.

Esslemont, (1978), Bahá'u'lláh en het nieuwe tijdperk. Stichting Bahá'í Literatuur, Den Haag.

8. Zolang biologen niet goed worden opgeleid in wiskunde, natuurkunde en scheikunde zullen fysici, chemici en ingenieurs door kunnen blijven gaan met het annexeren van biologische onderzoeksgebieden.

9. Gezien het feit dat veel wetenschappers hun gedachtengangen moeilijk op schrift kunnen vastleggen en het feit dat velen van hen wel moeiteloos kunnen praten over hun werk, verdient het aanbeveling dat wetenschappers alleen maar schriftelijk met elkaar communiceren. Ook uit het oogpunt van de bescherming van intellectueel eigendom biedt dit voordelen.

10. Het verhuizen van software kost vaak zoveel bedstro dat men er slapeloze nachten aan overhoudt.

11. De invoering van de kleurentelevisie heeft er weinig toe bijgedragen dat de informatieoverdracht minder zwart-wit is geworden.

Leo van der Heijden

Nijmegen, 27 januari 1984